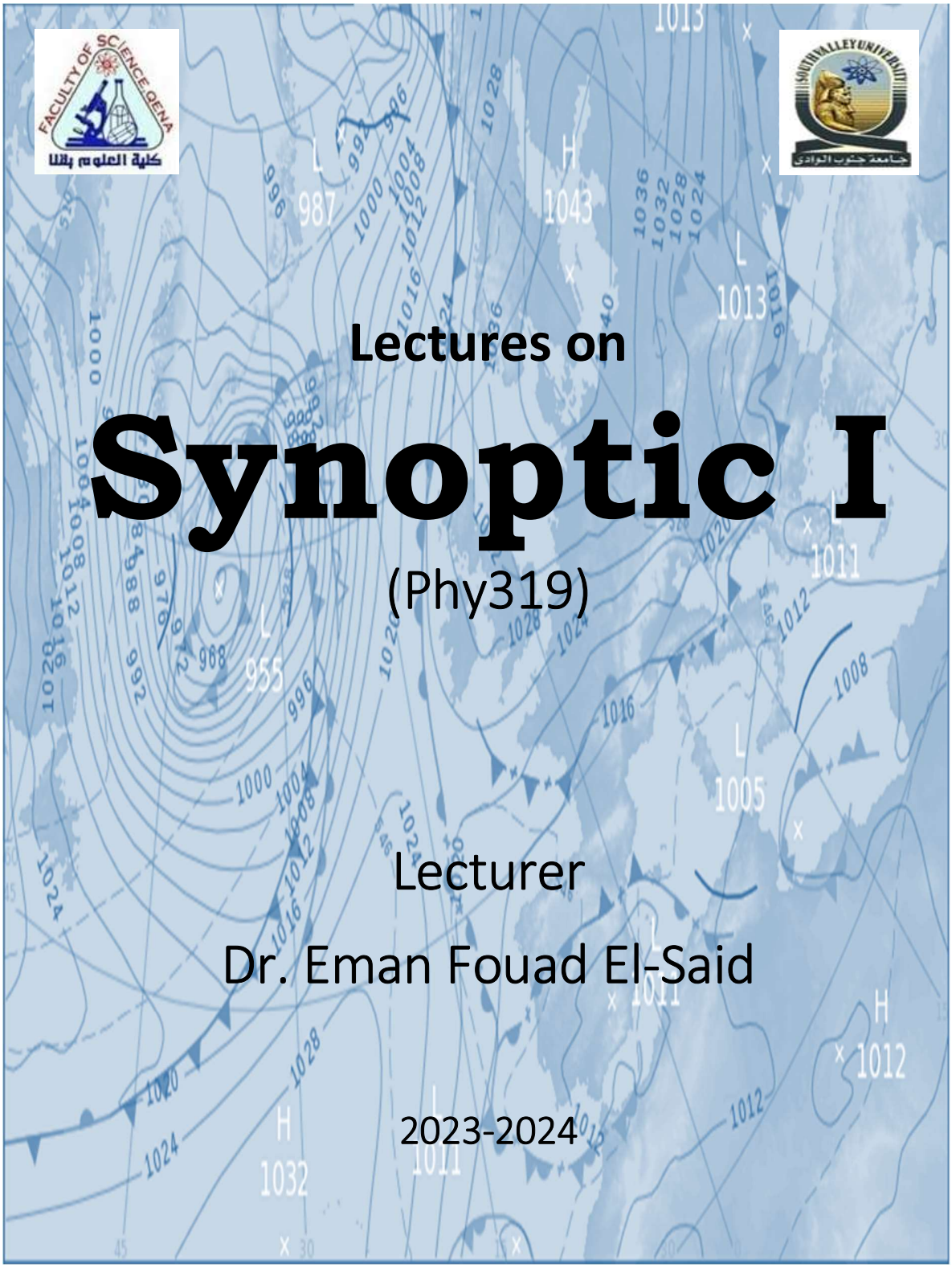

Lectures on

Synoptic I

(Phy319)

Lecturer

Dr. Eman Fouad El-Said

2023-2024

Table of Contents

CHAPTER 1: PRELIMINARIES

1.1: What is Synoptic Meteorology? 5
1.2: Scales of Motion 7
1.3: Outline of the Book 7

CHAPTER 2: OBSERVATIONS OF METEOROLOGICAL VARIABLES

2.1: The Measurement of Time 9
2.2: The Measurement of Pressure and Height 10
2.3: The Measurement of Temperature 12
2.4: The Measurement of Humidity 13
2.5: The Measurement of the Wind Field 15
2.6: Observation Stations 18
2.7: Weather Data Visualization 20

CHAPTER 3: KINEMATICS OF METEOROLOGICAL VARIABLES

3.1: The Scalar Meteorological Fields 21
3.2: Advection 26
3.2.1: Mathematical Derivation of Advection 29
3.3: Overview of Atmospheric Thermodynamics 30
3.3.1: Macroscopic Description of Moist Air 30
3.3.2: Kinetic Theory of Gases 32
3.3.3: The First Law of Thermodynamics 34
3.3.4: Potential Temperature 36
3.4: Kinematics of the Wind Field 39
3.4.1: Derivation of Flow Patterns 39
3.4.2: Translation 40
3.4.3: Divergence 41
3.4.4: Vorticity 43
3.4.5: Deformation 45

CHAPTER 4: SYNOPTIC FRONTS

4.1: Air Masses 47
4.2: General Characteristics of Synoptic Fronts 50

4.3: Frontogenesis 51
4.3.1: Derivation of Frontogenesis Function..... 54
4.3.2: Frontogenesis and Deformation 58
4.4: Cold Fronts 61
4.4.1: Katafront and Anafront Structure 64
4.5: Warm Fronts 66
4.6: Stationary Fronts and Occlusions 68
4.7: Coastal Fronts 71

CHAPTER 5: FUNDAMENTAL AND APPARENT FORCES

5.1: Introduction 74
5.2: The Pressure Gradient Force 75
5.2.1: Derivation of the Pressure Gradient Force 77
5.3: The Gravitational Force 78
5.4: The Frictional Force 79
5.4.1: Derivation of the Viscous Force 80
5.5: Introduction to the Apparent Forces 82
5.6: The Centrifugal Force 83
5.7: The Coriolis Force 85
5.7.1: Derivation of Apparent Forces 88
5.8: The Fundamental Equations of Motion 90

CHAPTER 6: THE GOVERNING EQUATIONS

6.1: Introducing Scale Analysis 93
6.1.1: Simplifying the Equations of Motion..... 94
6.2: The Hydrostatic Equation 96
6.3: The Thickness Equation 97
6.3.1: Reduction to Sea Level Pressure 99
6.3.2: Isobaric Charts 102
6.3.3: Thickness and Temperature Advection 103
6.4: Mass Continuity Equation..... 105
6.4.1: Derivation of Mass Continuity Equation 108
6.5: The Geostrophic Approximation 110
6.6: Thermal Wind Balance 113
6.6.1: Full Derivation of Thermal Wind Balance 119

End

Chapter 1:Preliminaries

1.1: What is Synoptic Meteorology?

Outside of field of meteorology, the adjective *synoptic* refers to a "summary or general view of a whole." The adjective has a more restrictive meaning to meteorologists, however, in that it refers to large spatial scales. The first routinely available weather maps, produced in the late 19th century, were derived from observations made in European cities having a relatively coarse characteristic spacing. These early meteorological analyses, referred to as **synoptic maps**, paved the way for the Norwegian cyclone model, which was developed during and shortly after World War I. Because only extratropical cyclones and fronts could be resolved on the early synoptic maps, *synoptic* ultimately became a term that referred to large-scale atmospheric disturbances. Hence, **synoptic meteorology** traditionally involves the study of weather systems, such as extratropical high and low-pressure systems, jet streams and associated waves, and fronts. As we will see, the width of synoptic-scale features such as troughs and ridges in the midlatitude westerlies and large extratropical cyclones and anticyclones is much greater than their depth. Although fronts and jets associated with the aforementioned synoptic-scale features are as long as the troughs and rides in the midlatitude westerlies, and have similar time scales, they are much narrower.

The study of weather phenomena on somewhat smaller spatial and temporal scales, **mesoscale meteorology**, includes the study of convective storms, land-sea breezes, gap winds, and mountain waves. In recent years, advances in observing and computing technology have allowed the boundary between synoptic and mesoscale meteorology to blur as an increasing volume of high-resolution information has become available. As the resolution of analyses, forecasts, and observations increases, mesoscale weather systems begin to come into focus on the maps that were once the exclusive realm of synoptic-scale weather systems. Today's synoptic meteorologist benefits from in-depth knowledge of mesoscale processes and their interactions with synoptic-scale weather systems. The earth system exhibits a continuous spatial and temporal spectrum of motion that defies simple categorization.

The question of whether to classify phenomena in terms of physical characteristics or controlling physical laws manifests itself in an interesting way in meteorology. Synoptic meteorology is largely based upon observation. On the other hand, dynamic meteorology is based on the acceptance of physical laws and deductions about atmospheric behavior based upon those laws. We can first observe a phenomenon and describe its characteristics, then analyze it to learn why it forms and why it behaves as it does, and ultimately to predict its behavior. Or we

can predict its existence based upon physical law, and then search for it in nature. Synoptic meteorologists usually take the former approach, whereas dynamic meteorologists usually take the latter approach. For example, the midlatitude cyclone was first observed, then analyzed, and much later numerically predicted. On the other hand, gravity waves were first discussed as solutions to a set of dynamical equations, and later were sought observationally. Today's synoptic meteorologist benefits from insights derived by physical laws (traditionally within the realm of dynamical meteorology) and the plethora of observational analysis based on our advances in observational technology and instrumentation.

Thus, knowledge of numerical modeling and modern observational systems, in addition to a solid traditional physics foundation in the atmospheric sciences, is consistent with increasingly high expectations for today's scientists to solve complex problems, often of considerable societal import. Atmospheric scientists who are able to synthesize theoretical concepts, observations, and conceptual and numerical models in their work are best able to contribute to scientific advance. The advantages of the interplay between practice and theory were recognized by pioneers in the atmospheric sciences, such as Vilhelm Bjerknes, who actively encouraged such diverse activities. Consider the following quote from C. -G. Rossby in 1934, a pioneer in the atmospheric sciences:

The principle task of any meteorological institution of education and research must be to bridge the gap between the mathematician and practical man, that is, to make the weather man realize the value of a modest theoretical education, and to induce the theoretical man to take an occasional glance at the weather map.

This quote embodies the spirit of atmospheric science and this philosophy remains as relevant today as it was in 1934.

Weather forecasting necessitates understanding a wide range of processes and phenomena acting on a variety of spatial and temporal scales. For example, forecasting for a coastal location requires information concerning the near-shore water temperature, the potential for land–sea breeze circulations, and the strength and orientation of the prevailing synoptic-scale wind flow. The prediction of precipitation type can benefit from knowledge of atmospheric thermodynamics and cloud physics. Other types of prediction, including air quality forecasting and seasonal climate prediction, also require knowledge that spans a broad spectrum of meteorological processes. Hence, weather forecasting and weather analysis are essentially topics in applied physics. In other words, the skill set necessary to become a proficient forecaster is the ability to synthesize information for a wide range of phenomena and to apply one's physics education (primarily classical mechanics, thermodynamics, and fluid dynamics) to understand and predict atmospheric phenomena.

1.2: Scales of Motion

As mentioned in the Preface, atmospheric motions occur over a broad continuum of space and time scales. The timescales of atmospheric motions range from under a second (in the case of small-scale turbulent motion), to as long as weeks (in the case of planetary waves). In order to examine atmospheric motions, we must identify the characteristic horizontal length and time scales, and these are often related to one another. The length scale can be related to the size of a weather system, whereas the time scale can be related to how long it would take an air parcel to circulate within the system.

Table 1.1. Summary of basic scales, with example phenomena

Scale	Length (km)	Time	Example phenomena
Microscale	<1	<1 h	Turbulence, PBL
Mesoscale	1–1,000	1 h–1 day	Thunderstorm, land–sea breeze
Synoptic	1,000–6,000	1 day–1 week	Upper-level troughs, ridges
Planetary	>6,000	>1 week	Polar front jet stream, trade winds

The values in Table 1.1 are typically used to define different scale regimes in atmospheric systems. The values listed in Table 1.1 are approximate; there are not usually sharp distinctions or abrupt transitions in the dynamics at a certain specific scale, and there are exceptions. However, generally speaking, meteorological phenomena having short temporal scales tend to have small spatial scales, and vice versa.

1.3: Outline of the Book

No single course (or single textbook) can comprehensively treat the variety of processes and phenomena described previously, but the goal is to introduce these topics so that the reader develops an appreciation for the essential physics behind large-scale atmospheric phenomena. The approach of this course is to synthesize what has been traditional to synoptic meteorology (i.e., observations) with the theoretical foundation being laid by dynamical meteorology. The synoptic meteorologist represents the intuitive component of this process, while the dynamic meteorologist represents the deductive component of this process. The most important application of dynamics to synoptic meteorology, which we will examine in this course, is called **quasigeostrophic theory**, which is based upon observations, but logically developed by dynamical meteorology.

After introductory sections on units and coordinate systems, the kinematics of scalar meteorological fields, with an emphasis on the pressure and height fields will be discussed. The kinematics of the vector wind field is the next topic treated. We will then present an elementary survey of atmospheric dynamics and atmospheric thermodynamics with specific applications to synoptic fronts and other synoptic-scale motions. These discussions will ultimately culminate in the examination of quasigeostrophic theory. In the second portion of these notes, we will apply quasigeostrophic theory to the analysis of extratropical cyclones, anticyclones, upper-level waves, and the jet stream. Recognizing that the existence of mesoscale phenomena (such as thunderstorms, squall lines, etc.) depends upon the synoptic-scale environment and an understanding of convection, we will conclude the course with a discussion of atmospheric stability and convection.

Chapter 2: Observation of Meteorological Variables

The basic scalar meteorological variables we measure are pressure, temperature, humidity, and wind. The purpose of this chapter is to describe briefly the fundamental principles underlying common measurement instruments.

2.1: The Measurement of Time

The most basic meteorological variable is time. Weather systems and centralized produces regularly flow across time zones, so to help reduce confusion and simplify the workload, meteorologists preferentially use **Universal Coordinated Time** (UTC), also known as **Greenwich Mean Time** (GMT) or **Zulu Time** (Z). In simple terms, UTC is the time and date in London, England, ignoring any daylight saving time rules that are observed there. Forecasters should be thoroughly familiar with how to convert their local time zone to UTC and back. In the United States, Eastern Standard Time (EST) is converted by subtracting 5 hours from UTC time, or 4 hours when Eastern Daylight Time (EDT) is in effect. A map of time zones is given in Figure 2.1.

Figure 2.1: A time zone map

2.2: The Measurement of Pressure and Height

A very familiar and important meteorological property is pressure, which is defined as force per unit area. The derived SI unit of pressure is kg $m^{-1}s^{-2}$ = Pa, where Pa is the unit called **Pascal**. However, this unit of pressure is not used often in meteorology. The common meteorological convention is to measure pressure in millibars, which is defined as 1 mb = 1 hPa = 100 Pa.

Pressure may also be measured in terms of the height of a column of mercury in an evacuated tube, and in such a case is expressed in inches of mercury (note that one inch of mercury equals 33.86 mb). The volume of a liquid-like mercury changes as a function of pressure, and, when the liquid is confined inside a tube, the pressure may be inferred from the height of the liquid in the tube. If the volume of the liquid is also a weak function of temperature, then suitable corrections must be made. Ideally, the liquid should be chosen so that its volume is as sensitive to pressure, and as independent of other variables as possible.

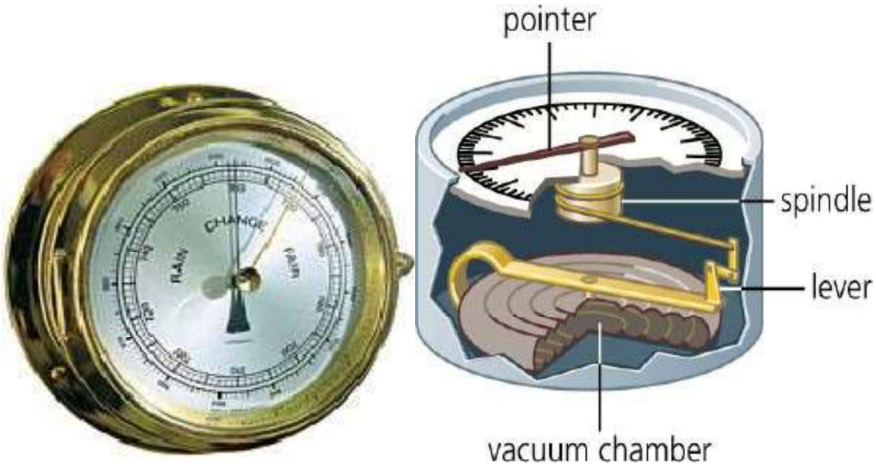

Figure 2.2: (Left) Actual aneroid barometer. (Right) Aneroid barometer schematic

The volume of some materials also changes as a function of pressure. Barometers that work on this principle are called **aneroid barometers**; the extent to which the material bends is a function of pressure, and this bending action is converted into the deflection of a lever on a scale. As shown in Figure 2.2, an aneroid barometer is operated by a metal cell containing only a very small amount of air. Increased air pressure causes the sides of the cells to come closer together. On one side there is a fixed point to the base of the barometer, while the other is connected by levers and pulleys to a rotating pointer that moves over the scale. Aneroid barometers also are sensitive to temperature to some extent, and suitable corrections may have to be made.

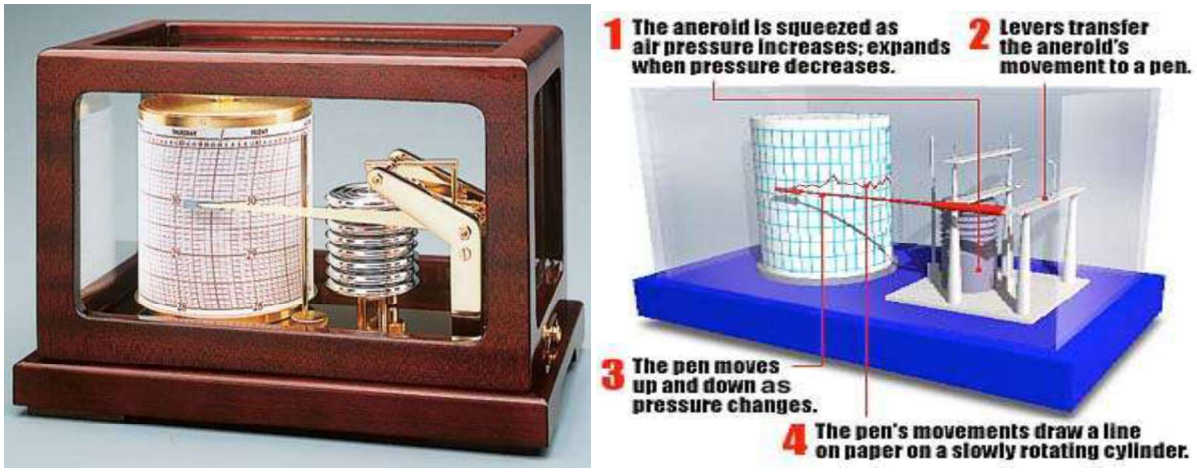

Figure 2.3: (Left) Actual barograph; (Right) Barograph schematic

The lever of some aneroid barometers is connected to a pen, which presses down upon a rotating cylinder containing a chart. Such a barometer is called a **barograph,** as shown in Figure 2.3. Good barometers are accurate to within 1 or 2 mb or better.

There are three primary pressure variable systems that are currently in use: station pressure (QFE), sea-level pressure (SLP), and altimeter setting (QNH). Station pressure is the actual, uncorrected pressure reading. A barometer that reads correctly at sea level and is brought to some other elevation, without adjustment, is displaying the station pressure. While it is not directly used in forecasting, it is the building block of all other pressure values. Sea-level pressure is that station pressure "reduced" numerically to sea level. The intent of this is to remove temperature bias from various stations at different elevations. The standard sea-level pressure is 1013.2 mb. Altimeter setting is station pressure value directly reduced to sea level. The altimeter setting is the value commonly heard on television and radio weathercasts in the United States and it is used for setting aircraft altimeter. The purpose of the altimeter setting is to remove elevation bias at various locations.

Height above the ground may be measured from an aircraft with a downward looking radar. Such a height is called the **radar altitude**. For a suitable environment (which will be demonstrated in a later chapter), knowledge of the pressure within the aircraft and the pressure at the observation station can be used to infer the height as a function of pressure and temperature. Heights are obtained that in general are good to within a meter or less in the lower depths of the troposphere.

2.3: The Measurement of Temperature

Figure 2.4: An actual thermograph

According to the kinetic theory of gases (which will be discussed in the next chapter), temperature is a measure of the amount of kinetic energy in the molecules of a substance, which manifests itself as how "hot" a substance is. The standard unit of temperature is given in degrees Kelvin (K) when computations are made. Temperature may also be measured in degrees Celsius (which is usually used on upper air weather charts) and in degrees Fahrenheit (which is usually used on surface weather charts in the United States). The temperature conversion formulas are made:

$$T(°C) = \frac{5}{9}[T(°F) - 32], \quad T(°F) = \frac{9}{5}[T(°C) + 32], \quad T(K) = T(°C) + 273.15$$

where °C is degrees Celsius and °F is degrees Fahrenheit.

Temperature, like pressure, may be measured from the amount of change in volume of a liquid such as mercury or alcohol confined inside a tube. It's very important to use a liquid that will not freeze if the temperature gets very cold. Temperature can also be measured electronically. The volume of some solid substances changes as a function of temperature, and hence the deflection of an electrically conductive substance can result in a change in the capacitance of a set of parallel plates. The electrical resistance of some materials changes as a function of temperature, and hence these devices are called **thermistors**. Temperatures can usually be measured to within 0.5 °C with such devices. Thermometers that are coupled to a pen and a moving chart are called **thermographs**.

Figure 2.5: A common microwave radiometer operating at an airport

An infrared or microwave radiometer (pointing upward if it is ground based and downward if it is airborne or on a satellite) can be used to obtain vertical profiles of the temperature field. Since the radiative properties of oxygen and water vapor in the infrared and microwave regions of the electromagnetic spectrum depend to a large extent on temperature, measurement of infrared and microwave radiation can be used to get an estimate of the vertical temperature profile. The infrared and microwave radiometers are **passive devices** in that they are **remote sensors** that do not radiate their own energy, but rather detect radiation from the atmosphere. These thermodynamic profiles are very useful in that they can make measurements at a fixed location nearly continuously in time.

2.4: The Measurement of Humidity

The Earth's air is made up of nitrogen, oxygen, argon, and other gases. The most important trace gas in Earth's atmosphere for the sake of meteorology is the gaseous phase of water, known as **water vapor**. Because of its important in determining the distribution of precipitation and atmospheric stability, several different measurements for moisture are commonly used:

- **Mixing ratio**: The mixing ratio q (units: g/kg) is simply the ratio of the mass of water vapor to the mass of dry air in a given volume. The greater the mixing ratio, the more water is contained in a given volume of air. On a summer day in Florida, a typical mixing ratio will be about 12 g/kg.

- **Relative humidity**: Relative humidity is defined as the ratio of the mixing ratio q to the saturation mixing ratio q_s. The saturation mixing ratio q_s (units: g/kg) represents the *maximum* possible mixing ratio for a given parcel of air and it is largely a function of temperature. If $q = q_s$, then the relative humidity is 100%. At this point, the air is considered to be saturated, and water vapor must condense into liquid droplets or ice crystals.

Humidity is perhaps the most difficult variable to measure. The electrical resistance of some materials varies as a function of humidity. These sensors are used electronically. It is useful to use a material whose resistance responds as linearly as possible on humidity. The **sling psychrometer** is a set of thermometers mounted side by side. One wick is left dry, while the other is wet with pure water. The device is spun through the air so that the "wet-bulb" thermometer attains the wet-bulb temperature as the water evaporates, while the "dry-bulb" thermometer simply measures the air temperature. Infrared and microwave radiometers can be used to estimate the vertical profile of water vapor and liquid water in a manner similar to that which can be used to determine the vertical temperature profile.

Figure 2.6: (Left) An actual sling psychometer; (Right) A schematic of a sling psychrometer

Clouds are best observed by satellite. Satellites in geosynchronous orbit (i.e. an orbit with an orbital period equal to the rotation period of the Earth) rotate about earth's axis at the same rate at which the Earth turns about its axis. Photographs of the same entire half of the Earth's disc are available at frequent intervals. Polar-orbiting satellites provide higher-resolution images because they are closer to Earth's surface. However, images of the same location are available only several times daily. Visible channels show clouds and surface features, while the infrared

channels show cloud-top and surface temperatures. Time-lapse movies or "loops" of images from a geosynchronous satellite are often used to view the evolution of cloud features.

2.5: The Measurement of the Wind Field

The wind field is the primary meteorological vector variable we measure, and is perhaps the most important. Meteorologists often express the wind speed (i.e. the magnitude of the velocity vector) in knots, one of which equals 0.514 m/s or 1.15 mph. The following conversion formulas are often useful.

- 1 meter = 39.37 inches (in.) = 3.2808 feet (ft)
- 1 kilometer (km) = 0.62137 statute miles
- 1 statute mile (mi) = 1.6093 km = 5280 ft
- 1 nautical mile (nm) = 1 min of latitude = 1.15 statute miles
- 1 m/s = 1.94 knots (kts) = 2.23 miles per hour (mph)
- 1° latitude = 111.137 km.

The measurement of wind is based upon two main principles:

1. The action of wind upon a fixed object produces a change in some properties of that object that depend upon the wind speed.
2. Some objects suspended in air move along (in the horizontal) at the same speed as the air and can be tracked.

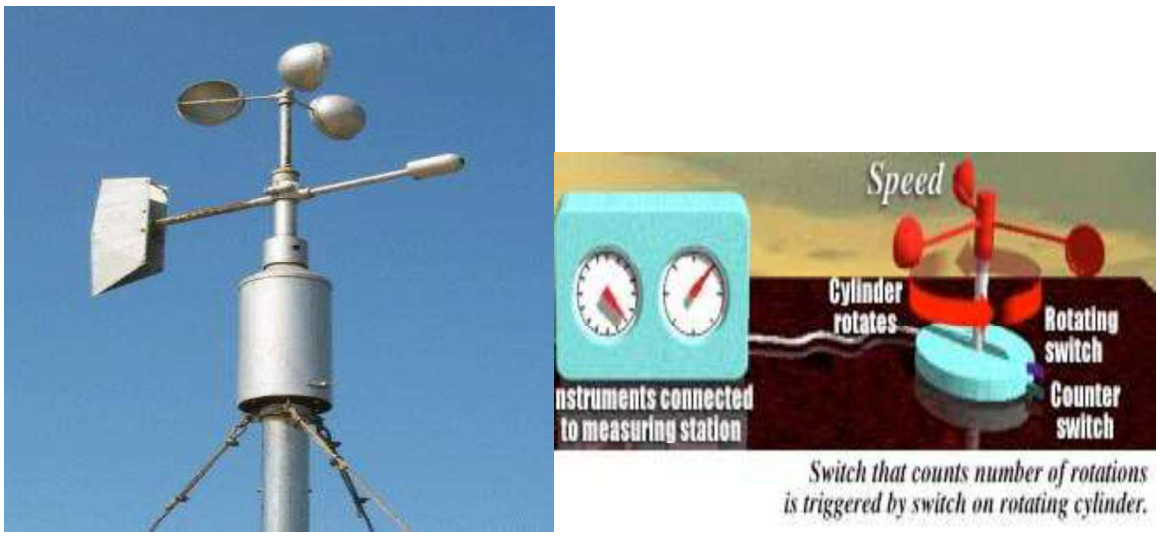

Figure 2.7: (Left) An actual anemometer. (Right) Schematic of an anemometer

Devices in which the wind speed is related quantitatively to a change in some property of the device are called **anemometers**. The torque induced by the wind on a number of rotating cups is called a **cup anemometer**. Some anemometers work on the principle that the pressure change across the device depends upon the wind speed and direction. These anemometers have no moving parts. Sonic anemometers employ the principle that the sound waves travel at the air velocity plus the velocity of sound in still air. Anemometers are usually mounted on towers, high enough above surrounding obstacles so that the wind measurements are represent of the free air above the ground. Anemometers are often located at 10 m above ground level (also called **AGL**), the so-called **anemometer level**.

Meteorologists usually express this direction of the wind in degrees relative to true north, the direction of the North Pole. Meteorologists must be extremely attentive to whether a direction describes where wind is *blowing from* or *blowing to*. The **meteorological wind direction** is the compass heading *from which* the wind is blowing. For example, northerly, easterly, southerly, and westerly winds are from 360 (north), 90 (east), 180 (south), and 270 (west) degrees, respectively. In other words, the meteorological wind direction (θ_{met}) is the angle made by the horizontal wind vector measured in a clockwise manner from the y-axis.
However, *wind vectors* express which direction winds are blowing toward. In operational meteorology, wind vectors are used primarily when working out physical equations and when using the hodograph, while nearly all weather charts use wind direction instead. Fortunately, when it comes to actual weather charts, the use of wind symbols in meteorology is never ambiguous. Vector symbols are always reserved for wind vectors, whereas wind barbs are always an indicator of wind direction

The wind may be estimated from the motion of objects that move along with the wind. There are many techniques for doing this. The most common method of this type involves the tracking of a balloon, which has a known ascent rate and which is released from the ground and visually tracked a theodolite (a precision instrument used for measuring angles in the horizontal and vertical planes). Balloons that are tracked by radar or by direction-finding devices (rotatable antennas that search for the strongest signal) are called **rawinsondes**. The accuracy of the standard rawinsonde varies from 1 m/s at low altitudes to 10-20 m/s near the tropopause around a jet. The accuracy diminishes when the balloon is far downstream at a low elevation angle.

Balloons may also be tracked with the use of navigation aids. Signals are received from several very low frequency (VLF) radio beacons around the world, and are re-transmitted downward to the fixed base station. The difference in time of arrival (measured by phase differences among the signals) of the radio beacons and a knowledge of the exact location of the beacons enables one to determine the precise location of the balloon. Winds may also be computed by determining the difference between the track taken by an aircraft as determined by an **inertial navigation system** (INS) aboard the aircraft and that expected by the orientation of

the aircraft. The INS determines the location of the aircraft from its initial position and measurements of the aircraft's acceleration as a function of time. The wind, therefore, blows the aircraft off course, and knowledge of this deviation enables one to determine the wind.

Figure 2.8: An actual rawinsonde.

Cloud elements may be tracked in sequences of satellite photographs in order to get an estimate of the wind field at cloud-top level. This method is very useful over data-void regions such as those over the ocean. However, one must determine the height of the cloud top from an inspection of infrared photographs, and by associating cloud-top temperature with the temperature of a representative sounding. Finally, pulsed Doppler radar may be used to estimate the motion of targets such as precipitation and clouds.

There are a number of types of platforms upon which instruments are placed. Surface measurements of pressure and humidity may be measured by an observer reading the scale of a simple barometer and a sling psychrometer. Temperature may be read off a simple thermometer. Automated networks of observation stations (as shown in Figure 2.10) send digitally processed signals to a central computer. Aircrafts are also often used as platforms. In some cases the data may be relayed via satellite to fixed stations. Tall towers have been instrumented at various level so that profiles of temperature and humidity as a function of pressure may be obtained in the boundary layer (i.e. the layer closest to the Earth that is most affected by surface friction). Instruments placed under balloons that are released into the air and travel upwards and that

transmit data by radio back to the ground are called **radiosondes**. Instruments placed under parachutes that are then dropped from an aircraft are called **dropsondes**, as shown in Figure 2.9. Finally, satellites are used as bases for the remote measurement of temperature and humidity in the atmosphere below.

2.6: Observation Stations

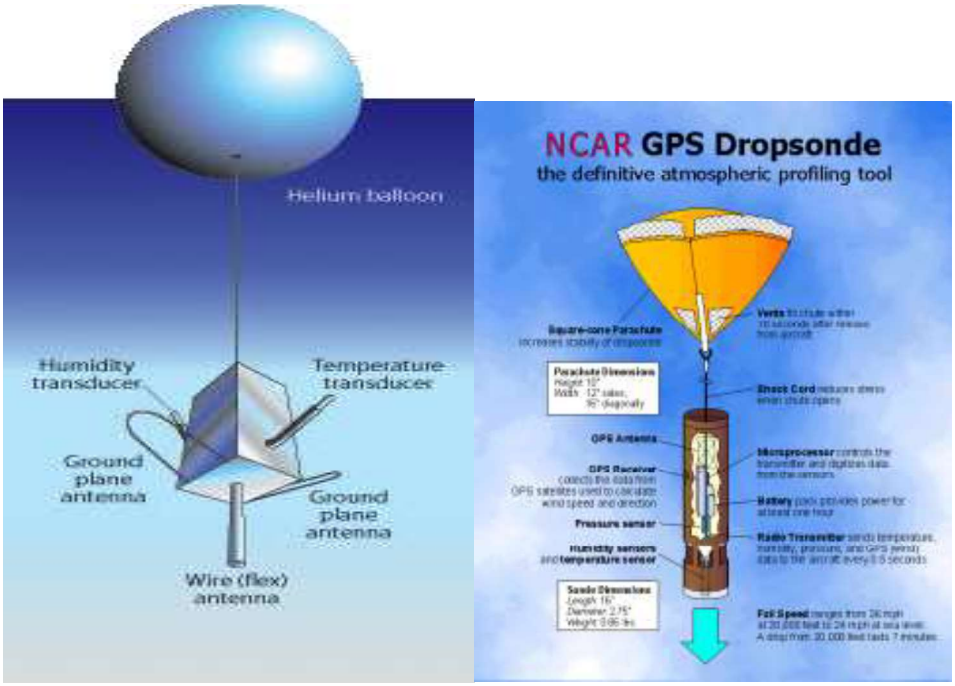

Figure 2.9: (Left) A schematic of a radiosonde. (Right) A schematic of a dropsonde.

Weather observations are taken daily every 1 to 6 hours at about 5,000 stations around the world and shared via data networks under the oversight of the World Meteorological Organization (WMO) and International Civil Aviation Organization (ICAO). Because of the close relationship of meteorology with aviation, a substantial number of weather stations are located at airports and are managed by aviation authorities. This is especially true in the United States, Canada, and Europe.

Figure 2.10: An automated surface observation system (ASOS)

The United States uses 3 station identifiers: ICAO location indicators, FAA location identifiers, and WMO station index. The ICAO codes were developed in the mid-1950s by the International Civil Aviation Organization, which standardizes and publishes the codes. The first one or two letters always represents the country or region (for example, a U.S. identifier is K---). The FAA codes were developed in the 1940s by the Civil Aeronautics Administration. In the U.S., where ICAO identifiers begin with K, FAA codes are generally equivalent to the second, third, and fourth letters. The WMO codes were developed as 5-digit numerical identifiers in 1948 and are widely used within meteorology. These codes were developed to resolve growing chaos caused by dozens of station code systems and weather dissemination formats that varied from coutnry to country. Much like the ICAO system, the first two digits identify the country or region and are known as block numbers (for example, the U.S. has a block number of 72). Meteorologists frequently come into contact with these codes when dealing with soundings, radiosonde observations, and synoptic observations.

METAR is the most common format for hourly surface observations in North American and Europe. At some stations, a METAR observation is transmitted every 20 minutes, and if a significant weather change occurs it is referred to as a SPECI (special) observation. The format is rather readable and is designed mostly for the aviation sector. The Federal Meteorological Handbook (http://www.ofcm.gov/fmh-1/fmh1.htm) on surface weather observations contains a full list of abbreviations for METAR reports.

As mentioned previously, radiosondes are the most important (and most reliable) source of weather data for the upper atmosphere. Twice a day, hundreds of radiosonde stations around world launch these instruments and monitor the primary meteorological variable. These are encoded in a code format known as WMO TEMP (or RAOB) and are disseminated worldwide, where they can be used in soundings and integrated into model forecasts. The Federal Meteorological Handbook (http://www.ofcm.gov/fmh3/pdf/13-app-e.pdf) on rawinsonde observations contains a full list of abbreviations for radiosonde codes.

2.7: Weather Data Visualization

After data is collected at various weather stations, the observational data is processed and presented in many forms. The most common forms of weather data visualization are: surface and upper-air weather maps; thermodynamic diagrams; numerical model output; satellite imagery; and radar imagery. These weather charts are openly available to the public through the internet. Below is a list of popular institutions that visualize real-time weather data:

- National Center for Atmospheric Research Real-Time Weather Data (NCAR-RAL): http://weather.rap.ucar.edu/
- Unisys Weather: http://weather.unisys.com/index.php
- Plymouth State Weather Center: http://vortex.plymouth.edu/index.html
- University of Oklahoma: http://hoot.metr.ou.edu/
- National Weather Service Storm Prediction Center (NWS-SPC): http://www.spc.noaa.gov/
- Pennsylvania State University Electronic Map Wall: http://mp1.met.psu.edu/~fxg1/ewall.html

In the next chapter, we will examine the kinematics of scalar meteorological fields and the vector wind field.

Chapter 3: Kinematics of Meteorological Variables

The basic meteorological variables are pressure, temperature, humidity, and the wind fields. The purpose of this chapter is to briefly describe the kinematics of these meteorological fields. We first consider pressure (at constant elevation) because it is the most commonly analyzed quantity.

3.1: The Scalar Meteorological Fields

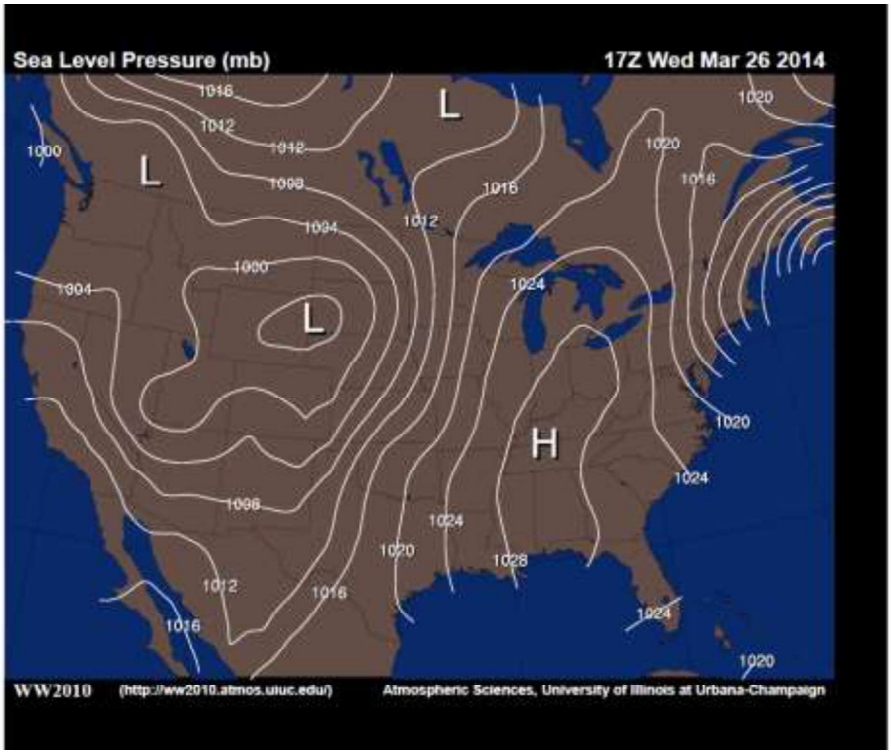

Figure 3.1: Sea-level pressure map of the continental U.S. on 26 March 2014 at 17 Z

A sea-level pressure map of the continental United States given in Figure 3.1. Typically on surface maps, lines of constant pressure (which is usually at a fixed elevation) are plotted. These lines are called **isobars**. Suppose we regard a curved isobar as an arc section of an imaginary circular isobar. The **radius of curvature** vector $\vec{R}$ is measured from the center, radially outward to the isobar. If pressure increases in the radially outward direction, then the isobar is considered to be **positively curved**. Conversely, if pressure decreases in the radially

outward direction, then the isobar is considered to be **negatively curved**. In the former case, pressure is an increasing function of distance from the center, and the radius of curvature is positive (such as the low-pressure center over Colorado in Figure 3.1). In the latter case, pressure is a decreasing function of distance from the center, and the radius of curvature is negative (such as the high-pressure center over Tennessee over Colorado in Figure 3.1). An isobar is **negatively curved** if the isobar is concave in the direction of increasing values of pressure. If an isobar is convex in the direction of increasing values of pressure, then the isobars are said to be **positively curved**.

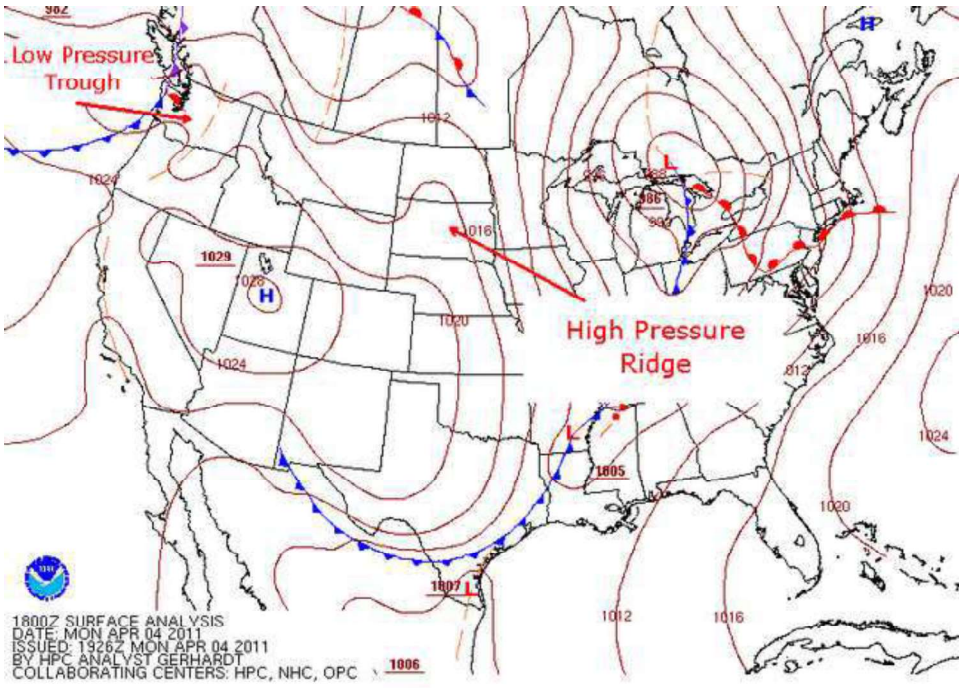

Figure 3.2 Annotated surface analysis chart for 18Z on 04 April 2011. Courtesy of NOAA. Trough axes are denoted by the dashed lines.

A **ridge axis** (or **ridge line**) may be defined as the locus of maximum negative curvature on a set of adjacent isobars. A **trough axis** (or **trough line**) may be defined as the locus of maximum positive curvature on a set of adjacent isobars. The symbol for a ridge axis is a sawtooth-shaped line, and the symbol for a trough axis is a dashed line. As shown in the surface analysis of Figure 3.2, trough axes are drawn over the low pressure trough in the Northwest US and over the Great Lakes near the Canadian border. Trough axes and ridge axes may have any orientation. **Tilted** troughs and ridges are those whose axes are not oriented strictly in the north-south direction. For example, the axes of positively (negatively) tilted troughs lean toward the east (west) with increasing latitude. In Figure 3.2, we see a positively tilted trough over the Northwest US, and a negatively tilted trough over the Great Lakes. As we will show later,

negatively tilted troughs are usually indicators of potentially severe weather, whereas positively tilted troughs often are signs of a weakening weather system.

Alternatively, one may think of positively and negatively tilted troughs and ridges as those that lean in the direction of the basic flow or against the direction of the basic flow, respectively, with increasing latitude. Troughs in easterly flow are found, for example, in coastal fronts along the east coast of the United States, in thermal troughs along the west coast of the United States, and north of developing cyclones in the central United States. (Since most of the pressure troughs we observe are in the midlatitude westerlies, troughs in easterly flow are often called **inverted troughs**. This terminology is misleading since the definition of a trough is independent of its orientation). Zonally oriented troughs are often found along zonally oriented warm fronts and stationary fronts (such as the trough axis over the Great Lakes). On surface maps, the relative strength of troughs and ridges are governed by the spacing between the isobars. Thus, strong ridges (troughs) have more tightly spaced isobars than weak ridges (ridges).

Features in the pressure field such as highs, lows, troughs, and ridges usually exhibit some motion. We often attribute motion to low- and high-pressure centers and to troughs and ridges, as if the lows and highs and troughs and ridges were solid bodies embedded within the flow of the atmosphere. In fact, the motion of lows, highs, troughs, and ridges is usually only "apparent". These features are "propagating" when they re-form on one side and dissipate on the other. Air is continually being circulated into and out of these pressure-field features. In a sense, air is ingested, processed, and expelled from these features, just as air enters the human body, is processed, and is expelled in a transformed state. Thus, lows, highs, troughs, and ridges cannot be considered by themselves in isolated from their environment. The behavior of the pressure systems depends to some extent upon the trajectories of air parcels entering the systems. The injection of warm or moist or cold or dry air can be dynamically important.

Systems that move eastward or westward move **zonally**, while those that move northward or southward move **meridionally**. Troughs in the midlatitude westerlies that have a component of motion toward the equator are said to be **digging**. Troughs that have component of motion toward the pole are said to be **lifting out**. Pressure systems not only move, but they also intensify or weaken, or just have central pressures that change without any corresponding change in intensity. When the pressure in a high or along a ridge rises, it is said that the high or ridge is **building**. When the pressure falls in a high or along a ridge it is said that the high or ridge is **weakening**. When the pressure in a low or along a trough falls, it is said that the low or trough is **deepening**. Intensification occurs only if the spacing between isobars decreases. When the pressure rises in a low or along a trough it is said that the low or trough is **filling**. It is likely, but not always true, that deepening lows and troughs are also intensifying, and it is also likely, but not always true, that building highs and ridges are intensifying, and vice versa.

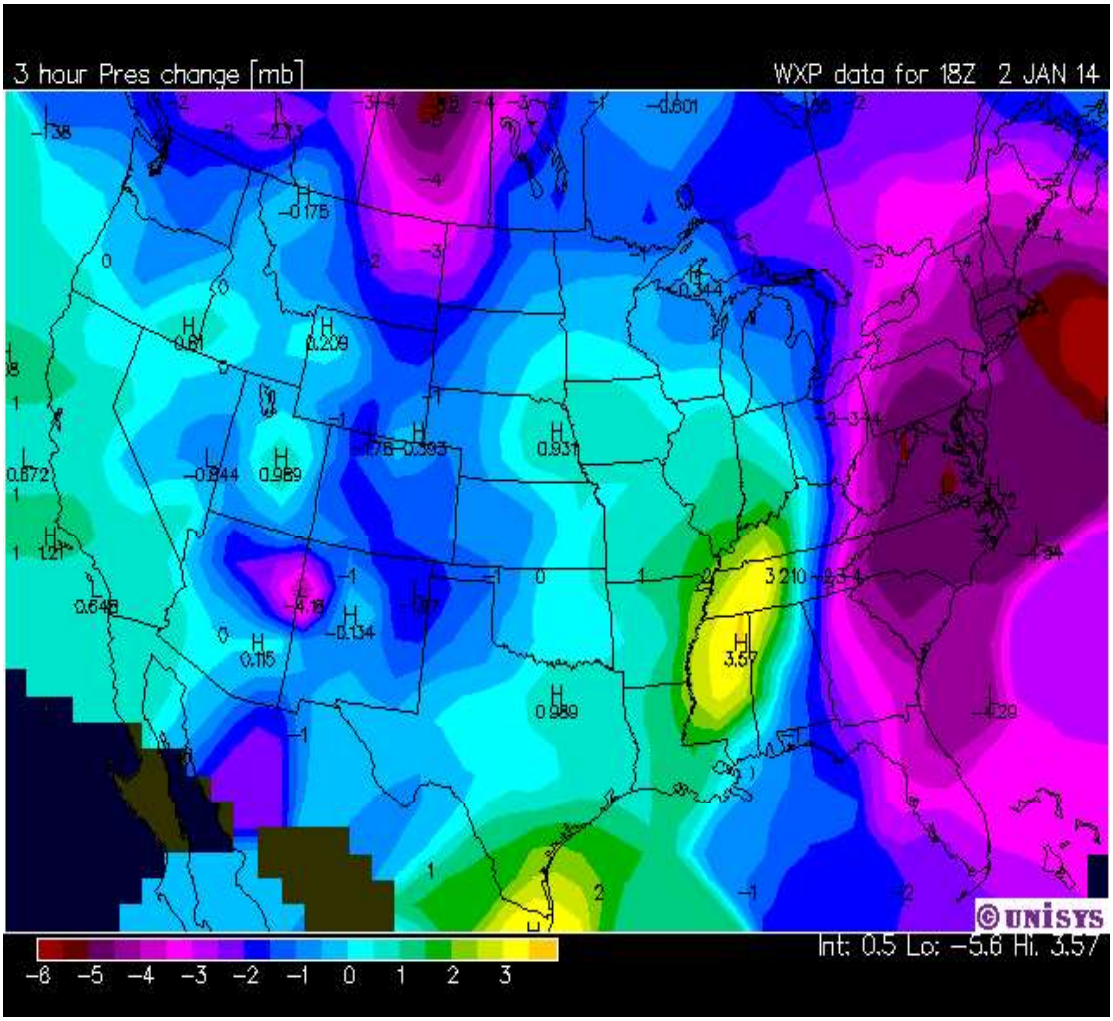

Figure 3.3 Map of 3 hour surface pressure change from 18Z on 2 January 2014. Courtesy of UNISYS.

The rate at which intensity of the pressure field changes is called the **pressure tendency** and lines of constant pressure tendency are called **isallobars**. An isoballaric tendency map is given in Figure 3.3. The positive isallobaric tendency over Mississippi indicates that the pressure is rising locally. The rise in pressure could mean that a ridge axis or a high-pressure center has a component of motion that is toward the observer, or that a trough axis or a low-pressure center has a component of motion away from the observer, or that a nearby high-pressure area or ridge is stationary, and building, or that a nearby low-pressure area or trough is stationary and filling, or a combination of all the aforementioned. The pressure tendency field is important because it provides a mean of predicting the movement of surface pressure systems. Generally speaking, **lows tend to move from an adjacent region of greatest pressure rises toward an adjacent region of greatest pressure falls; highs tend to move from an adjacent region of greatest pressure falls toward a region of greatest pressure rises.** Based on this rule, Figure 3.3 suggests that frontal system along the eastern US will tend to move in an

eastward or east-northeastward direction. The exact direction of motion depends also on the intensity and symmetry of the pressure field.

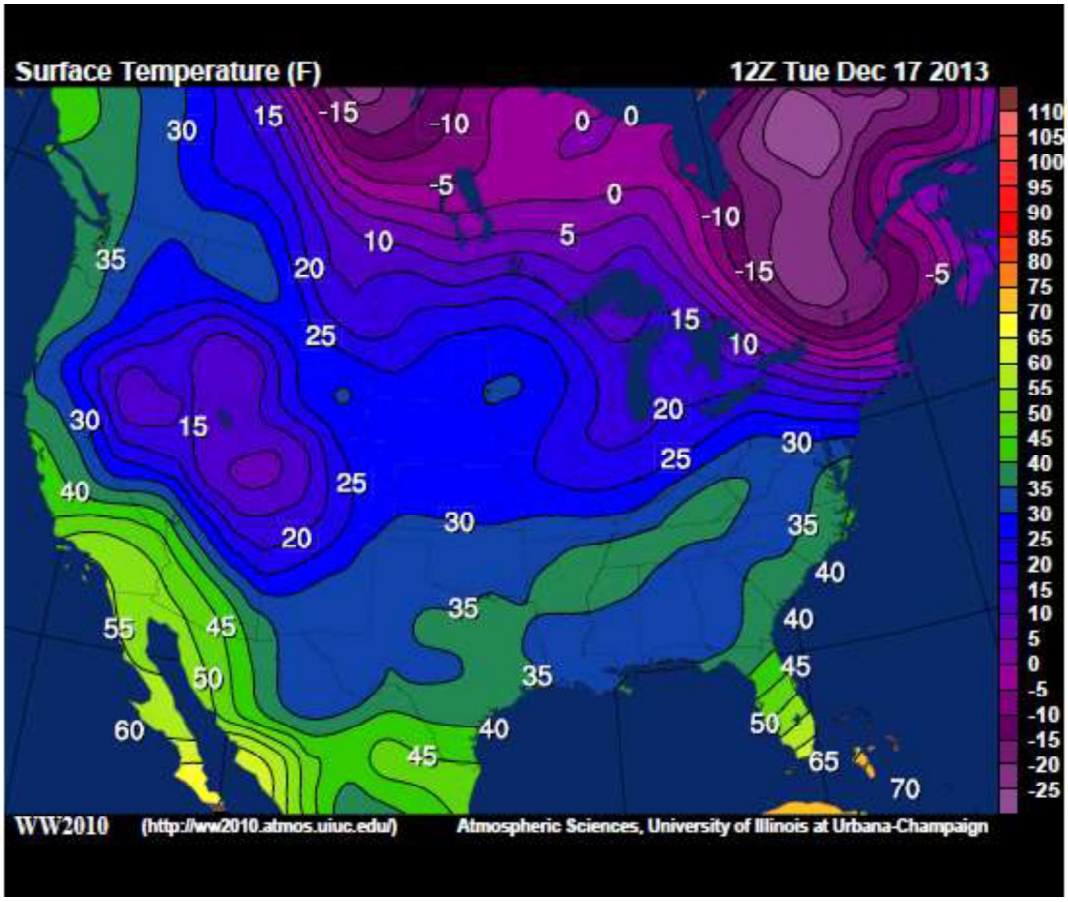

Figure 3.4: Surface temperature map of the continental U.S. on 17 December 2013 at 12Z

A surface temperature map of the continental United States is given in Figure 3.4. The discussion on the kinematics of the pressure field is also valid for other scalar fields such as the temperature field and the moisture field. A line of constant temperature is called an **isotherm** and an **isallotherm** is a line of constant temperature tendency. There is some additional terminology often used to describe features in the temperature and moisture fields. A ridge in the temperature field is sometimes called a **warm tongue**. A trough in the temperature field is sometimes called a **cold tongue**. A local minimum in the temperature field is sometimes referred to as a **cold pool**.

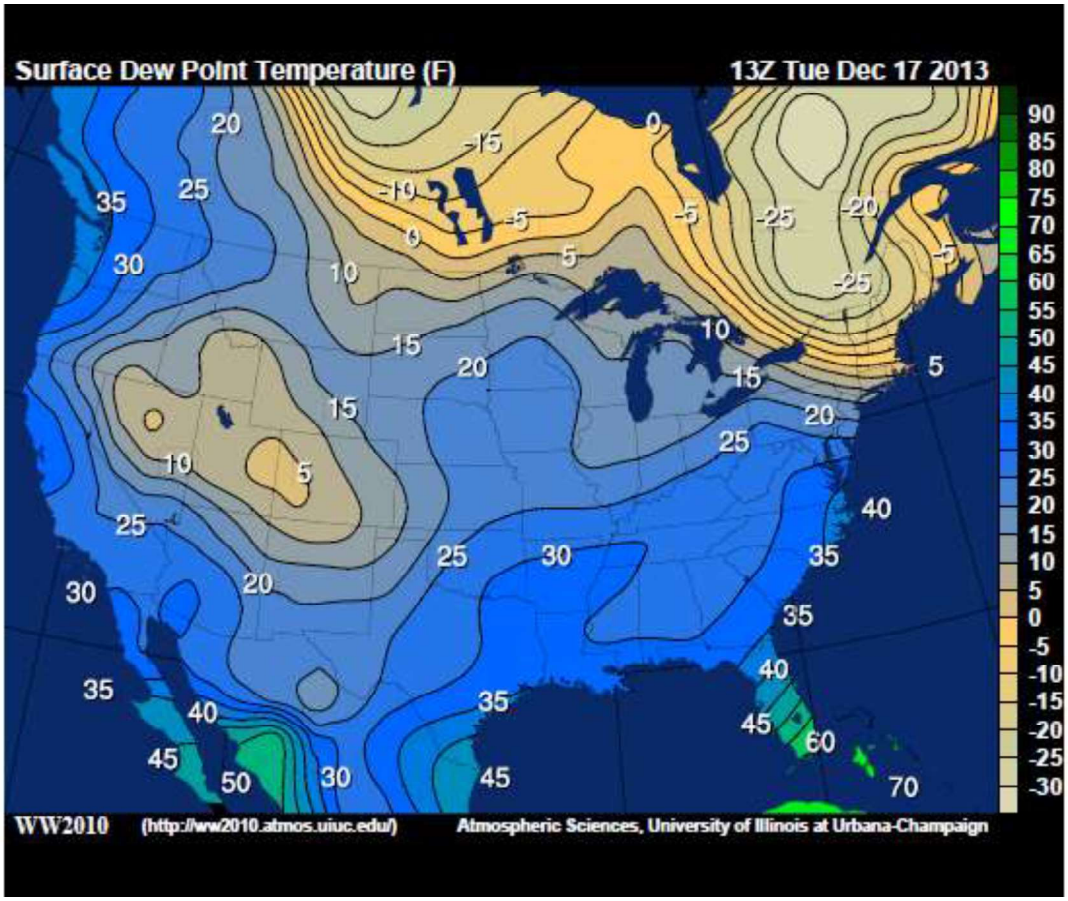

Figure 3.5 Surface dewpoint of the continental U.S. on 17 December 2013 at 13Z

A surface dewpoint map of the continental United States is given in Figure 3.5. A line of constant humidity is called an **isohume**. A ridge in the water-vapor field is often called a **moist tongue** or **moist axis**, while a trough in the water-vapor field is sometimes called a **dry tongue** or **dry slot**.

3.2: Advection

The atmosphere is a continuously evolving medium and so the fundamental variables discussed in the previous section is ceaselessly subject to temporal changes. But what does it really mean to say "The temperature has changed in the last hour"? In the broadest sense this statement could have two meanings. It could mean that the temperature of an individual air parcel, moving past a thermometer, is changing as it migrates through space. In this case, we would be considering the change in temperature experienced while moving with a parcel of air. However, the statement could also mean that the temperature of the air parcels currently in contact with the thermometer is lower than that of air parcels that used to reside there but have since been replaced by the importation of these colder ones. In this case we would be considering

the changes in temperature as measured at a fixed geographic point. These two notions of temporal change are clearly not the same, but one might wonder if and how they are physically related. We will consider an example to illustrate this relationship.

Imagine a winter day in Madison, Wisconsin characterized by biting northwesterly winds which are importing cold arctic air southward out of central Canada. From the fixed geographical point of my back porch, the temperature drops with the passage of time. If, however, I could ride along with the flow of the air, I would likely find that the temperature does not change over the passage of time. In other words, a parcel with $T = -3°F$ passing my porch at 8 am still has $T = -3°F$ at 2 pm even though it has traveled nearly to Chicago, Illinois by that time. Therefore, the steady drop in temperature I observe at my porch is a result of the continuous importation of colder air parcels from Canada. We can write an expression for this relationship we've developed:

$$\begin{array}{c}\textit{Change with Time}\\ \textit{Following an Air}\\ \textit{Parcel}\end{array} = \begin{array}{c}\textit{Change with Time}\\ \textit{at a Fixed}\\ \textit{Location}\end{array} - \begin{array}{c}\textit{Rate of Importation}\\ \textit{of Temperature by}\\ \textit{Movement of Air}\end{array}$$

The left hand side of our expression is called the **Lagrangian rate of change** and it physically describes how the temperature of an air parcel changes during its motion. The first term on the right hand side of our expression is called the **Eulerian rate of change** and it physically describes how the temperature changes at a fixed location over time. The second term on the right hand side is called **advection** and it physically describes the rate of importation by the flow.

Advection is one of the most important processes in synoptic meteorology. Based on our above example, there are three factors that govern the magnitude of advection:

(i) magnitude of the wind speed,
(ii) the spacing of the isotherms, and
(iii) the orientation of the wind vector with respect to the isotherms.

In particular, in order to maximize the magnitude of advection, there should be a strong wind field that blows perpendicular to tightly spaced isotherms (see Figure 3.6). Conversely, no advection occurs if the winds are parallel to isotherms. These considerations suggest the following mathematical relationship for the advection of a scalar meteorological variable ψ

$$|ADV(\psi)| = |\vec{V}||\nabla\psi| \cos\theta$$

where $|\vec{V}|$ is the magnitude of the wind field (i.e. the wind speed). $\nabla\psi$ is defined as the **gradient** of the scale meterological variable ψ. Physically, $\nabla\psi$ us a vector that describes the rate of change of the function ψ, i.e., $\nabla\psi$ is the derivative of variable ψ. Mathematically, the direction

of $\nabla\psi$ points in the direction of maximum increase of ψ and the magnitude of $\nabla\psi$ gives the slope of ψ in the direction of maximum increase.

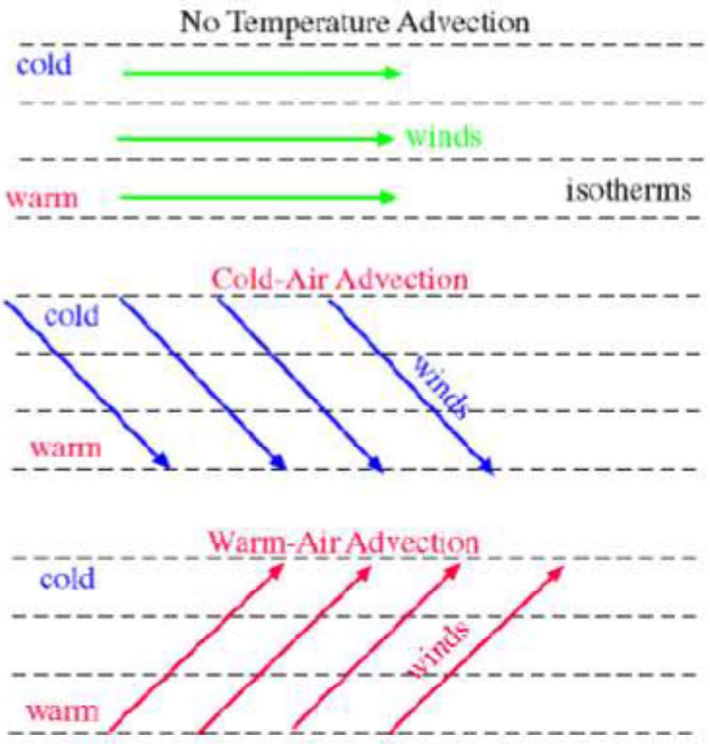

Figure 3.6 Schematic diagram of warm and cold advection

Consider the schematic diagram of warm and cold advection shown in Figure 3.6. Since the gradient vector points ***towards*** higher values of temperatures, this implies that ∇T points in the northerly direction. Moreover, note that ∇T always points perpendicular to isotherms. This is a general property of gradient vector and thus, it will apply to the gradient of any scalar variable. In the case of no temperature advection, $\vec{V}$ points perpendicular to ∇T. In the case of cold (warm) advection, $\vec{V}$ points in the same (opposite) direction as ∇T. Physically, this states that cold (warm) advection involves the transport of air parcel across cold (warm) isotherms to warm (cold) isotherms.

The above discussion can be generalized to discuss the advection of any scalar quantity. When the scalar quantity represents temperature, a positive (negative) value of advection is called **warm advection** (**cold advection**). When the scalar quantity represents water vapor, a positive (negative) value of advection is termed **moisture advection** (**dry advection**).

**3.2.1: Mathematical Derivation of Advection

The relationship between the Lagrangian rate of change and Eulerian rate of change can be made mathematically rigorous. Doing so will assist us later in the development of the equations of motion that govern the mid-latitude atmosphere. Let's consider an arbitrary scalar (or vector) quantity that we will call Q. If Q is a function of space and time, then $Q = Q(x, y, z, t)$. From differential calculus, the total differential of Q is given by

$$dQ = \left(\frac{\partial Q}{\partial x}\right)_{y,z,t} dx + \left(\frac{\partial Q}{\partial y}\right)_{x,z,t} dy + \left(\frac{\partial Q}{\partial z}\right)_{x,y,t} dz + \left(\frac{\partial Q}{\partial t}\right)_{x,y,z} dt$$

where the subscripts refer to the independent variables that are held constant while taking the indicated partial derivatives. Dividing both sides by dt, the total differential of t which represents a time increment, the resulting expression is

$$\frac{dQ}{dt} = \left(\frac{\partial Q}{\partial x}\right)_{y,z,t} \frac{dx}{dt} + \left(\frac{\partial Q}{\partial y}\right)_{x,z,t} \frac{dy}{dt} + \left(\frac{\partial Q}{\partial z}\right)_{x,y,t} \frac{dz}{dt} + \left(\frac{\partial Q}{\partial t}\right)_{x,y,z} \frac{dt}{dt}$$

The rates of change of $x, y, or\ z$ with respect to time are simply the components of the velocity vectors. Let's define these components as $u = dx/dt$, $v = dy/dt$, and $w = dz/dt$, respectively. Substituting these expressions gives

$$\frac{dQ}{dt} = \left(\frac{\partial Q}{\partial t}\right)_{x,y,z} + u\left(\frac{\partial Q}{\partial x}\right)_{y,z,t} + v\left(\frac{\partial Q}{\partial y}\right)_{x,z,t} + w\left(\frac{\partial Q}{\partial z}\right)_{x,y,t}$$

This can be written in vector notation as

$$\frac{dQ}{dt} = \left(\frac{\partial Q}{\partial t}\right) + \vec{V} \cdot \nabla Q \Rightarrow \left(\frac{\partial Q}{\partial t}\right) = \frac{dQ}{dt} - \vec{V} \cdot \nabla Q$$

We see that dQ/dt corresponds to the Lagrangian rate of change, $\partial Q/\partial t$ corresponds to the Eulerian rate of change, and the rate of importation by the flow is represented by $-\vec{V} \cdot \nabla Q$. Thus, $-\vec{V} \cdot \nabla Q$ will be referred to as advection of Q. The minus sign indicates that advection is considered positive when the rate of import in directed from positive values of Q to negative values of Q. Thus, the Eulerian (fixed location) change is equal to the sum of the Lagrangian (parcel following) change and advection.

In the previous example, we imagined a temperature drop at my back porch. We also surmised that the temperature of individual air parcels did not undergo any change as the day wore on. Thus, the advective change at the porch must be negative – there must be negative

temperature, or cold air advection (i.e. $-\vec{V} \cdot \nabla Q < 0$), occurring in Madison on this day. Clearly, the situation of northwesterly winds importing cold air southward out of Canada fits the bill.

3.3: Overview of Atmospheric Thermodynamics

The relationships between the scalar meteorological variables that we discussed previously are part of the general field of physics known as thermodynamics. **Thermodynamics** is a branch of physics concerned with heat and temperature and their relation to energy and work. A quantitative description of thermal phenomena requires a careful definition of such important terms as *temperature, heat, and internal energy*. Moreover, thermodynamics states that the behavior of these variables is subject to general constraints that are common to all materials and these constraints are expressed in the laws of thermodynamics. In this section, we will discuss the properties of these variables that are most relevant to synoptic meteorology

3.3.1: Macroscopic Description of Moist Air

Here, we examine the properties of a gas of mass *m* confined to a container of volume V at a pressure P and a temperature T. It is useful to know how these quantities are related. In general, the equation that interrelates these quantities, called *the equation of state*, is very complicated. However, if the gas is maintained at a low density, the equation of state is quite simple and can be found experimentally. Such a low-density gas is commonly referred to as an *ideal gas.* In our atmosphere, air matches the description of an ideal gas. For our purposes, we can separate air into two basic components: dry air components (such as nitrogen, oxygen, etc.) and water vapor. The equation of state for the dry air component can be written as

$$P_d = \rho_d R_d T$$

where P_d is the pressure associated with dry air, ρ_d is the density of dry air, and $R_d = 287\, J\, K^{-1}\, kg^{-1}$ is known as the dry air constant. The equation of state for water vapor can be written as

$$e = \rho_v R_v T$$

where e is the pressure associated with water vapor (also known as **vapor pressure**), ρ_v is the density of water vapor, and $R_v = 461\, J\, K^{-1}\, kg^{-1}$ is water vapor gas constant.

It's important to note that $R_d < R_m \Rightarrow \rho_v < \rho_d$, which leads to common observational fact that moist air is less dense than dry air (assuming that the temperature is the same). This also means that the amount of water vapor in the air affects the density of air within the atmosphere.

How can we write the equation of state for moist air? This can be derived by noting that the density of moist air can be written as

$$\rho = \rho_d + \rho_v = \frac{P_d}{R_d T} + \frac{e}{R_v T} = \frac{P_d}{R_d T} + \frac{e}{R_d \left(\frac{R_v}{R_d}\right) T}$$

Now, the total pressure exerted by moist air is $P = P_d + e$. Substituting this into the above equation gives

$$\rho = \frac{P - e}{R_d T} + \frac{e}{R_d \left(\frac{R_v}{R_d}\right) T} = \frac{P}{R_d T} - \frac{e}{R_d T} + \frac{e}{R_d \left(\frac{R_v}{R_d}\right) T} = \frac{P}{R_d T}\left[1 - \frac{e}{P} + \frac{e\left(\frac{R_d}{R_v}\right)}{P}\right]$$
$$= \frac{P}{R_d T}\left[1 - \frac{e}{P}\left(1 - \frac{R_d}{R_v}\right)\right]$$

Rearranging this expression gives

$$P = \rho R_d T \left[\frac{1}{1 - \frac{e}{P}\left(1 - \frac{R_d}{R_v}\right)}\right]$$

The term in the bracket is a correction term that accounts for the amount of water vapor in the air. Now, we can define a new variable known as the **virtual temperature T_v**, which is given by

$$T_v = T\left[1 - \frac{e}{P}\left(1 - \frac{R_d}{R_v}\right)\right]^{-1}$$

Thus, the equation of state for moist air can be written as $P = \rho R_d T_v$.

Virtual temperature T_v is an expression of temperature that takes into account the density of water vapor. Water vapor is over a third less dense than dry air, so adding it to dry air reduces its density. Virtual temperature is simply the temperature of a hypothetical mass of dry air whose density equals that of the sample containing water vapor. It can be shown that the virtual temperature can be approximated with the formula is $T_v \approx T + q/6$, where T is measured in degrees Celsius or Kelvin and q is the water vapor mixing ratio. It can be seen that by increasing the moisture, T_v will be as much as several degrees higher than the ambient air temperature. This increases the buoyancy of air.

Another common variable used to describe moist air is the **dewpoint temperature**. Dewpoint temperature T_d is the temperature at which saturation will occur if the air is cooled, omitting any change in pressure. When this point is reached, water vapor will condense, which leads to clouds and precipitation in the atmosphere. Dewpoint temperature is proportional to the amount of water vapor in the air, so it makes a good indicator of absolute (actual) moisture.

Since the dewpoint temperature is usually compared to the actual air temperature, another variable used to provide a measure of moisture is **dewpoint depression.** Dewpoint depression T_{dd} is simply the difference between the actual air temperature and the dewpoint temperature, $T_{dd} = T - T_d$. The lower the value, the closer the air is to saturation and the higher the relative humidity. A dewpoint depression of less than 5°C at a given level in the atmosphere is considered to be suitable for the formation of clouds.

3.3.2: Kinetic Theory of Gases

In the previous subsection, we discussed the properties of an ideal gas using macroscopic, measurable variables such as pressure, volume, and temperature. We shall now show that such large-scale properties can be described on a microscopic scale. This theory will provide us with a physical basis for our understanding of the concept of temperature.

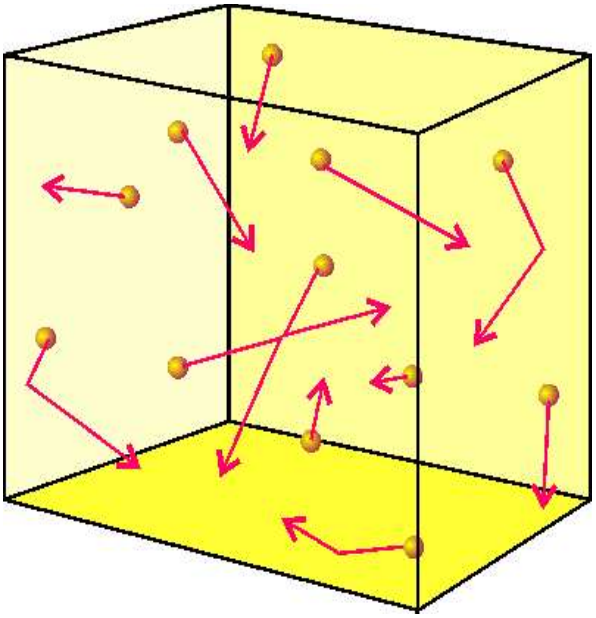

Figure 3.7 Schematic of gas contained with a container

Just as before, we examine the properties of a gas of mass m confined to a container of volume V at a pressure P and a temperature T. For the properties of air in our atmosphere, we can also add the following additional assumptions:

- All molecules in the gas are identical. This means that gas under consideration is a pure substance, rather than a heterogeneous mixture.
- The molecules interact only through short-range forces during elastic collisions. This means that, in the collisions, both kinetic energy and momentum are constant.
- The molecules obey Newton's laws of motion

- The number of molecules in the gas is large and the average separation between molecules is larger compared with their dimensions. This means that the volume of the molecules is negligible compared with the volume of the container.

Consider a one-dimensional gas in a one-dimensional box of length L. The change in momentum after the molecule collides with the wall is

$$\Delta p_x = 2mv_x$$

Since the molecule must travel a distance 2L before returning to the same wall, the rate at which the molecules imparts momentum to the wall is given by Newton's 2nd law:

$$F_{mol} = \frac{\Delta p}{\Delta t} = \frac{2mv_x}{2L/v_x} = \frac{m{v_x}^2}{L}$$

If there are N molecules in the box, then the average force on the wall is

$$\langle F \rangle = \frac{Nm\langle {v_x}^2 \rangle}{L}$$

The pressure on the wall is given by

$$P = \frac{\langle F \rangle}{A} = \frac{Nm\langle {v_x}^2 \rangle}{LA} \Rightarrow PV = Nm\langle {v_x}^2 \rangle$$

Since the molecules are equally probable to move in all three directions of space, then we have

$$PV = \frac{1}{3}Nm\langle v^2 \rangle \Rightarrow P = \frac{2}{3}\left(\frac{N}{V}\right)\left(\frac{1}{2}m\langle v^2 \rangle\right) = \frac{2}{3}\left(\frac{N}{V}\right)\langle KE \rangle$$

This result indicates that **the pressure is proportional to the number of molecules per unit volume and the average kinetic energy of the molecules**. Since pressure is proportional to temperature, this means that **temperature is a direct measure of the average molecular kinetic energy of the gas.** Therefore, according to the kinetic theory of gases, temperature is an expression of the amount of kinetic energy in the molecules of a substance. In meteorology, this manifests itself as heat.

3.3.3: The First Law of Thermodynamics

One of the fundamental laws of physics is the conservation of energy, which asserts that the total energy of the universe remains constant. This principle can be applied to examine macroscopic systems in the atmosphere. The first law of thermodynamics is essentially a law of conservation of energy for macroscopic systems. Conservation can be imposed by requiring that the variation of the total energy of the system and its environment is identically zero. However, in order to make this precise, one should be able to say what exactly the energy of a macroscopic system is in the first place.

At the outset, it is important that we make a major distinction between internal energy and heat. Internal energy is all the energy of a system that is associated with its microscopic components (i.e. atoms and molecules). Thus, the internal energy includes translational kinetic energy, rotational kinetic energy of the molecules, the potential energy within molecules, and the potential energy between the molecules. Heat is defined as the *transfer* of energy across the boundary of a system due to temperature differences between the system and its surroundings. When you *heat* a substance, you are transferring energy into it by placing it in contact with surroundings that have a higher temperature.

The first law of thermodynamics says that a change in internal energy is due to

- **Heat Q**: Energy flow between a system and its environment due to a temperature gradient across a boundary and a finite thermal conductivity of the boundary and/or;
- **Work W**: Mechanical energy (and any other kind of energy) transfer across the boundary.

This indicates that work and heat are both defined to describe energy transfer across a system boundary. This law can be written mathematically as

$$dU = dQ + dW$$

where dU is the differential change in internal energy, dQ is the transfer of energy via heat, and dW is the differential work done on the system.

In the atmosphere, the system is usually specified as an air parcel (which is an infinitesimal amount of air) and the environment is the environmental air surrounding the air parcel. If some external forces are acting upon the air by virtue of its interaction with the environment then there will be a change in the internal energy. If the system is an open system, then energy will be exchanged between the system and the environment in the form of heat. This implies that the change in internal energy should be equal to the work done on the system plus the heat added into the system. For the atmosphere, the work done on the system primarily occurs due to change in the volume of the air parcel. In particular, energy *enters* the air parcel

when work is done to compress the air parcel. Thus, the work can be calculate by using the common definition of work

$$dW = F\,dr = (PA)\,dr = -P\,dV$$

where the minus sign indicates that compression of the parcel increases the parcel's energy. Therefore, the first law can be written as

$$dU = dQ - P\,dV$$

Increases in internal energy in the form of molecular motions are manifested as increases in temperature. This was experimentally verified by English physicist James Joule (1818-1889). Joule showed following a series of lab experiments that when a gas expands into a vaccum without doing external work ($dW = 0$) and without taking in or giving out heat ($dQ = 0$), that the temperature of the gas does not change. By the first law of thermodynamics, $dW = 0$ and $dQ = 0$ implies that $dU = 0$. This implies that the internal energy of a gas is a function of temperature only (i.e. independent of its volume when the temperature is held constant).

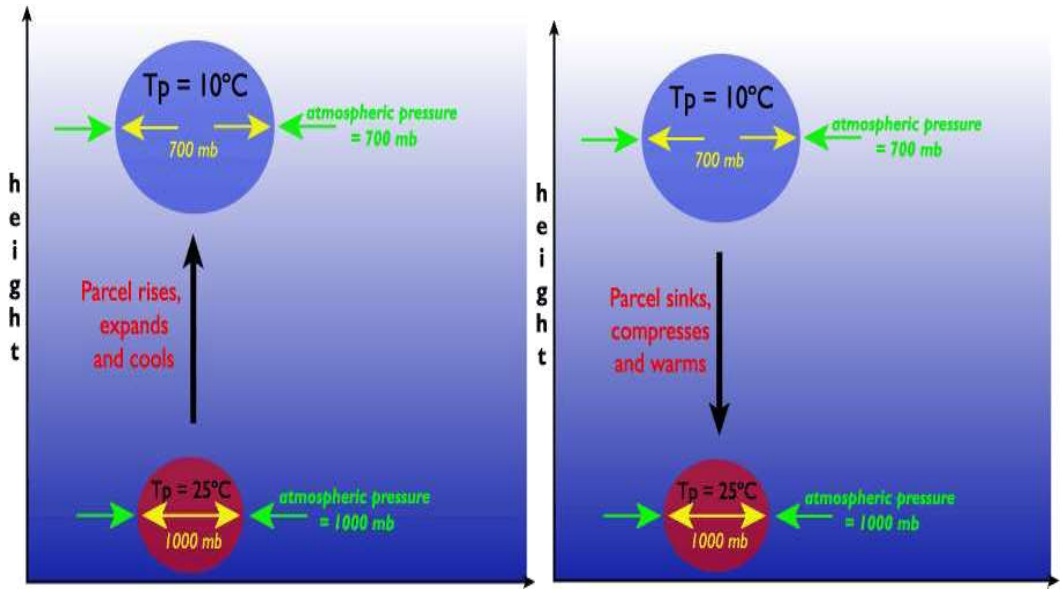

Figure 3.8 (Left) Schematic of a rising air parcel. (Right) Schematic of a sinking air parcel.

The first law can be used to explain why rising air tends to cool whereas sinking air tends to warm. Suppose that we have a rising air parcel that is insulated from its environment such that no heat is added or taken away from the parcel. This is known as an adiabatic process. As the air parcel rises, it enters into regions of lower pressure. This causes the air parcel to expand since the lower pressure outside allows the air molecules to push out on the parcel walls. This means that air parcels is doing work on the environment at the expense of its own internal energy. Therefore, the parcel will cool as it rises. Conversely, a sinking parcel compresses since it is

moving into a region of higher pressure. Due to the parcel compression, the air molecules (which compose the air parcel) gains internal energy and thus, the parcel will warm.

3.3.4: Potential Temperature

Many atmospheric processes are close to adiabatic so it is useful to have a physical parameter that can be used as a tracer under adiabatic conditions. This variable is known as the potential temperature and it is given by

$$\theta = T\left(\frac{P_0}{P}\right)^{R_d/c_p}$$

where T is the current temperature (in Kelvin), R_d is the dry air gas constant, and c_p is the specific heat at constant pressure (which is defined as the amount of heat required to raise the temperature of a 1 kg system by 1 degree Kelvin). The specific heat varies depending upon the system in question, but for air, the specific heat at constant pressure is experimentally verified to be $1004\,J\,kg^{-1}\,K^{-1}$. The **potential temperature** of a parcel of fluid at pressure P is the temperature that the parcel would acquire if adiabatically brought to a standard reference pressure P_0, usually 1000 millibars.

What is the use of potential temperature? Potential temperature can be used to compare the temperature of air parcels that are at different levels in the troposphere. As we have previously seen, temperature tends to decrease with height. This fact makes it more difficult to note which regions in the troposphere are experiencing warm air advection and cold air advection. Therefore, bringing air parcels adiabatically to a standard level (1000 millibars) allows comparisons to be made between air parcels at different elevations, similar to the idea of reduced sea-level pressure measurements. If the potential temperature of an air parcel at one pressure level is colder than air parcels at other pressure levels, a forecaster can infer cold air advection or a cold pocket exists at the pressure level with the lowest potential temperature.

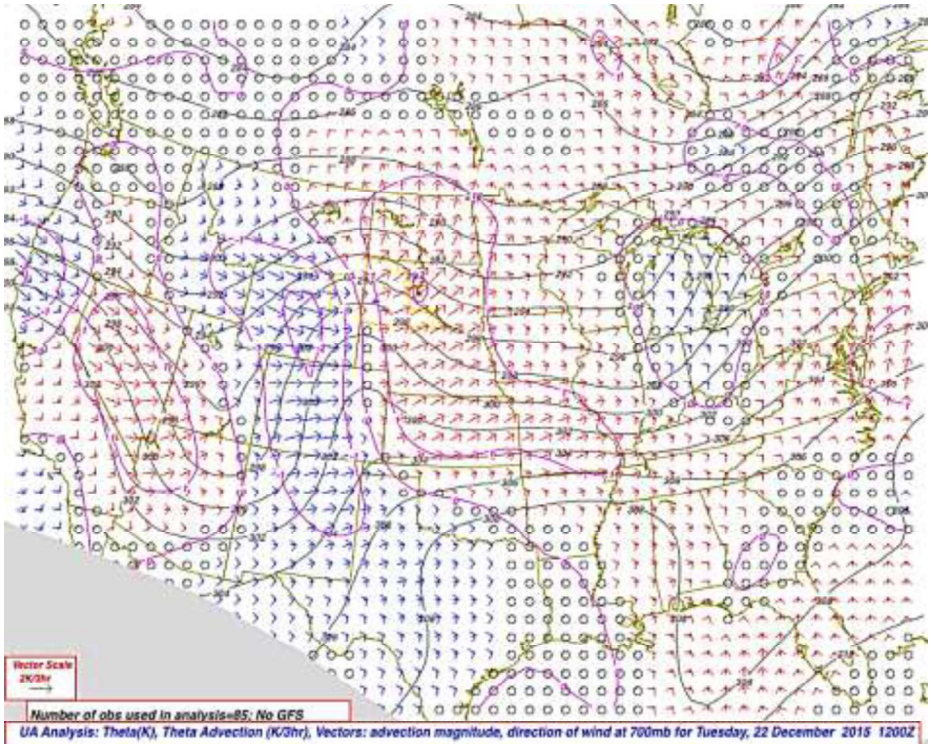

Figure 3.9 700-mb θ map of the continental US at 22 December 2015 at 1200 Z

Finding the potential temperature at a constant pressure level over an area produces one type of θ-chart, in which higher (lower) θ represents warmer (cooler) air. For example, θ can be found at 700 mb, as shown in Figure 3.9. Each location at 700 mb drops a parcel from the 700 to 1000 mb level and the temperature is read off at 1000 mb and thus, this is the 700 mb θ (θ is always given in degrees Kelvin).

A vertical cross section of θ can be produced by finding the areal distribution of θ at many pressure levels, then connecting the points of equal θ. At this point, sloping constant θ surfaces can be plotted. Air parcels tend to travel along constant Theta surfaces. This makes sense because constant θ surfaces represent "constant density" surfaces. The path of least resistance on an air parcel that is advecting is for it to remain at the same density as its environment. The term that describes this process is isentropic lifting / descent. Isentropic lifting (descent) occurs whenever warm air advection (cold air advection) or flow of one air mass over another occurs. Less dense air will tend to glide up and over more dense air (thus low level warm air advection leads to rising air) when less dense air advects toward more dense air.

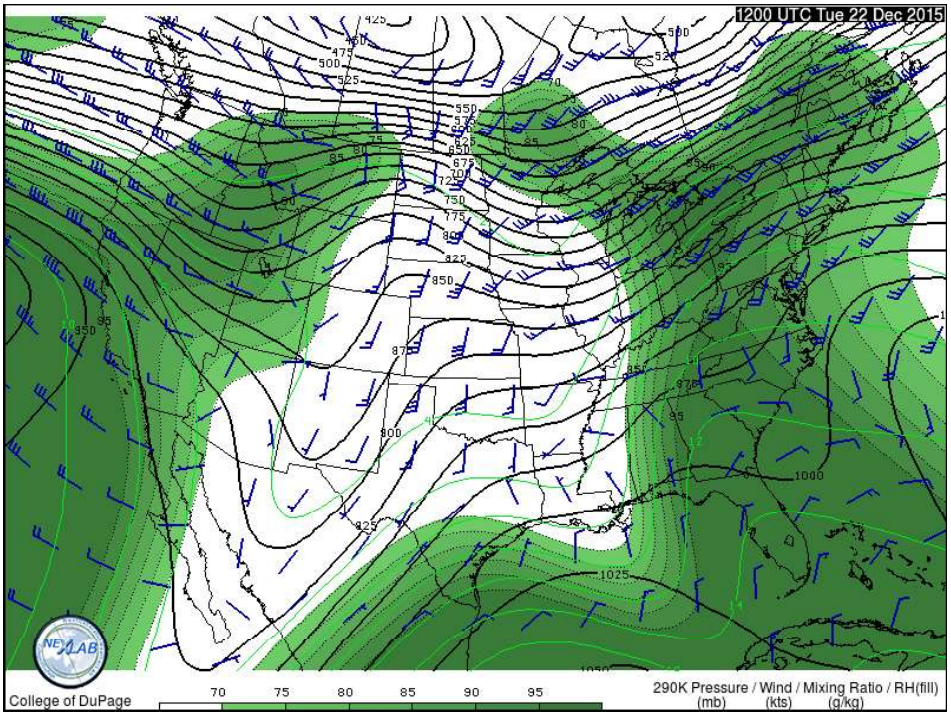

Figure 3.10 290 K isentropic surface map of the continental US at 22 December 2015 at 1200 Z

You will hear isentropic (i.e. constant θ) lifting referenced to often in forecast discussions. The trajectories that wind vectors take over isentropic surfaces determine how much lifting or sinking will take place due to advection. NWS forecasters are experts on these processes and use them as a major part of their forecasting process. The different ways of graphing θ can be quite complex, but the key points to remember are that: (1) air parcels in a convectively stable environment tend to advect along constant θ surfaces and (2) low level warm air advection produces isentropic lifting and uplift while cold air advection produces isentropic downglide and sinking.

While potential temperature can be used to compare temperatures at different elevations and the trajectory air parcels will take (rising or sinking), equivalent potential temperature can be used to compare BOTH moisture content and temperature of the air. The equivalent potential temperature θ_e is found by lowering an air parcel to the 1000 mb level AND releasing the latent heat in the parcel. The lifting of a parcel from its original pressure level to the upper levels of the troposphere will release the latent heat of condensation and freezing in that parcel. The more moisture the parcel contains the more latent heat that can be released. θ_e is used operationally to map out which regions have the most unstable and thus positively buoyant air. The θ_e of an air parcel increases with increasing temperature and increasing moisture content. Therefore, in a region with adequate instability, areas of relatively high θ_e (called $\boldsymbol{\theta_e}$ **ridges**) are often the burst

points for thermodynamically induced thunderstorms and MCS's. θ_e ridges can often be found in those areas experiencing the greatest warm air advection and moisture advection.

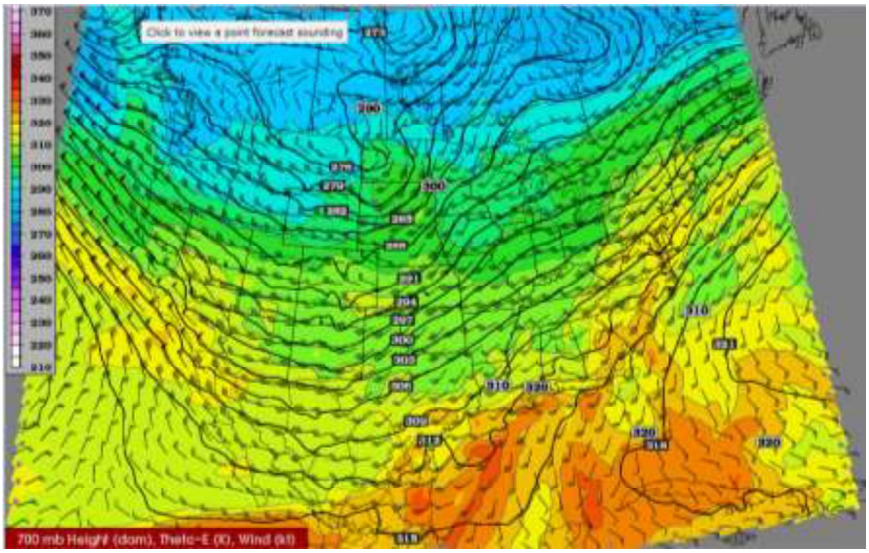

Figure 3.11 700-mb θ_e map of the continental US at 22 December 2015 at 1200 Z

3.4: Kinematics of the Wind Field

As can be readily discerned from inspection of any satellite animation or clouds or water vapor, the wind field varies zonally and meridionally. Even though it appears that there are an innumerable number of wind field patterns within the atmosphere at any given point in time, it turns out that the horizontal wind field can be decomposed into four types of flow patterns: **translation, divergence, vorticity, and deformation**. We will examine each type of flow pattern below.

**3.4.1: Derivation of Flow Patterns

The physical properties of the horizontal wind field can be described by considering the Taylor-series expansion of the wind field about the point (x_0, y_0). We will consider what happens to air parcels only near the origin so that higher-order nonlinear terms can be neglected. Therefore, we have

$$u(x,y) = u_0 + \left(\frac{\partial u}{\partial x}\right)_0 x + \left(\frac{\partial u}{\partial y}\right)_0 y + O(2),$$

$$v(x,y) = v_0 + \left(\frac{\partial v}{\partial x}\right)_0 x + \left(\frac{\partial v}{\partial y}\right)_0 y + O(2),$$

Through algebraic manipulations, we have

$$u(x,y) = u_0 + \frac{1}{2}\left[\left(\frac{\partial u}{\partial x}\right) - \left(\frac{\partial v}{\partial y}\right) + \left(\frac{\partial v}{\partial y}\right) + \left(\frac{\partial u}{\partial x}\right)\right]_0 x + \frac{1}{2}\left[\left(\frac{\partial u}{\partial y}\right) - \left(\frac{\partial v}{\partial x}\right) + \left(\frac{\partial v}{\partial x}\right) + \left(\frac{\partial u}{\partial y}\right)\right]_0 y + O(2),$$

$$v(x,y) = v_0 + \frac{1}{2}\left[\left(\frac{\partial v}{\partial x}\right) - \left(\frac{\partial u}{\partial y}\right) + \left(\frac{\partial u}{\partial y}\right) + \left(\frac{\partial v}{\partial x}\right)\right]_0 x + \frac{1}{2}\left[\left(\frac{\partial v}{\partial y}\right) - \left(\frac{\partial u}{\partial x}\right) + \left(\frac{\partial u}{\partial x}\right) + \left(\frac{\partial v}{\partial y}\right)\right]_0 y + O(2),$$

Defining

$$D = \left(\frac{\partial u}{\partial x}\right) + \left(\frac{\partial v}{\partial y}\right), \qquad \zeta = \left(\frac{\partial v}{\partial x}\right) - \left(\frac{\partial u}{\partial y}\right), \qquad F_1 = \left(\frac{\partial u}{\partial x}\right) - \left(\frac{\partial v}{\partial y}\right), \qquad F_2 = \left(\frac{\partial u}{\partial y}\right) + \left(\frac{\partial v}{\partial x}\right)$$

We have

$$u(x,y) = u_0 + \frac{1}{2}(D + F_1)x - \frac{1}{2}(\zeta - F_2)y,$$

$$v(x,y) = v_0 + \frac{1}{2}(\zeta + F_2)x - \frac{1}{2}(D - F_1)y$$

This analysis indicates that the horizontal wind field can be decomposed into four types of flow patterns: translation ($u_0.v_0$), divergence (D), relative vertical vorticity (ζ), and deformation (F_1, F_2).

3.4.2: Translation

A wind field of pure **uniform translation** is given by Figure 3.12. For a field of pure translation, air parcels near the origin are translated downstream at the same rate of speed regardless of their initial location.

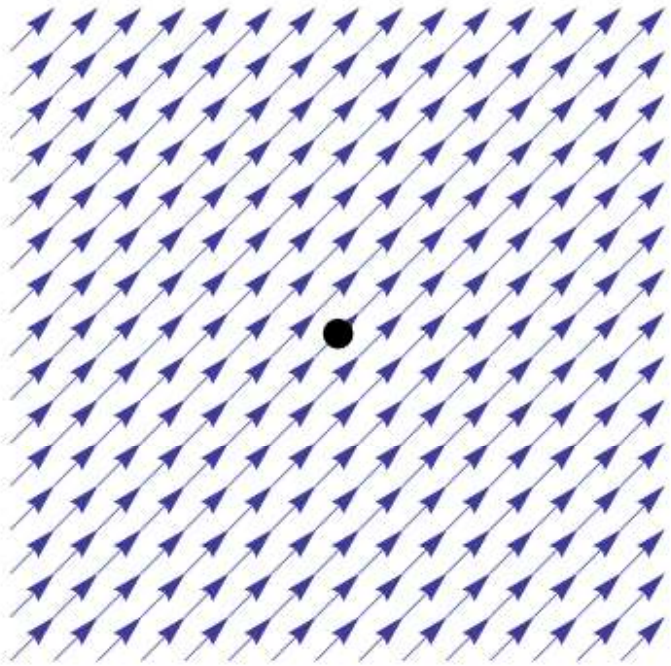

Figure 3.12: The effects of uniform translation on a fluid element

3.4.3: Divergence

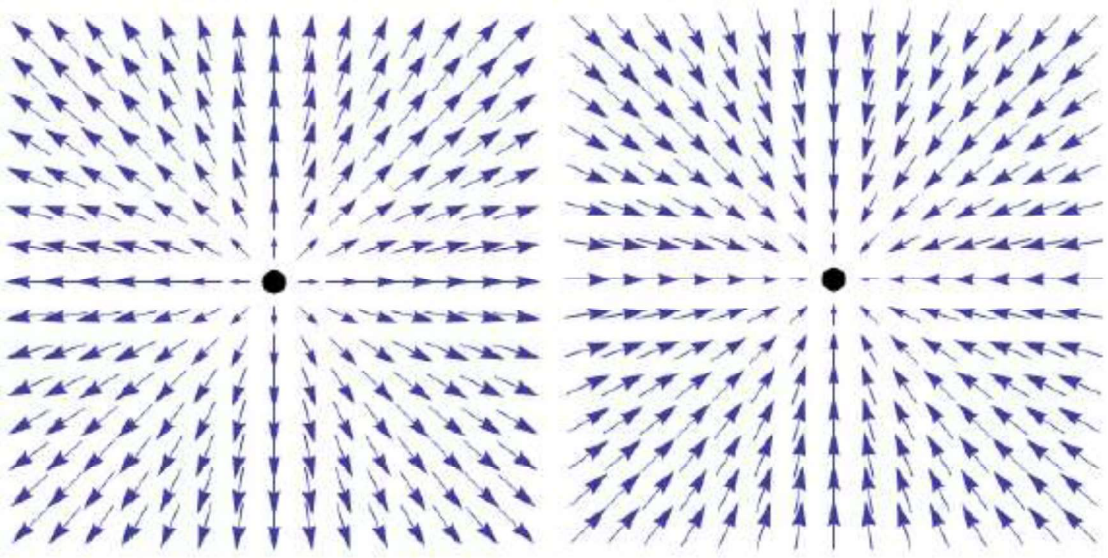

Figure 3.13 (Left) A field of positive divergence. (Right) A field of negative divergence (i.e. convergence)

Figure 3.13 illustrates the wind field of pure divergence. The divergence provides us with a measure of how much the vector wind field is "spreading out" at each point. For a field of pure divergence, the area of air parcels is expanded as the fluid moves in all directions away from the origin. If the direction of the vector field is reversed, we obtain a wind field of pure convergence as the fluid moves in all directions towards the center. For a field of pure convergence, the area of air parcels is contracted independent of direction.

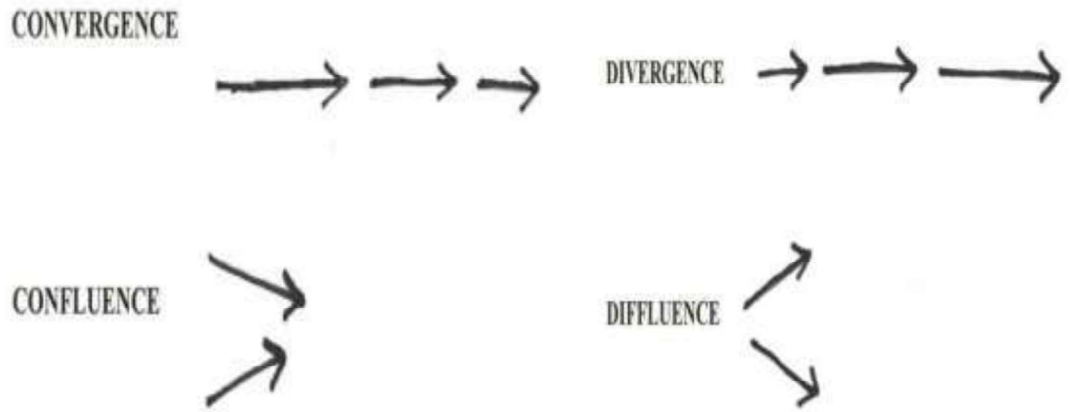

Figure 3.14 Schematic of convergence, divergence, confluence, and diffluence

Divergence in the wind field can be split into two components: **speed divergence** and **directional divergence**. Speed divergence is due to a change in wind speed along the direction of flow. Speed divergence is associated with a downstream increase of wind speed. Directional divergence (also called **diffluence**) is the directional spreading of the wind. The corresponding term for directional convergence is **confluence**. Diffluence (confluence) occurs when the flow spreads out (contracts) downstream (as shown in Figure 3.14). Thus, divergence is associated with a downstream increase in wind speed (i.e. stretching of air parcels) alone or with diffluence (i.e. spreading of air parcels) alone. A downstream decrease in wind speed, shrinking, coupled with diffluence may be divergent if the magnitude of the latter outweighs the former. Similarly, a downstream increase in wind speed, stretching, coupled with confluence, may be convergent if the latter outweighs the former. Observations suggest that synoptic-scale values of divergence are very small and consequently stretching is usually accompanied by confluence and shrinking is usually by diffluence. Therefore, it's not correct to associate diffluence with divergence and confluence with convergence as a general rule.

3.4.4: Vorticity

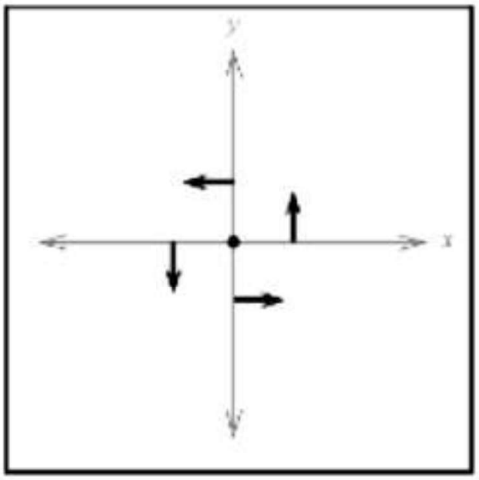

Figure 3.15 A field of pure, positive vorticity

Figure 3.15 illustrates a wind field of pure vorticity. As is shown, vorticity is associated with the local rotation of the air flow. In the Northern Hemisphere, a counterclockwise rotation of the air is associated with positive (or cyclonic) vorticity, whereas a clockwise rotation of the air is associated with negative (or anticyclonic) vorticity. Therefore, **cyclonic vorticity** is characterized by a component of rotation about the local vertical that is in the same direction as the Earth's axis of rotation, whereas **anticyclonic vorticity** is characterized by a component of rotation about the local vertical that is in the opposite direction as the Earth's axis of rotation. Since the rate of rotation is uniform (independent of direction), the area and shape of the air parcel are preserved. Vorticity is also designed as **cyclonic** and **anticyclonic**.

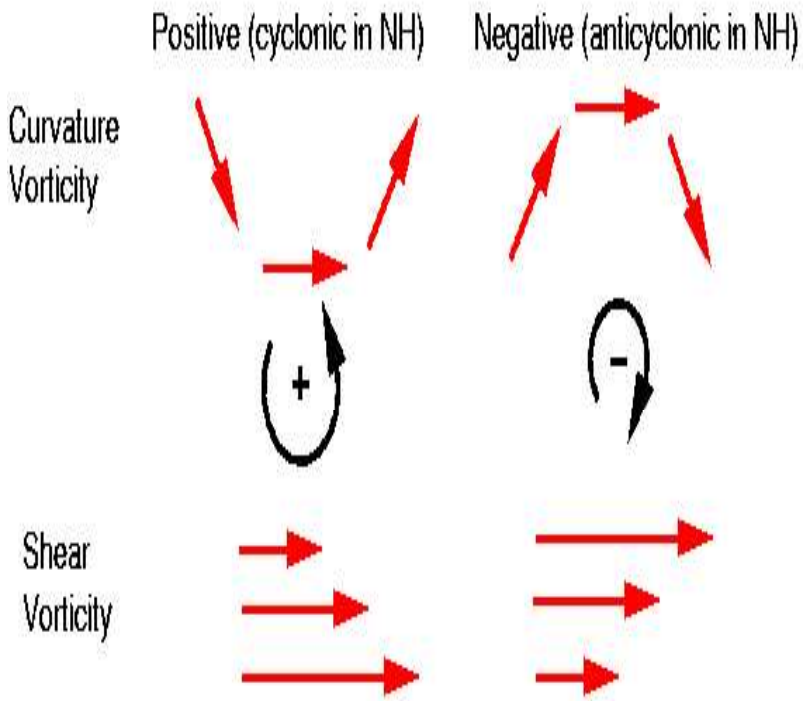

Figure 3.16 Schematic of curvature vorticity and shear vorticity in the northern hemisphere

Similar to divergence, vorticity in the wind field can be split into two components: curvature vorticity and shear vorticity (as shown in Figure 3.16). **Curvature vorticity** is associated with a change in wind direction over some horizontal distance. This change will result in either a counter-clockwise or clockwise curvature. **Shear vorticity** is associated with a change in speed over some horizontal distance. Unlike the individual contributions from each component for divergence, the individual contributions from each term for vorticity do not act in the opposite sense for synoptic-scale motions. Positive vorticity can be produced by

- Wind speed increasing when moving away from the center point of a trough or low (positive shear vorticity).
- A counterclockwise curvature in the wind flow, which occurs in troughs or lows (positive curvature vorticity).

Negative vorticity can be produced by

- Wind speed decreasing when moving away from the center point of a trough (negative shear vorticity).
- A clockwise curvature in the wind flow, which occurs in ridges or highs (negative curvature vorticity).

Cyclonic shear poleward of a trough in the westerlies enhances the cyclonic vorticity associated with curvature, while anticyclonic shear equatorward of the trough counteracts the cyclonic curvature vorticity. Similarly, cyclonic shear poleward of a ridge in the westerlies counteracts the anticyclonic vorticity associated with curvature, while anticyclonic shear equatorward of the ridges enhances the anticyclonic curvature vorticity.

3.4.5: Deformation

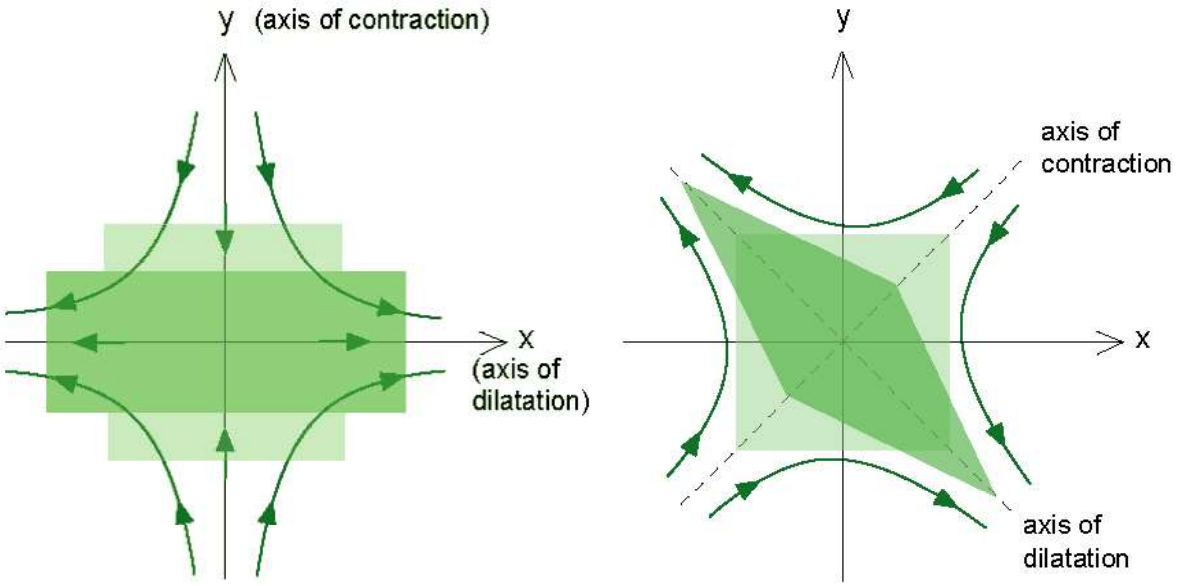

Figure 3.17 (Left) A field of pure, positive stretching deformation. (Right) A field of pure, positive shearing deformation

Figure 3.17 demonstrates a wind field of pure stretching deformation. This flow field pattern is stretched along the *x*-axis and compressed along the *y*-axis. In fact, these two axes have special names: the flow is stretched along the **axis of dilatation** while it is compressed along the **axis of contraction**.

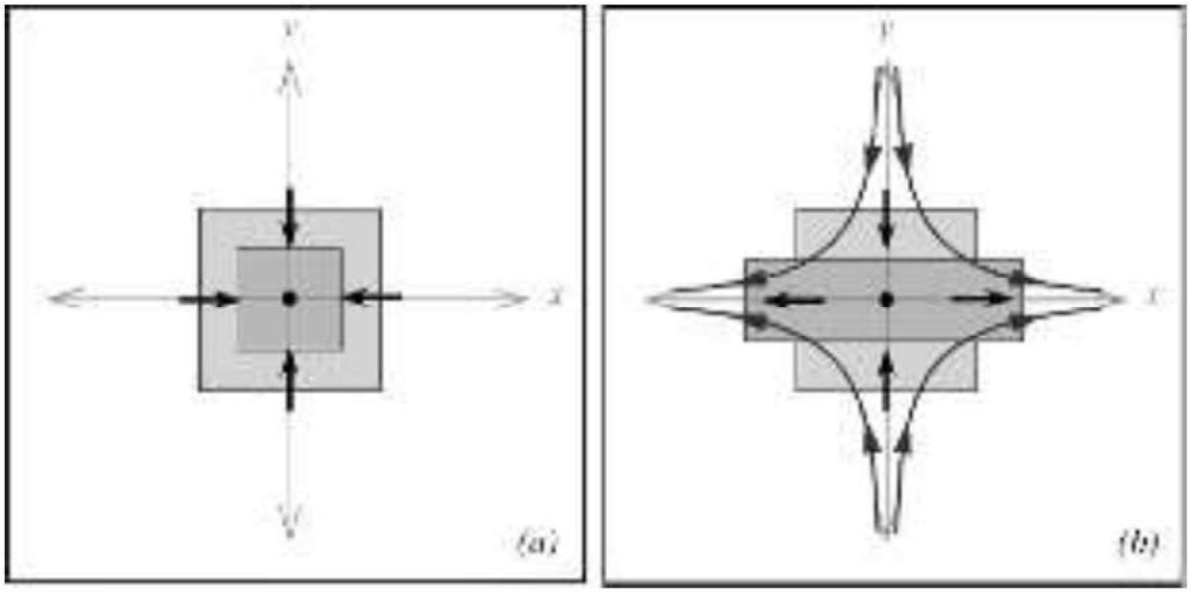

Figure 3.18 (a) A fluid element in a field of pure convergence. The lighter square represents the initially square element. Note that the area of the fluid element is decreased in a field of convergence. (b) A fluid element in a field of pure stretching deformation. The original square is deformed into a rectangle whose area is the same as that of the square

It is important to distinguish between deformation and convergence as they are commonly confused. If we consider the area of an air parcel bounded by curve C embedded within a field of pure convergence as shown in Figure 3.18, we see immediately that the area will become progressively smaller under the influence of the convergent flow. If the same fluid parcel were placed in a field of pure stretching deformation, however, the shape of the originally square air parcel would be deformed into a rectangle while preserving its area.

Figure 3.17 also demonstrates a wind field of pure shearing deformation. For a field of pure shearing deformation, the flow is similar to the stretching deformation rotated counterclockwise by 45^0. We are usually most interested in the total deformation field given by

$$F = \sqrt{{F_1}^2 + {F_2}^2}$$

Unlike divergence, deformation on the synoptic-scale is not necessarily very small. Whereas the effects of stretching and confluence/diffluence counteract each other as far as divergence is concerned, the effects of stretching and confluence/diffluence usually act in concert. As we will see in the next chapter, deformation tends to be extremely important for intensifying surface fronts.

Chapter 4: Synoptic Fronts

Inspection of satellite imagery frequently reveals long, narrow cloud bands that often correspond to frontal zones. Why do fronts matter? Whether the systematic lowering and thickening of stratiform clouds accompanying the approach of a warm front, or the formation of convective storms along a cold front, it is clear that fronts can strongly influence weather conditions. For this reason, forecasts must account for their movement, type, intensity, and influence on cloud and precipitation. Depending on the static stability of air in the vicinity of a frontal system, fronts can trigger severe, organized convective storms. The presence of enhanced vertical wind shear in frontal zones contributes to the organization and severity of convective storms that form in their vicinity. In some situations, convective storms can develop in succession along frontal boundaries, resulting in flash flooding as sequential cells move over the same areas repeatedly. Both the horizontal wind shift and vertical wind shear accompanying frontal zones have important implications for aviation forecasting, and the timing of fronts can be critical to determining the amount and type of precipitation in a given location.

To understand and predict frontal weather, we must first understand the mechanisms that lead to frontal formation and structure. We begin the chapter with a discussion of introductory thermodynamics.

4.1: Air Masses

The *Glossary of Meteorology* defines a front as the "*interface* or transition zone between two **air masses** of different **density**". This requires use of a density variable, such as potential temperature or density, to identify a front. Since fronts are defined as the boundary between two regions of contrasting air density, it's helpful to examine air masses. Air masses are traditionally classified according to the scheme developed by Tor Bergeron in 1928. This sorts air masses by moisture (continental, c; or maritime, m) and temperature (arctic, A; polar P; tropical T; or equatorial E). The air mass may be further classified according to whether it is significantly warmer or colder than the surface it is passing over. An air mass that is warmer than Earth's surface gains the suffix "w". Since it is being cooled from below, it is prone to forming a stable inversion near the surface, favoring haze and leading to stratus and fog if it has high moisture content. Likewise an air mass that is cooler than the Earth's surface has the suffix "k", which means that it is being heated from below. A "k" air mass is destabilizing, and as a result it is prone to wind gusts, low-level wind shear, and cumuliform clouds.

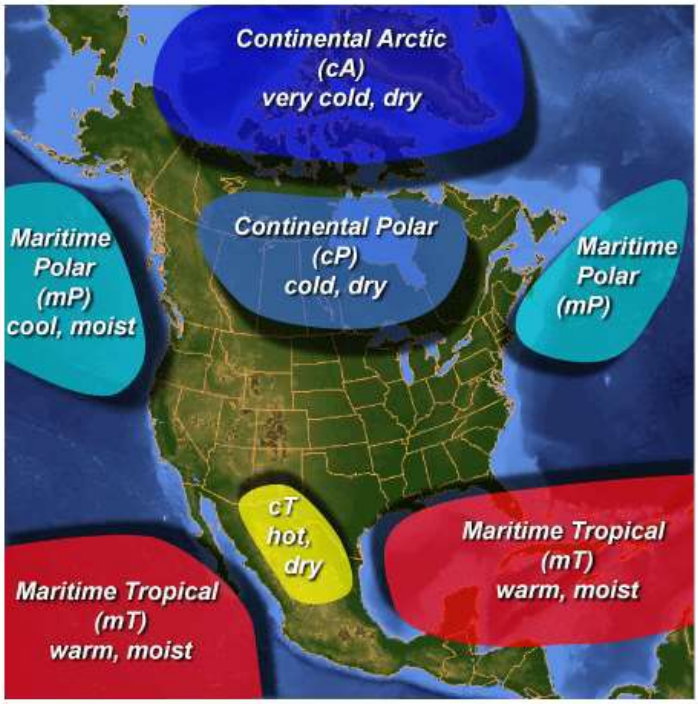

Figure 4.1 Schematic of common air masses to the continental US

Once an air mass is identified, its abbreviation may be written near the center of the mass. The abbreviation is comprised of the moisture letter, the temperature letter, and the relative temperature letter if applicable. This annotation communicates basic information about the air mass to other forecasters and end user. Again it must be remembered that these classifications are idealized air mass archetypes, and air mass may originate from other regions and have ambiguous characteristics. The primary archetypes are as follows: continental polar (cP), continental tropical (cT), maritime polar (mP), maritime tropical (mT), and arctic (A), as shown in Figure 4.1.

Continental polar (cP) air forms due to radiational cooling of air over cold or frozen terrain. Its most common source in North America is far northern Canada and the Arctic basin. In the winter, source regions can extend south into the United States if fresh snow cover blankets a large region. When cP air reaches the warm waters of the Gulf of Mexico and Atlantic, it becomes cPk and forms extensive streets of stratocumulus and cumulus clouds.

Continental tropical (cT) air is associated with strong heating of dry terrain by the sun. Its most common source region is Arizona, New Mexico, and northern Mexico, especially during the spring and summer. The most common characteristics are fair skies, warm temperatures, and low dew points. The dryline, a surface feature found in the Great Plains, is a boundary separating this type of air from maritime tropical air, and where strong westerlies carry the light buoyant air eastward above the tropical air mass it is known as an **elevated mixed layer** (EML) and forms a

capping inversion at the interface beneath. In the 1930s and 1940s, this EML was occasionally classified as an air mass type called Superior. The northern incursion of maritime air in late summer causes the onset of monsoon rains in the Desert Southwest.

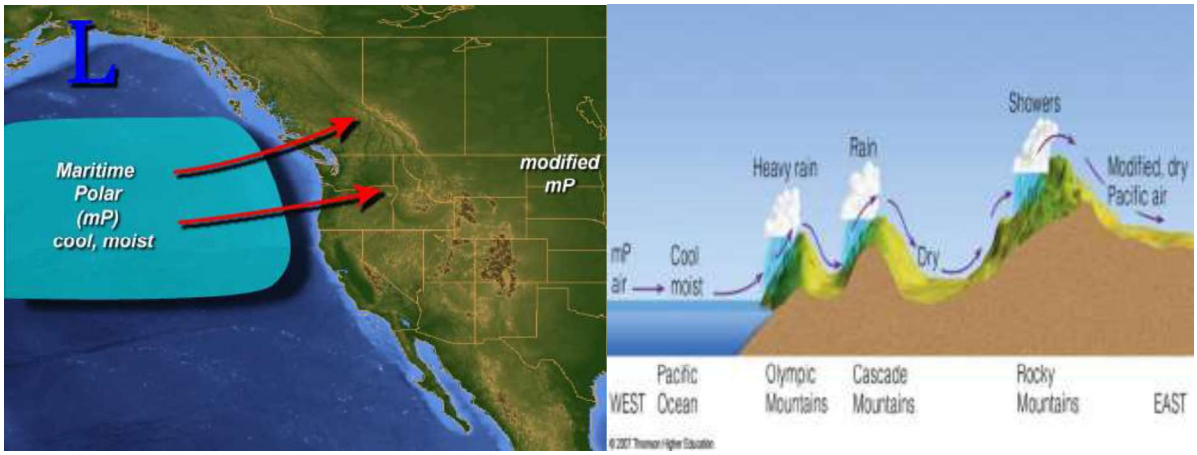

Figure 4.2 Schematic of mP air mass

Maritime polar (mP) air forms when air masses stagnate over cool ocean surfaces. It tends to originate over Asia as cP air and tends to be unstable. The temperature of an mP air mass is similar to that of the cool ocean waters it rests over, usually from 30 to 60°F. Nearly all weather systems that come ashore on the west coast of the United States usher in maritime polar air. As shown in Figure 4.2, mP air is modified by the time it reaches the interior of the US, although it is milder than cP air.

Maritime tropical (mT) air is found across all tropical oceans, and due to the high evaporation of these warm waters the air mass goins large values of dew point -- 60 to 80°F. Maritime tropical air contains abundant and rich moisture, but since the ocean absorbs most of the incoming solar energy, convective instability tends to be weak. When this air mass is advected onshore as a mTk air mass, it tends to gain considerably more heat and it destabilizes further, producing clouds and thunderstorms. Since tropical oceans cover a substantial percentage of the globe, maritime tropical air is the single most common air mass. Furthermore, the strong solar heating of land masses in the Tropics allows extensive infiltration of this air inland. Even when the air mass moves inland, evapotranspiration from damp tropical terrain and vegetation helps offset the moisture lost from storm clouds.

4.2: General Characteristics of Synoptic Fronts

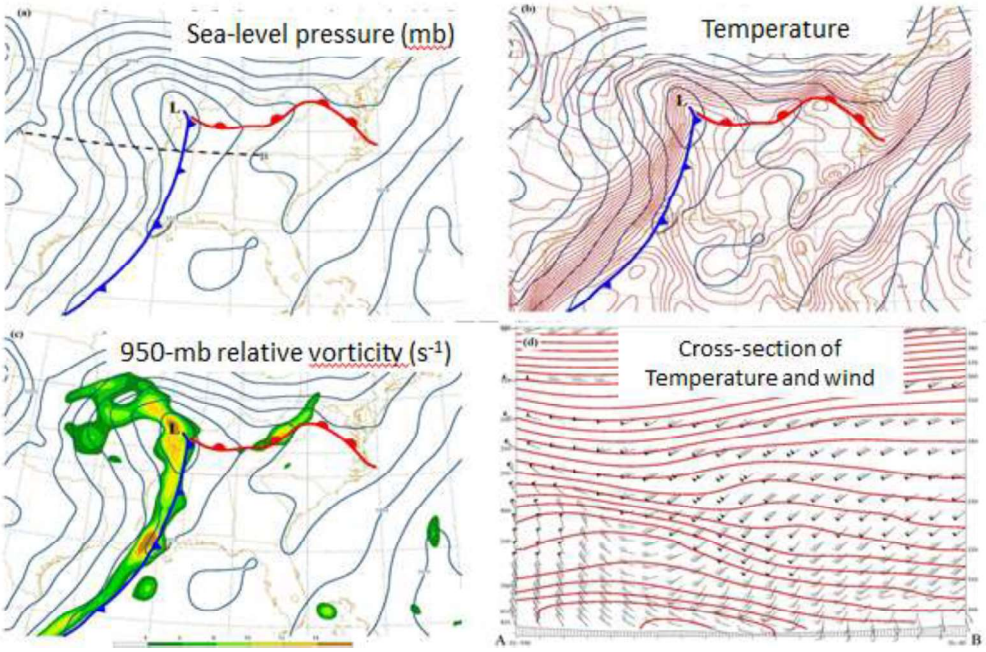

Figure 4.3 Schematic of cold and warm fronts

Since enhanced horizontal gradients of temperature associated with frontal zones are also zones of strong vertical wind shear by thermal wind balance, then strong and deep frontal zones would necessarily accompany strong upper-level winds. We will see in a future chapter that these frontal zones are accompanied with the midlatitude jet stream. Moreover, one would expect strong vertical circulations to be associated with frontal zones, as air parcels moving into or out of the frontal zone would experience a marked change in the magnitude of the horizontal temperature gradient. On a basic level, this is one reason why fronts are often associated with bands of cloud and precipitation.

Noting that frontal zones are long and narrow, we can define spatial scales characteristic of frontal zones as synoptic scale (1000 km) in the along-front direction, and one order of magnitude less than this in the cross-front direction (100 km). Therefore, the cross-front horizontal scale is therefore decidedly mesoscale. Owing to their along-front dimension, and also because these air mass boundaries were originally analyzed on early synoptic maps, we shall refer to these boundaries as **synoptic fronts** in order to distinguish them from the other air mass boundaries that are fully meridional (such as drylines, gust fronts, etc.). Observations demonstrate that fronts display the following characteristics:

- Enhanced horizontal contrasts of temperature and/or moisture
- A relative minimum of pressure (trough) and maximum of cyclonic vorticity along the front;
- Strong vertical wind shear, and horizontal wind shift consistent with a pressure trough and cyclonic vorticity;
- Large static stability within the frontal zone;
- Ascending air, clouds, and precipitation near the front (depending on moisture availability and other factors); and
- Greatest intensity near the surface, weakening with height

A synoptic front whose intensity is strongest near the ground is called a **surface front**. Surface fronts usually are usually formed downstream from upper-level troughs and upstream from upper-level ridges. Intense frontal zones are not only found at the surface; observational and theoretical studies have documented the formation of strong fronts near the tropopause as well. The strong vertical wind shear accompanying these systems can result in clear-air turbulence, which is of interest to the aviation industry, among others. In this chapter, we will focus our attention on surface fronts.

4.3: Frontogenesis

Frontogenesis refers to an increase in the magnitude of the horizontal density gradient, whereas **frontolysis** refers to a decrease in the magnitude of the horizontal density gradient. A traditional measure of frontogenesis was introduced by Norwegian meteorologist, Sverre Pettersen, to explore the kinematic processes leading to change in the strength of the gradient of a scalar field following a moving air parcel. If we choose potential temperature as our scalar field, the **frontogenesis function** (F) is defined as the time rate of change of the magnitude of the horizontal potential temperature gradient following the flow. More generally, for any orientation of coordinate axes and for cases in which an along-front potential temperature gradient is present, $F = d/dt\ |\nabla_h \theta|$. The advantage of defining F with potential temperature, rather than temperature, is that in regions of complex terrain, the potential temperature can help to isolate synoptic features (including fronts) by correcting the temperature to a common pressure level, thereby reducing the portion of the temperature gradient due to elevation. Also, potential temperature is a conservative variable for adiabatic flow.

Here, the different physical mechanisms that can lead to changes in the potential temperature gradient following the flow will be examined on a conceptual level. Pettersen demonstrated that the frontogenesis function can be written as

$$F_{equiv} = \frac{d}{dt}|\nabla_h \theta| = F_{shear} + F_{stretch} + F_{tilt} + F_{heat}$$

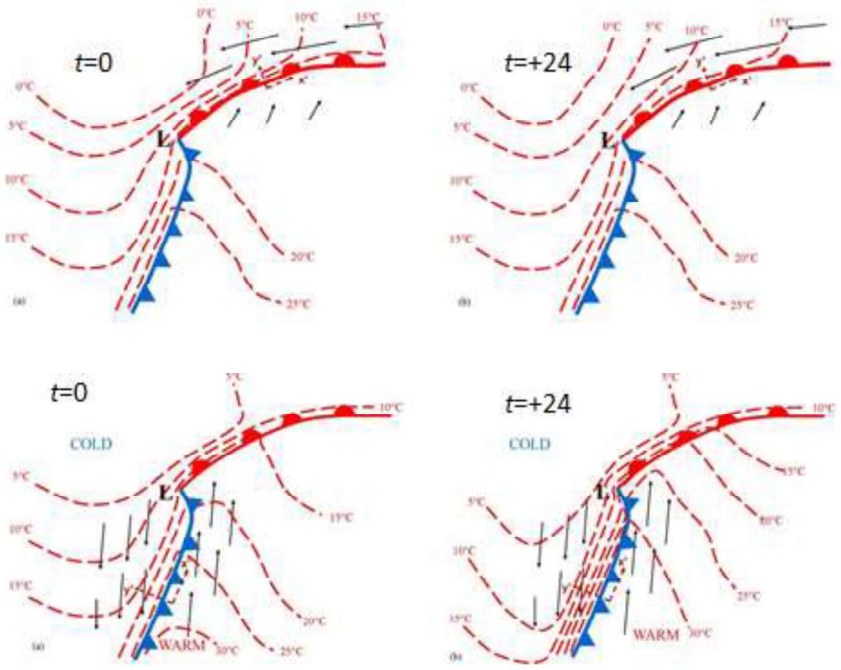

Figure 4.4 Schematic of the effect of F_{shear}. Top panel depicts shearing frontolysis along the warm front, whereas bottom panel depicts frontogenesis along the cold front.

F_{shear} represents the effects of horizontal shear on the horizontal temperature gradient. Shearing frontogenesis describes the change in frontal strength due to differential potential temperature advection by the front-parallel wind component. For shearing frontogenesis, a strengthened temperature gradient results from cold advection in the cold air and warm advection in the warm, both of which act to increase the frontal contrast. Shearing can also have a frontolytic effect when warm advection occurs within cold air or cold advection occurs within warm air, both of which act to decrease the frontal contrast.

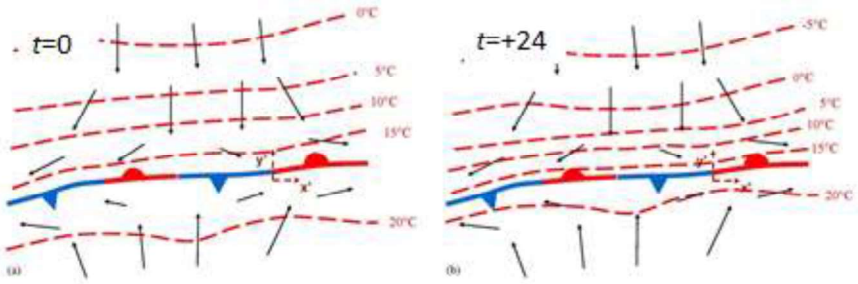

Figure 4.5 Schematic of the effect of $F_{stretch}$, depicting frontogenesis.

$F_{stretch}$ represents the kinematic effect of confluence/diffluence on the horizontal temperature gradient. Confluence acts to increase the horizontal potential temperature gradient, while diffluence acts to decrease the horizontal potential temperature gradient. Confluence and diffluence contribute to both convergence (divergence) and horizontal (nondivergent) deformation. Because of the smaller cross-front distance scale, the confluence term tends to be larger than the shearing term.

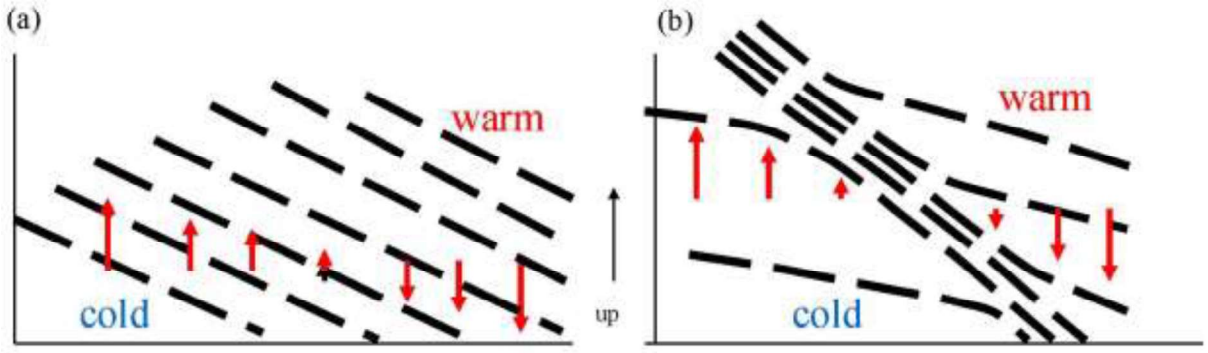

Figure 4.6 Schematic of the effect of F_{tilt}, depicting frontogenesis.

F_{tilt} represents kinematically the tilting of the vertical potential temperature gradient onto the horizontal. In a statically stable atmosphere, rising motion and its associated adiabatic cooling on the cold side, and sinking motion and its associated adiabatic warming on the warm side, increase the temperature gradient. Near the Earth's surface, the vertical motion is small, and the effect of tilting is often relatively weak.

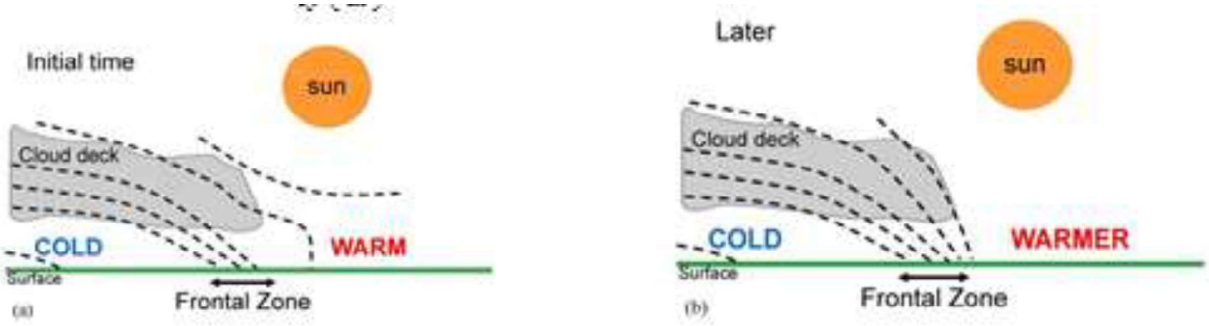

Figure 4.7 Schematic of the effect of F_{heat}, depicting frontogenesis.

F_{heat} represents a horizontal variation in diabatic heating. For example, heating of the warm side of a front by the sun during the day, if it is clear there, without heating on the cold, cloudy side, if it is cloudy there, is a frontogenetical process. At night the effect of long-wave cooling is dominant, so that cooling on the clear, warm side, with restricted cooling on the cold, cloudy side, represents a frontolytical process. Differential heating along the boundary between snow cover and bare ground can act frontogenetically. If a surface cold front is very shallow, and relatively warm air is present above the shallow cold air mass, then heating by the sun may result in the total destruction of the cold air mass, and hence in the destruction of the front. In the High Plains area of the United States, a shallow cold front may be turned into a dryline by this mechanism.

**4.3.1: Derivation of Frontogenesis Function

To examine frontogenesis, we need to examine the evolution of θ, which means that we need to derive an expression for the rate of change of θ. The first law of thermodynamics is usually derived by considering a system in thermodynamic equilibrium, that is, a system that is initially at rest and after exchanging heat with its surroundings and doing work on the surroundings is again at rest. For such a system the first law states that *the change in internal energy of the system is equal to the difference between the heat added to the system and the work done by the system*. A Lagrangian control volume consisting of a specified mass of fluid may be regarded as a thermodynamic system. However, unless the fluid is at rest, it will not be in thermodynamic equilibrium. Nevertheless, the first law of thermodynamics still applies. To show that this is the case, we note that the total thermodynamic energy of the control volume is considered to consist of the sum of the internal energy (due to the kinetic energy of the individual molecules) and the kinetic energy due to the macroscopic motion of the fluid. The rate of change of this total thermodynamic energy is equal to the rate of diabatic heating plus the rate at which work is done on the fluid parcel by external forces.

If we let e designate the internal energy per unit mass, then the total thermodynamic energy contained in a Lagrangian fluid element of density ρ and volume δV is $\rho\left[e+\frac{1}{2}U^2\right]\delta V$. In the absence of viscous forces, the external forces that act on a fluid element are the pressure force, the gravitational force, and the Coriolis force. Our job is to determine the rate at which work is done on the fluid element by each of these forces.

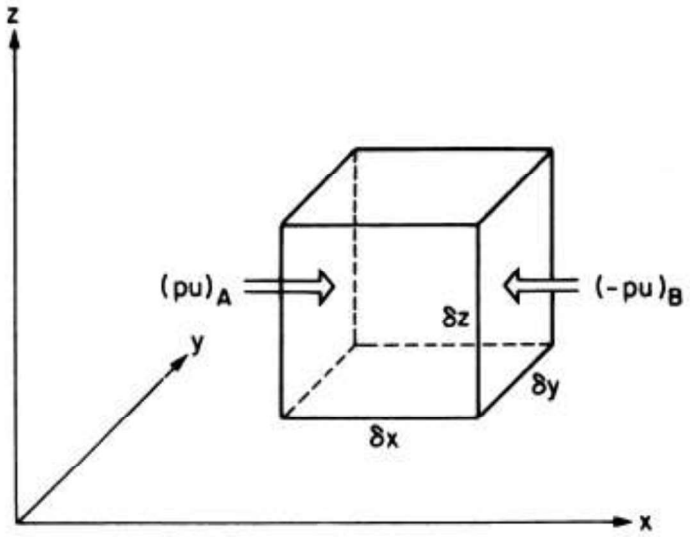

Figure 4.8 Rate of work done on a fluid element due to the *x* component of the pressure force

First, we note that the Coriolis force is perpendicular to the velocity vector, it can do no work. Second, we note the rate at which the gravitational force does work on the mass element is $\rho g w \delta V$, where w is the vertical velocity. The rate at which work is done on the fluid element by the x component of the pressure force is illustrated in Figure 4.8. Recall from introductory physics that pressure is force per unit area and that the rate at which a force does work (i.e. the power) is given by $\vec{F}\cdot\vec{U}$. We see that the rate at which the surrounding fluid does work on the element due to the pressure force on the two boundary surfaces in the *y,z* plane is given by

$$(Pu)_A\delta y\delta z-(Pu)_B\delta y\delta z$$

Note that the negative sign is needed before the second term because the work done on the fluid element is positive if u is negative across face B. Now by expanding in a power series we can write

$$(Pu)_B=(Pu)_A+\left[\frac{\partial}{\partial x}(Pu)\right]_A\delta x+\cdots$$

Thus, the net rate at which the pressure force does work due to the *x* component of motion is

$$[(Pu)_A - (Pu)_B]\delta y \delta z = -\left[\frac{\partial}{\partial x}(Pu)\right]_A \delta V$$

Generalizing to three dimensions, we have that the total rate at which work is done by the pressure force is

$$-\nabla \cdot \left(P\vec{U}\right)\delta V$$

Applying the principle of energy conservation to our Lagrangian control volume (neglecting effects of molecular viscosity), we thus obtain

$$\frac{D}{Dt}\left[\rho\left(e + \frac{1}{2}U^2\right)\delta V\right] = -\nabla \cdot \left(P\vec{U}\right)\delta V + \rho g w \delta V + \rho \dot{Q}\delta V$$

Here, $\dot{Q}$ is the rate of heating per unit mass due to radiation, conduction, and latent heat release. Using the chain rule, we can rewrite the above expression as

$$\rho\delta V \frac{D}{Dt}\left(e + \frac{1}{2}U^2\right) + \left(e + \frac{1}{2}U^2\right)\frac{D(\rho\delta V)}{Dt} = -\vec{U} \cdot \nabla P\, \delta V - P\nabla \cdot \vec{U}\delta V - \rho g w \delta V + \rho\dot{Q}\delta V$$

Now based on the mass continuity equation, the second term on the left hand side of the expression vanishes so that we have

$$\rho\frac{De}{Dt} + \rho\frac{D}{Dt}\left(\frac{1}{2}U^2\right) = -\vec{U} \cdot \nabla P - P\nabla \cdot \vec{U} - \rho g w + \rho\dot{Q}$$

We can simplify by this expression by using the vector momentum equation. If we take the dot product of $\vec{U}$ with the momentum equation, we obtain

$$\vec{U} \cdot \frac{D\vec{U}}{Dt} = -\frac{1}{\rho}\vec{U} \cdot \nabla P + \vec{g} \cdot \vec{U} \Rightarrow \rho\frac{D}{Dt}\left(\frac{1}{2}U^2\right) = -\vec{U} \cdot \nabla P + \rho g w$$

Using this in our expression for energy conservation gives

$$\rho\frac{De}{Dt} = -\rho\nabla \cdot \vec{U} + \rho\dot{Q}$$

This is known as the thermal energy equation. This can be written in a more familiar form by using the continuity equation. From the continuity equation, we note that

$$\frac{1}{\rho}\nabla \cdot \vec{U} = -\frac{1}{\rho^2}\frac{D\rho}{Dt} = \frac{D\alpha}{Dt}$$

where $\alpha = \rho^{-1}$ is known as the specific volume. We also note that for dry air, the internal energy per unit mass is given by $e = c_v T$, where c_v is the specific heat at constant volume. This gives us

$$c_v \frac{DT}{Dt} + P\frac{D\alpha}{Dt} = \dot{Q}$$

This is known as the **thermodynamic energy equation**, which is the first law of thermodynamics applied to a moving fluid.

We can write the thermodynamic energy equation in terms of potential temperature θ. First, taking the total derivative of the ideal gas law (in terms of specific volume) gives

$$\frac{D}{Dt}(P\alpha) = R_d\frac{DT}{Dt} \Rightarrow P\frac{D\alpha}{Dt} = R_d\frac{DT}{Dt} - \alpha\frac{DP}{Dt}$$

Substituting this into the thermodynamic energy equation and noting that $c_p = c_v + R_d$, we have

$$c_p\frac{DT}{dt} - \alpha\frac{DP}{Dt} = \dot{Q}$$

Dividing both sides by T and using the ideal gas law, we obtain

$$c_p\frac{D\ln T}{Dt} - R_d\frac{D\ln P}{Dt} = \frac{\dot{Q}}{T}$$

Now, by the definition of potential temperature

$$\theta = T\left(\frac{P_0}{P}\right)^{R_d/c_p} \Rightarrow \ln\theta = \ln T + \frac{R_d}{c_p}(\ln P_0 - \ln P) \Rightarrow c_p\frac{D\ln\theta}{Dt} = c_p\frac{D\ln T}{Dt} - R_d\frac{D\ln P}{Dt}$$

Therefore, we have

$$c_p\frac{D\ln\theta}{Dt} = \frac{\dot{Q}}{T} \Rightarrow \frac{D\theta}{Dt} = \frac{\dot{Q}\theta}{c_p T}$$

By differentiating with respect to y (i.e. the along front direction), we obtain the equation for the time rate of change of the strength of baroclinicity along a front

$$F \equiv \frac{d}{dt}\left(-\frac{\partial\theta}{\partial y}\right) = \frac{\partial u}{\partial y}\frac{\partial\theta}{\partial x} + \frac{\partial v}{\partial y}\frac{\partial\theta}{\partial y} + \frac{\partial w}{\partial y}\frac{\partial\theta}{\partial z} - \frac{\partial}{\partial y}\left(\frac{\dot{Q}\theta}{c_p T}\right)$$

where F is known as **the scalar frontogenesis function.**

The first term is known as the shearing frontogenesis term. Shear frontogenesis describes the change in front strength due to differential temperature advection by the *front-parallel* wind component. Along the cold front given in the bottom panel of Figure 4.4, both $\partial u/\partial y$ and $\partial\theta/\partial x$ are negative, giving a positive contribution to F. This means cold (warm)-air advection in the cold (warm) air. Along the warm front in the top panel of Figure 4.4, $\partial\theta/\partial x$ is positive, but $\partial u/\partial y$ is negative, giving a negative contribution to F. This means along the warm front, shearing acts in a frontolytical sense.

The second term is the confluence or stretching term. Confluence frontogenesis describes the change in front strength due to *stretching*. Along the front in Figure 4.5, both $\partial\theta/\partial y$ and $\partial v/\partial y$ are negative, giving a positive contribution to F. This means along the front, confluence acts in a frontogenetical sense. The third term is the tilting term and it usually acts to strengthen fronts *above* the Earth's surface, as in Figure 4.6. In that figure, $\partial\theta/\partial z$ is negative (temperature decreases above the surface), and $\partial w/\partial y$ is also negative (rising motion in the cold air, sinking in the warm air), leading to frontogenesis.

The fourth term is the differential diabatic heating term, which takes into account all diabatic processes together (such as differential solar radiation, differential surface heating due to soil characteristics, differential heat surface flux, etc.). In Figure 4.7, we see the effects of differential solar radiation. Based on the figure, the diabatic heating rate in the warm air exceeds the diabatic heating rate in the cold air. This makes $\partial/\partial y\left(\dot{Q}\theta/c_p T\right)$ positive, causing frontogenesis.

4.3.2: Frontogenesis and Deformation

If the effects of tilting and differential diabatic heating can be neglected, then the frontogenesis function can be written as

$$F = \frac{d}{dt}|\nabla_h\theta| = \frac{\nabla_h\theta}{2}(D\cos 2\beta - \delta)$$

where β is the angle between the isentropes (i.e. lines of constant θ) and the axis of dilatation, δ is the horizontal divergence, and D is the total deformation. We observe from the above equation that frontogenesis occurs whenever a nonzero horizontal potential temperature gradient coincides with convergence $\delta < 0$, and whenever the total deformation field acts upon isentropes that are oriented within 45° of the axis of dilatation, as shown in Figure 4.8. For angles between isentropes and the axis of dilatation that are between 45° and 90°, frontolysis occurs. Divergence ($\delta > 0$) also contributes to frontolysis. Vorticity does not contribute directly to frontogenesis or frontolysis, but can affect frontogenesis or frontolysis by rotating the isentropes, thereby changing the angle between the isentropes and the axis of dilatation, which affects F. This approximation essentially states that the geometry of the horizontal flow has a strong influence on frontogenesis in most situation and thus the two main processes (parameters) that make significant separate contributions to frontogenesis is divergence and deformation.

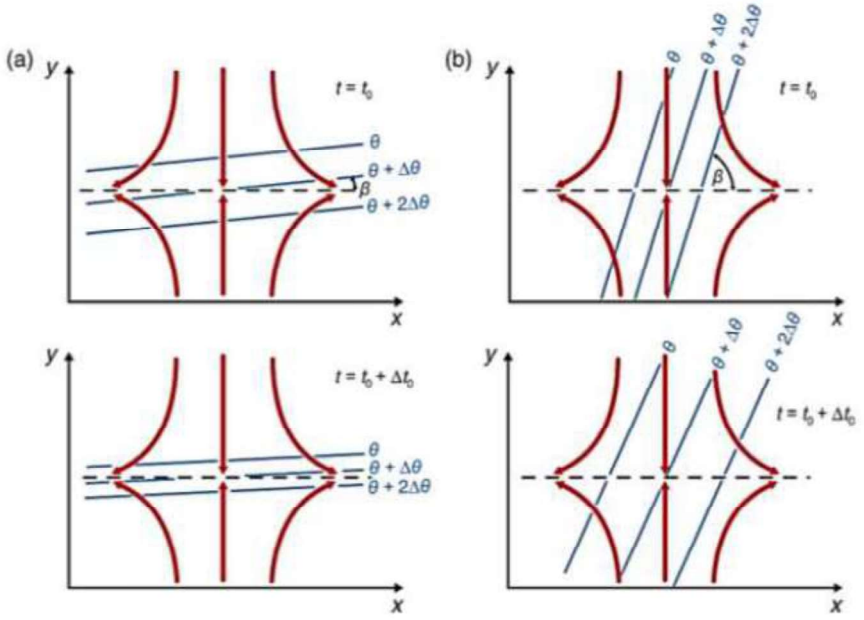

Figure 4.9 Schematic illustration of the relationship between isentropes (blue contours) and an idealized wind field dominated by deformation (red streamlines) in a situation of (a) frontogenesis and (b) frontolysis. The axis of dilatation (black dotted line) and angle β are also indicated.

Now that we have reviewed the general properties of fronts and have examined the kinematic processes responsible for their evolution, it remains to illustrate examples of different types of frontal structure and associated weather. Our goal is to extend beyond a basic discussion of the main frontal types — to focus on some of the key structural differences leading to contrasting weather in their vicinity. The basic frontal types — cold, warm, stationary, and occluded — are loosely defined based on the sense of local movement and temperature tendency in the frontal zone. Fronts that are moving slowly can be categorized as stationary fronts, and other fronts may require examination of sequential analyses to discern their movement. The mechanism of

movement of fronts varies with type, but the frontal kinematics outlined in the preceding section is generally relevant to all types of fronts.

4.4: Cold Fronts

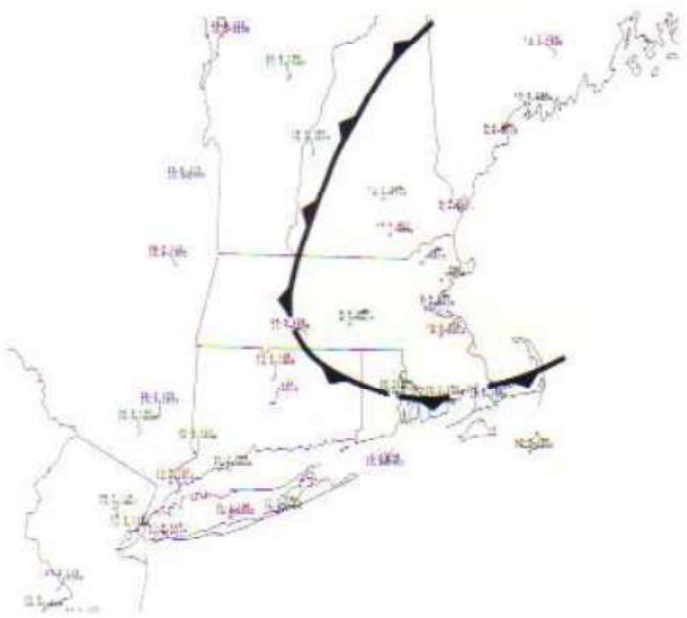

Figure 4.10 Example of a New England back-door cold front 0000 UTC, April 29, 1990.

When a cold air mass advances equatorward, equatorward and eastward, or eastward relative to the warm air mass, the front is called a **cold front**. When the cold air advances westward or equatorward and westward, the front is called a **back-door cold front** because synoptic-scale weather systems in the midlatitudes usually have an eastward component of motion. The former usually trail off in an equatorward direction from a surface cyclone, and are followed by a cold, surface anticyclone. Synoptic-scale vertical motion is usually downward, and an upper-level ridge is found upstream with respect to the flow aloft. Back-door cold fronts are common in the northeastern part of the United States during the spring and summer, east of the Rocky Mountains any time of year, and sometimes in the Great Plains during the period from fall through spring. The spring and summer New England back-door cold front is influenced strongly by the relatively cold ocean upstream.

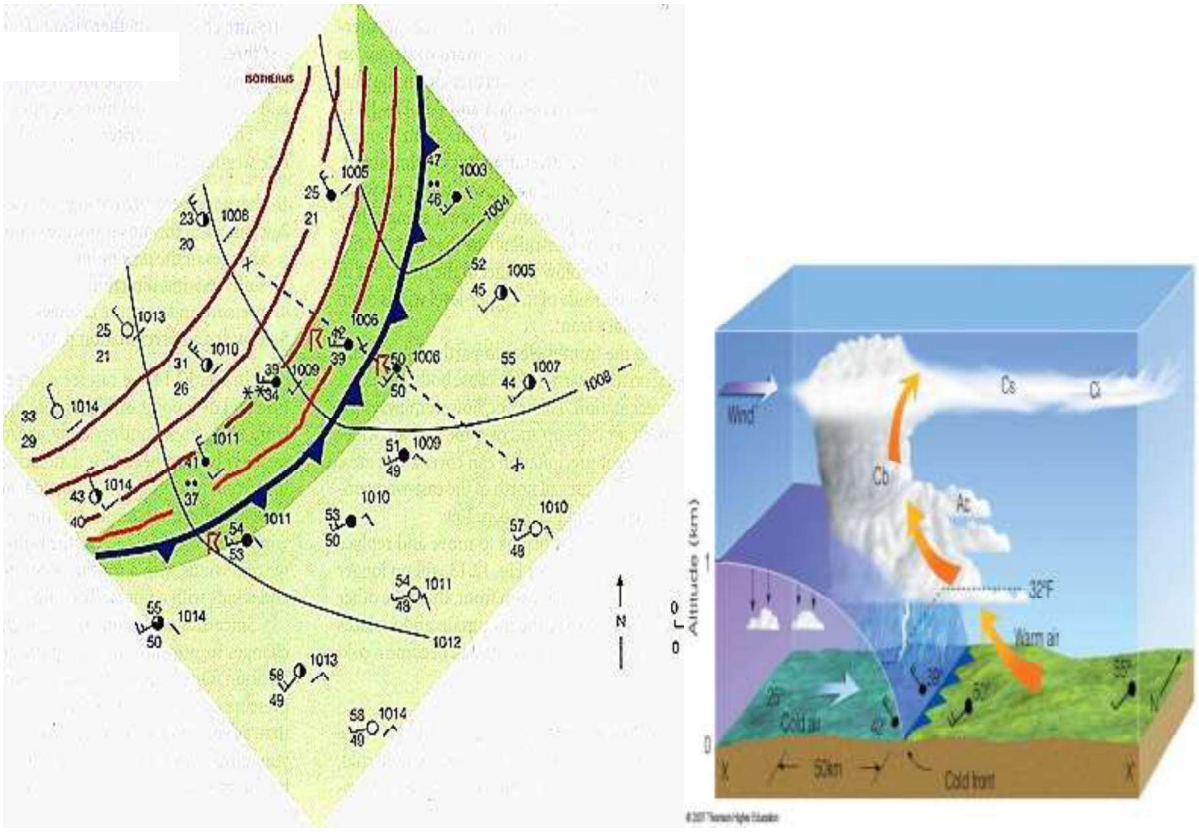

Figure 4.11 (Left) Surface map associated with cold front (Right) Vertical cross section of cold front

The surface frontal zone (i.e., band of surface temperature gradient much greater in magnitude than the synoptic-scale horizontal temperature gradient) is usually found on the cold side of the wind shift associated with a surface pressure trough. The wind veers (backs) along the wind-shift line equatorward (poleward) of the cyclone. It is common practice to identify the front symbol (line along which there are toothlike triangles pointing from the cold side toward the warm side) with the wind-shift line along which there is a maximum in cyclonic vorticity. Just as or shortly after the wind has shifted, the temperature drops and the pressure rises. One is in the frontal zone from the time the wind shifts direction and the temperature begins to drop until the time the temperature no longer falls rapidly.

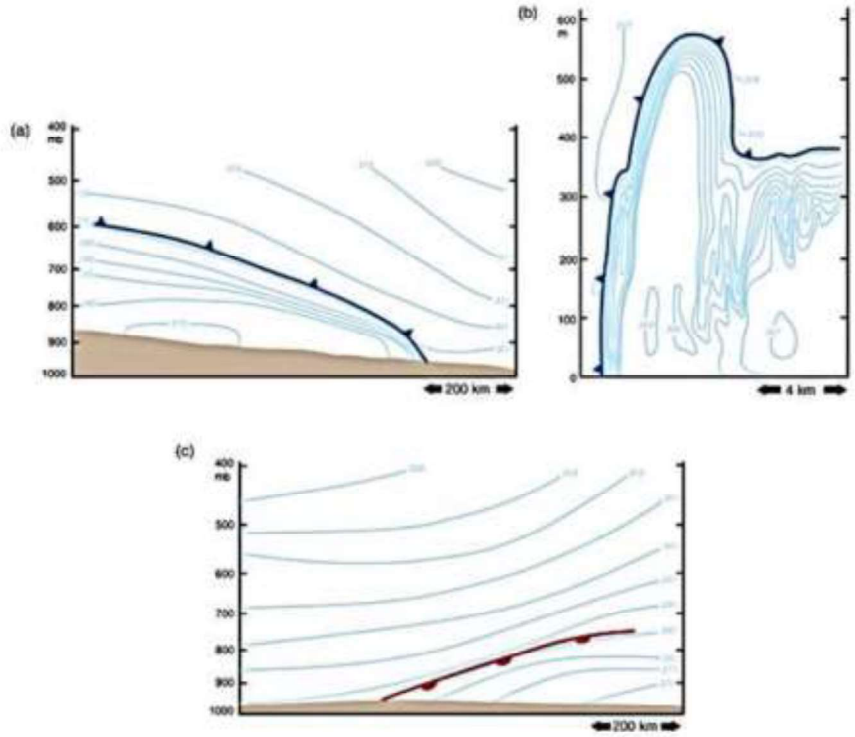

Figure 4.12 Examples of synoptic fronts as seen in approximately front-normal vertical cross-section of potential temperature (blue contours). (a) Cold front analyzed by Sanders (1955) using rawinsonde observations. (b) Strong cold front analyzed by Shapiro et al. (1985) based on observations obtained from an instrumental tower (observations were time-to-space converted). (c) Warm front analyzed by Bluestein (1993) using rawinsonde observations.

The surface front is most intense at the ground, and weakens with height. It can intensify dramatically on time scales as short as 12 hours. The frontal zone is marked by strong static stability; it is associated with strong vertical wind shear, which is associated to some extent with the surface temperature gradient, in accord with the thermal wind relation. The frontal zone is steepest near the ground. A narrow jet of rising air is often located just above the leading edge of the surface front. A narrow cloud line ("rope cloud") or band of precipitation may be located along the rising jet if there is sufficient moisture. Below the frontal zone in the cold air at low levels, the lapse rate (i.e. the change in temperature with height) may be nearly adiabatic, and hence there is strong turbulent mixing that creates gusty surface winds.

The movement of a cold front is not necessarily determined by the difference between the wind components normal to the front on either side of it. Movement is best correlated with the wind component normal to the front in the cold air. The movement of the surface cold front should be dependent upon the front-normal isallobaric gradient. The trough associated with a frontal zone moves from a region where surface pressures are rising to a region where surface pressures are falling. Because the zone of temperature gradient is located on the cold side of the wind-shift line, we expect to find strong cold advection there. Moreover, the cold advection is

associated with sinking motion and surface pressure rises. Thus, it's not surprising that frontal movement is associated with the front-normal wind speed in the cold air. The distribution of clouds on either side of a front depends upon the vertical motion, the front-relative flow, and the availability of moisture upstream from the front. The front-relative flow in eastward-moving fronts is likely to be rear-to-front, owing to strong westerlies aloft. The front-relative flow in equatorward-moving fronts is more likely to be front to rear, especially if there is a poleward component of flow aloft downstream from a trough. Frontal motion can also be influenced by diabatic effects such as latent cooling resulting from the evaporation of precipitation (latent cooling influences the surface pressure field and therefore also affects the isallobaric gradient).

4.4.1: Katafront and Anafront Structure

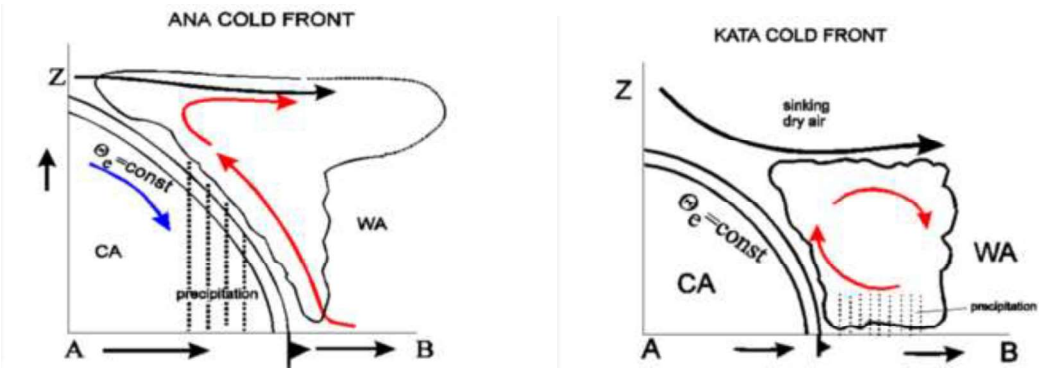

Figure 4.13 Comparing kata cold front and ana cold front

Broadly speaking, cold fronts can be divided into two types: **ana** and **kata** cold fronts. These types can be described both in terms of classical frontal theory and in terms of conveyor belts. The main feature which separates the different types of cold front is the orientation of the jet relative to the front in the middle and upper levels of the troposphere: In the case of an ana cold front, the jet axis and dry intrusion are parallel to the frontal cloud band, and form a well pronounced rear cloud edge. In the case of a kata cold front, the jet axis crosses the frontal cloud band.

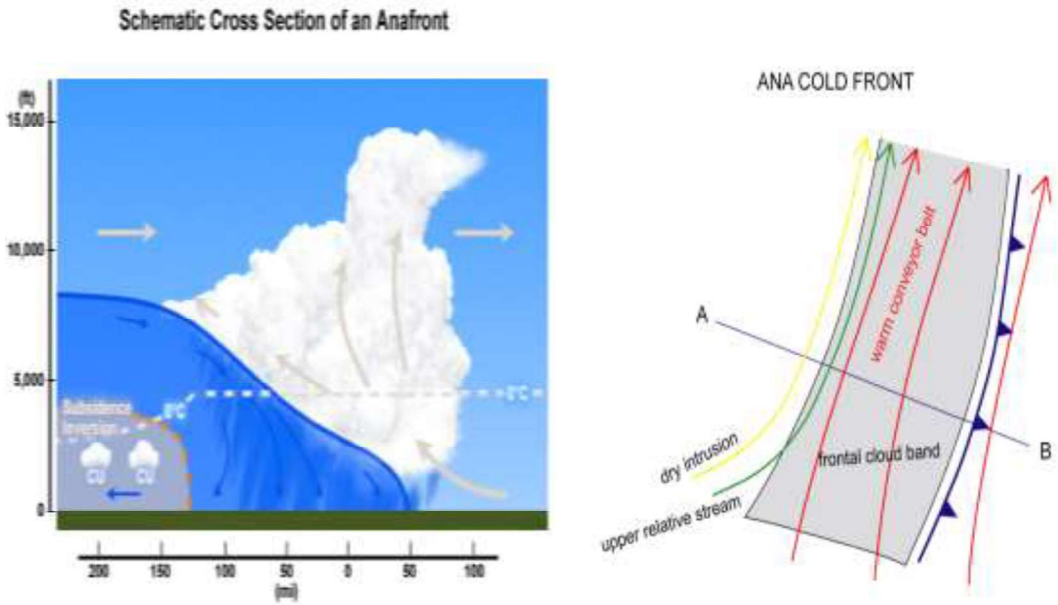

Figure 4.14 Schematic of ana cold front

For ana cold fronts, the cold air moves rapidly against warm air, creating convergence within the baroclinic zone between the two air masses. Convergence forces the warm, moist air to ascend along the frontal surface. The developing cloud band is inclined rearward with height. The main zone of cloudiness and precipitation is located behind the surface front. The frontal cloud band and precipitation are related to an ascending **warm conveyor belt**, which has a rearward component relative to the movement of the front, causing the frontal cloud band and precipitation to appear behind the surface front. Parallel to the warm conveyor belt there is a dry stream (dry intrusion). The sharp rear cloud edge of frontal cloudiness marks the transition between the two relative streams.

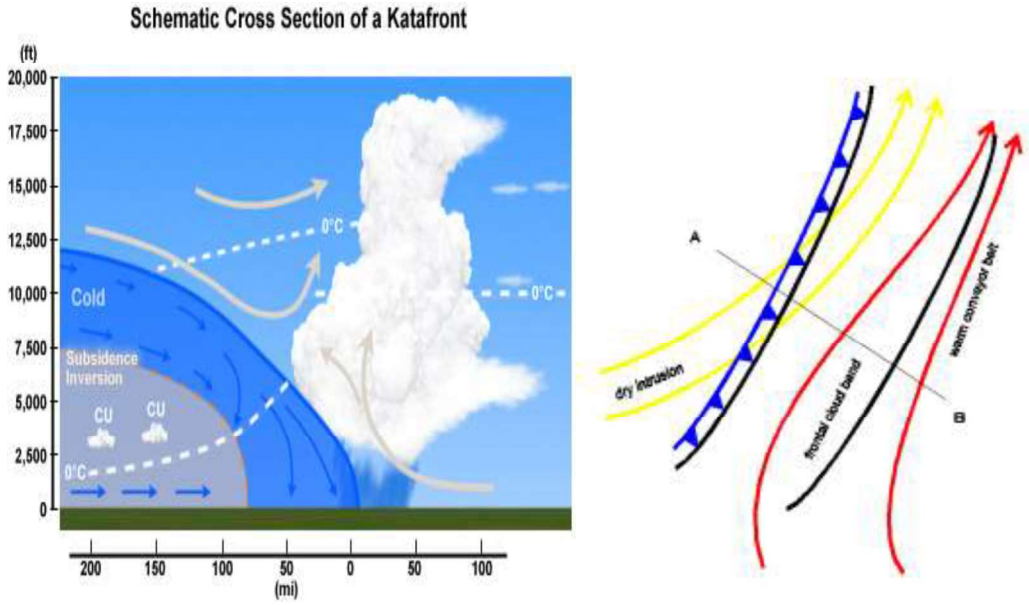

Figure 4.15 Schematic of kata cold front

For kata cold fronts, the ascent of warm air is restricted by dry descending air originating from behind the front and, consequently, dissipating the higher clouds. The main zones of cloudiness and precipitation appear in front of the surface front. Unlike the ana cold front, the ascending warm conveyor belt is overrun by the dry intrusion. The dry air originates from upper levels of the troposphere and crosses the cold front from behind. The warm conveyor belt acquires a component which is inclined forwards relative to the movement of the cold front. Therefore, frontal clouds and precipitation tend to lie ahead of the surface front. The cloud tops in the area of the dry airstream are relatively low, whereas on the leading edge of this area the cloud tops are higher. This area indicates the so-called upper Cold Front. The air mass which is advected by the dry intrusion is colder than the air within the warm conveyor belt. The intrusion cools air above and, later, also ahead of the cold front.

4.5: Warm Fronts

When the warm air mass advances poleward, poleward and eastward, and sometimes eastward relative to the cold air mass, the surface front is called a **warm front**. The poleward or poleward and eastward movement of a warm front is usually associated with strong low-level warm advection east or poleward and east of a developing or intensifying surface cyclone. However, not all surface cyclones are associated with warm fronts, or with warm fronts with well-defined wind-shift lines.

The wind veers when a warm front passes. Low clouds and fog often clear away, as drier air not having a history of ascent arrives. In the Southern Plains, however, warm frontal passage may mark the return of stratocumulus overcast from the Gulf of Mexico. Relatively warm, Atlantic air sometimes circulates from the east around the north side of a cyclone near the Great Lakes and eventually advances westward, southwestward, southward, and even southeastward. This feature could be called a **back-door warm front**.

In this High Plains of the United States, the passage of a lee trough usually marks the shift to dry, potentially warm air from the west. This warming along the leading edge of the downslope air may be rather pronounced, especially when the air mass being displaced is cold, Arctic air that had arrived after the passage of a Norther. This type of warm front is sometimes referred to as a **chinook front**. Strong downslope wind storms are common in the foothills of the Rockies as the lee trough/chinook front passes east of the Continental Divide. The potential for damaging winds is a function of wind direction, vertical wind profile, and static stability upstream.

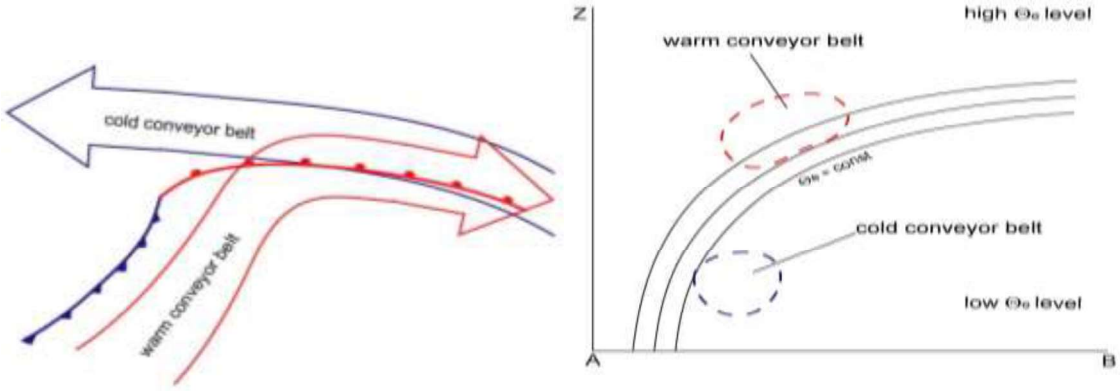

Figure 4.16 Schematic of warm front using conveyor belt theory

The idealized structure and physical background of a warm front can be explained with the conveyor belt theory. Frontal cloud band and precipitation are in general determined by the ascending warm conveyor belt, which has its greatest upward motion between 700 and 500 hPa. The warm conveyor belt starts behind the frontal surface in the lower levels of the troposphere, crosses the surface front and rises to the upper levels of the troposphere. There the warm conveyor belt turns to the right (anticyclonically) and stops rising, when the relative wind turns to a direction parallel to the front. If there is enough humidity in the atmosphere, the result of this ascending Warm Conveyor Belt is condensation and more and more higher cloudiness.

The cold conveyor belt in the lower layers, approaching the warm front perpendicularly in a descending motion, turns immediately in front of the surface Warm Front parallel to the surface front line. From there on the cold conveyor belt ascends parallel to the warm front below

the warm conveyor belt. Due to the evaporation of the precipitation from the warm conveyor belt within the dry air of the cold conveyor belt, the latter quickly becomes moister and saturation may occur with the consequence of a possible merging of the cloud systems of warm and cold Conveyor belt to form a dense nimbostratus.

Generally speaking, warm fronts are weaker than cold fronts. This implies that warm fronts are usually less steeply sloped than cold fronts and tend to have smaller temperature contrasts than cold fronts. Moreover, the wind shift along warm fronts is often not as pronounced as along cold fronts, which is related to the fact that warm fronts also tend to be have weaker temperature gradients than cold fronts.

4.6: Stationary Fronts and Occlusions

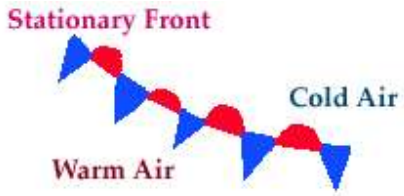

Figure 4.17 Schematic of stationary front

When neither the cold air mass nor the warm air mass advances much relative to each other, the front that separates the two is referred to as **stationary**. Rising motion above the frontal zone is typically associated with warm advection. This brand of rising motion is often referred to as **overrunning**, since the warm air mass overruns the cool air mass. Precipitation associated with overrunning is usually stratiform and light owing to the high static stability in the frontal zone.

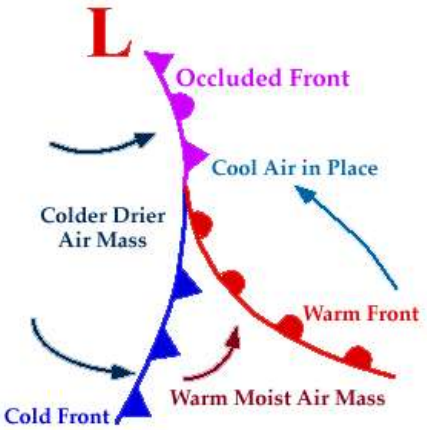

Figure 4.18 Schematic of basic occluded front

As cold fronts slow to a halt, often as a result of cyclogenesis to the west or equatorward and to the west, they become stationary. It is common for the stationary front to move back poleward as a warm front as the new cyclone deepens and moves poleward and eastward. When precipitation falls along and north of a stationary front, flooding is sometimes possible, since the region experiencing precipitation may do so for a long time.

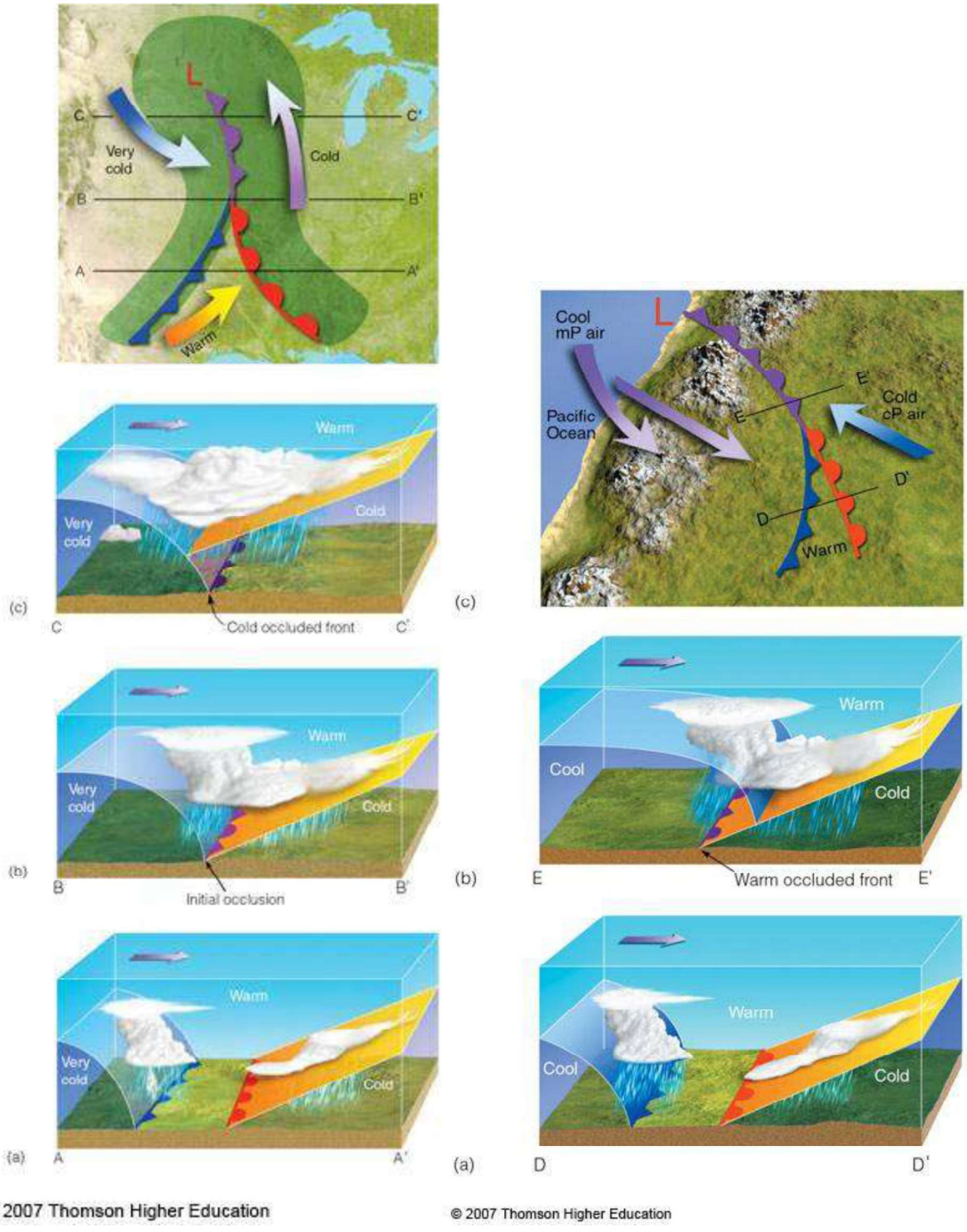

© 2007 Thomson Higher Education

Figure 4.19 Basic evolution of a cold occlusion and warm occlusion

According to polar-front theory, if a cold front overtakes a warm front equatorward of a cyclone the resulting wind and temperature field is referred to as an **occlusion**, since the warm air at the surface is blocked off from the ground. The surface boundary along which the cold front meets the warm front is called an **occluded front**. For an occlusion, the warm air mass is pinched in between the upstream and downstream cold air masses. Occluded fronts in which the advancing cold air is warmer than the retreating cold air are called **warm occlusions**. **Cold occlusions** are occluded fronts in which the advancing cold air is colder than the retreating cold air.

Occluded fronts that move across the Pacific Northwest and then downslope east of the Rockies are usually warm occlusions. A relatively mild, maritime air mass is warmed through adiabatic compression in the lee of the mountains and advances relative to a retreating, cold, continental air mass. These occluded fronts are called **trowals** in Canada. In the lee of the mountains, these fronts may behave more like warm fronts. Occluded fronts in the eastern United States are often cold occlusions, as relatively cold, continental air advances relative to retreating warm Atlantic air.

However, verification of the classic occlusion through analysis of observational data has been difficult! There are currently several other conceptual models for the formation of occluded fronts, which would go beyond the scope of these notes.

4.7: Coastal Fronts

A common feature along the southeastern U.S. coast, the Texas coast, and in coastal New England is a frontal zone that forms preferentially along the coast. The **coastal front** is a shallow (i.e. less than 1 km deep) mesoscale zone of strong horizontal temperature gradient (on the order of 10°C/10 km) at the surface that separates relatively warm, maritime air from cold, continental air. The coastal front has a time scale of 6 – 12 hours, which is somewhat less than the synoptic time scale of days. Coastal fronts are often found during the early and middle winter along the east coast of New England and the Carolina and Texas coasts, all of which are curved in a concave manner. During the early winter, there can be a substantial land-sea temperature contrast, because the ocean temperature is still relatively warm compared to the air temperatures over land. When cold, continental air flow offshore along a concave coastline, there is a relative maximum in diabatic heating.

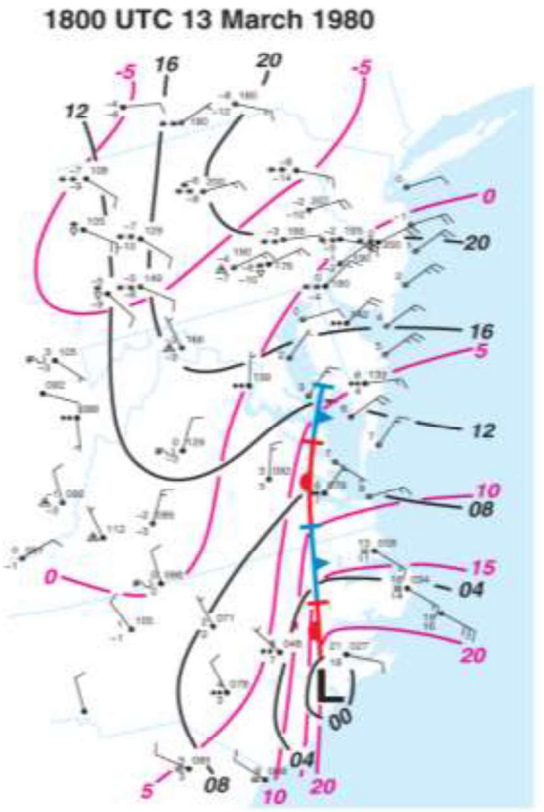

Figure 4.20 Surface analysis of Carolina coastal front on 14 March 1980 at 1800 UTC

Coastal fronts usually behave like stationary fronts or warm fronts. They often move toward the cold air mass, and are marked by a convergence zone, along which there is a shift in wind direction. The maximum amount of accumulated precipitation is found along a band on the cold side of the front. Sometimes the coastal front separates frozen precipitation (on the cold side) from rain (along the warm side), or heavy precipitation from light precipitation.

Coastal frontogenesis in New England occurs when there is an anticyclone associated with a cold air mass to the north or northeast of New England, and when a trough approaches from the west at low to middle levels. The cold air flows southward and southwestward, and my become trapped by the Appalachian mountains. This phenomenon is known also as **cold air damming**, since the relatively dense, cold air cannot be lifted easily to the west over the mountains: Less energy is required to deflect the airflow around the mountains. The quasistationary ridge that forms as a hydrostatic consequence of the trapped cold air mass is often referred to as the **Baker ridge**.

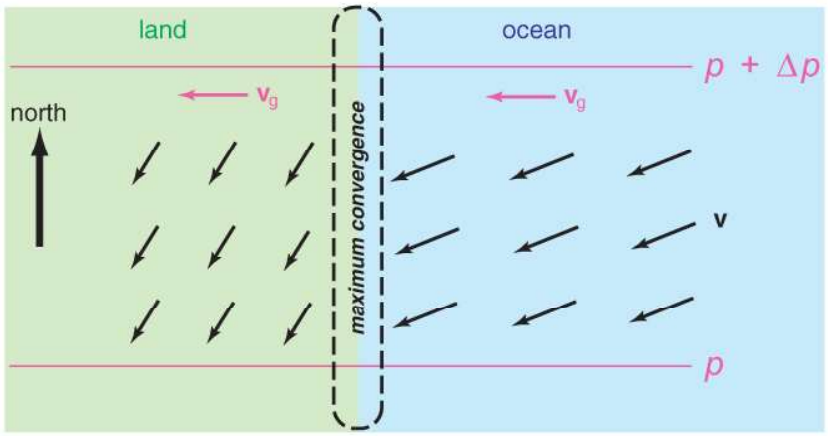

Figure 4.21 Schematic of coastal frontogenesis

The combination of cold air over the land and relatively warm air over the ocean produces a land-to-ocean directed horizontal temperature gradient. Although differential friction between the land and ocean can account for a band of convergence when there is onshore flow, it is not generally considered to be significant. In addition, heating of the cold, continental air from below by the relatively warm ocean results in **land breeze**, in which an offshore wind component along the shore contributes to a band of convergence along the coast. This band of convergence acts to increase the temperature gradient, that is, to promote frontogenesis.

To summarize, the characteristics of coastal fronts have been shown to include the following:

- the presence of a shallow front separating cold continental air from warm maritime air;
- most common occurrence during the cold season (November -- March) and along concave coastlines (e.g., New England, Carolinas, Texas);
- quasistationary or warm-frontal structure and movement, often migrating inland with time;
- heaviest precipitation on cold side of front due to enhanced life there, espectially with an extratropical cyclone located to the south;
- coastal fronts often form the eastern boundary of a cold-air damming event
- an "inverted trough" in the sea level pressure pattern can accompany the coastal front;
- coastal fronts can be accompanied by convection, even severe weather in some cases.

Chapter 5: Elementary Atmospheric Dynamics

The fluid atmosphere is a physical object and therefore, its motion is governed by the laws of physics. The purpose of this chapter is to describe the basic dynamics of the basic meteorological variables (i.e. pressure, temperature, humidity, and wind). We begin the discussion by describing the major forces that are active in the atmosphere.

5.1: Introduction

Newton's second law states that the rate of change of momentum of an object (i.e. its acceleration) equals the sum of all the forces acting on that object:

$$\frac{dp}{dt} = F_{net} \Rightarrow F_{net} = ma$$

This powerful statement is valid only for motions measured in a non-accelerating coordinate system, i.e. one that is fixed in space (or moving at a constant velocity). Such a coordinate system is known as an **inertial reference frame**. The most convenient $x, y,$ and z coordinates by which we measure motions on Earth refer to a grid based upon latitude and longitude (for the x and y coordinate directions) and elevation above sea level (for the z coordinate direction). Since the Earth rotates on its axis and revolves around the Sun, this Earth-based (x, y, z) coordinate system undergoes constant acceleration. This fact is easily proven using a globe. After finding your location on the globe, consider the fact that what you view at that location as the immutable direction east is, in fact, constantly changing direction (to an observer fixed in space) as the Earth rotates on its axis. Thus our Earth-based coordinates are non-inertial (i.e. accelerating). This being the case, Newton's second law can only be applied to the motion of objects on Earth if we correct for the acceleration of our coordinate system.

The collection of forces required to adequately represent Newton's second law on the rotating Earth can therefore be split into two broad categories. The first of these includes forces that would affect objects even in the absence of rotation, the so-called **fundamental forces**. The most important of these fundamental forces are (1) the pressure gradient force, (2) the gravitational force, and (3) the frictional force, all of which we will investigate below. The other group of forces that we must consider in a full treatment of Newton's second law arises from the

need to correct for the acceleration of our Earth-based coordinate system. We will refer to such forces as **apparent forces**. The two important apparent forces to be investigated in this chapter are (1) the centrifugal force and (2) the Coriolis force. We begin this examination by considering the nature of the pressure gradient force.

5.2: The Pressure Gradient Force

As can be readily discerned from inspection of any surface weather map, the pressure field varies zonally and meridionally. This spatial variability of pressure implies the presence of pressure gradients throughout the atmosphere. The **pressure gradient force** defines the force causing the air to respond to the pressure gradient.

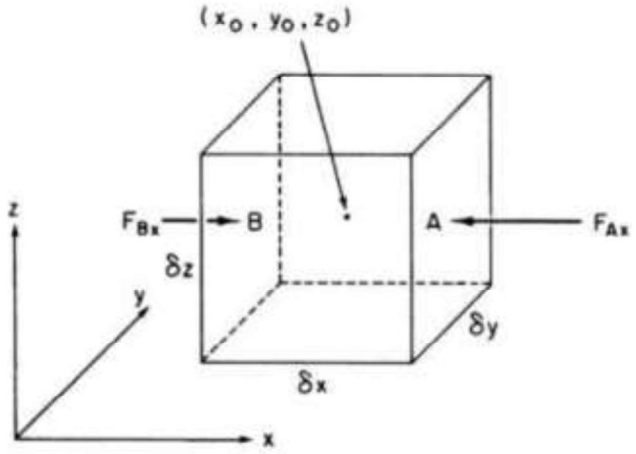

Figure 5.1 The *x*-component of the pressure gradient force acting on a fluid element

In order to examine the pressure gradient force (PGF) we will consider the pressure exerted by the atmosphere on sides A and B of the air parcel illustrated in Figure 5.1. The pressure exerted on sides A and B arises from the fact that random molecular motions compel molecules to strike the sides. Each time a molecule strikes the side of the fluid element, a certain amount of momentum is transferred to that side (according to Newton's 2nd law). The total momentum transfer is the sum of all the individual momentum transfers from each molecule. Since $dp/dt = F_{net}$, the total momentum transferred each second defines the force exerted by the atmosphere on the side of the fluid element. Since $P = F_{net}/A$, dividing this total force by the area of the side of the fluid element defines the pressure that is exerted on that side.

The above considerations show that the magnitude of the PGF is largely proportional to the pressure gradient. It can be shown that the expression for the pressure gradient force (per unit mass) between two points can be written as

$$\frac{F_{pressure}}{m} = -\frac{1}{\rho}\nabla P \approx -\frac{1}{\rho}\frac{P_1 - P_2}{D}$$

where P_1 and P_2 are the pressure at the two points (here it's assumed that $P_1 > P_2$) and D is the distance between the two points. The density prefactor, $1/\rho$, is included to account for the mass of the air. The negative sign in the above expression indicates that pressure gradient force is a vector that directed opposite of the pressure gradient. Physically, this states that the pressure gradient force compels air to move from regions of higher pressure to lower pressure. On surface weather charts, the above expression implies that the pressure gradient force is proportional to the spacing between isobars. Tightly packed isobars imply a strong pressure gradient force, whereas loosely packed isobars implies a weak pressure gradient force.

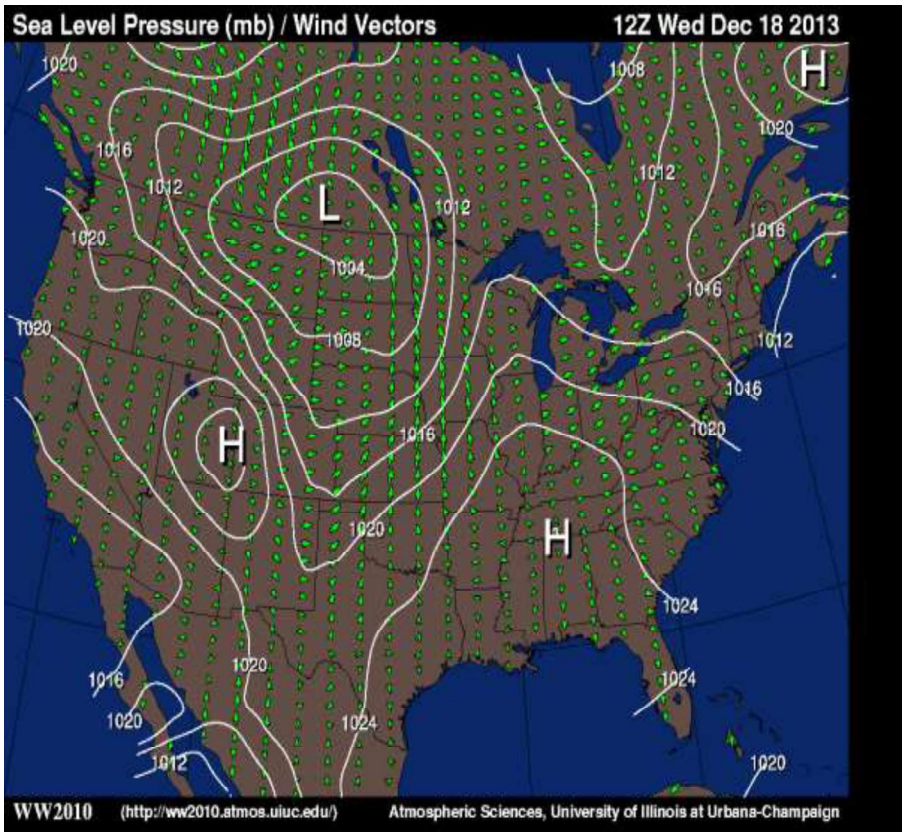

Figure 5.2: Sea-level pressure map at 12 Z on 18 December 2013 with wind vectors superimposed

Physically, the pressure gradient force demonstrates that any spatial variability of pressure in the atmosphere leads to the acceleration of air parcels. Since the change in pressure is directly proportional to the magnitude of pressure gradient force, this implies that the

acceleration of air parcels should increase as isobars become more closely spaced, as shown in Figure 5.2.

**5.2.1: Derivation of the Pressure Gradient Force

Let's assume that the air parcel in Figure 5.1 is an infinitesimal fluid element. If we define the pressure at the center of the fluid element to be p_0, then we can use a Taylor series expansion to determine the pressure on sides A and B

$$P_A \approx P_0 + \frac{\partial P}{\partial x}\left(\frac{\delta x}{2}\right)$$

$$P_B \approx P_0 - \frac{\partial P}{\partial x}\left(\frac{\delta x}{2}\right)$$

The x-direction pressure force on side A can be expressed as

$$F_{A,x} = -\left(P_0 + \frac{\partial P}{\partial x}\frac{\delta x}{2}\right)\delta y \delta z$$

The x-direction pressure force on side B can be expressed as

$$F_{B,x} = \left(P_0 - \frac{\partial P}{\partial x}\frac{\delta x}{2}\right)\delta y \delta z$$

Therefore, the net x-direction pressure force acting on the fluid element is

$$F_{net,x} = F_{A,x} + F_{B,x} = -\frac{\partial P}{\partial x}\delta x \delta y \delta z$$

The net force per unit mass acting in the x-direction on the fluid element is

$$\frac{F_x}{m} = -\frac{1}{\rho}\frac{\partial P}{\partial x}$$

This procedure can be generalized to three dimensions to give

$$\frac{\vec{F}_{pressure}}{m} = -\frac{1}{\rho}\nabla P$$

5.3: The Gravitational Force

Newton's law of universal gravitation says that any two elements of mass in the universe attract each other with a force proportional to their masses and inversely proportional to the distance between their centers of mass. This is represented symbolically as

$$\vec{F}_{gravity} = -G\,\frac{Mm}{r^2}\frac{\vec{r}}{r}$$

where $G = 6.67 \times 10^{-11}\ N\ m^2\ kg^{-2}$ is called **the universal gravitational constant**, $\vec{r}$ is the position vector directed from the center of mass of M to the center of mass of m. For an air parcel in the atmosphere, M is the mass of the Earth and m is the mass of an air parcel. Thus, we can express the gravitational force per unit mass as

$$\frac{F_{gravity}}{m} = -G\,\frac{M}{r^2}\frac{\vec{r}}{r}$$

In the above expression, $\vec{r}$ is the position vector directed from the center of the Earth to the center of mass of an air parcel in the atmosphere. Many applications in synoptic meteorology use height above sea level z as the vertical coordinate. This suggests that a parcel of air at a high elevation in the atmosphere might experience a smaller gravitational force than one located at sea level (i.e. nearer the center of gravity of the Earth). Though this is strictly true, the difference is very small from the surface to any level in the troposphere (lowest 10-12 km of the atmosphere) and we use a constant value of the gravitational force per unit mass, g^* where

$$\vec{g}^* = -G\frac{M}{a^2}\frac{\vec{r}}{r} \approx 9.80\ m/s^2$$

with a being the radius of the Earth, as a consequence.

5.4: The Frictional Force

Most of us have some conceptual understanding of friction and its effect on the behavior of solids. A textbook, for instance, that is pushed across a table feels the effect of the friction between itself and the tabletop and begins to decelerate immediately. In fact, the only reason the textbook does not continue to slide along the table indefinitely is that a force, the friction force, is applied opposite to its motion. The frictional force in this simple example is quantified as: $f = \mu N$, where N is the normal force of the table and μ is the **coefficient of friction** (which is a measure of the resistance to motion that results from pushing the book over the table).

This simplistic view of friction has to be modified when one considers the frictional force acting on a fluid parcel. Fluids, being collections of discrete atoms or molecules, are subject to internal friction (called **viscosity**) among these particles which cause the fluid to resist the tendency to flow. We will try to gain some insight into the nature of this resistance and how to express the physics in mathematical terms.

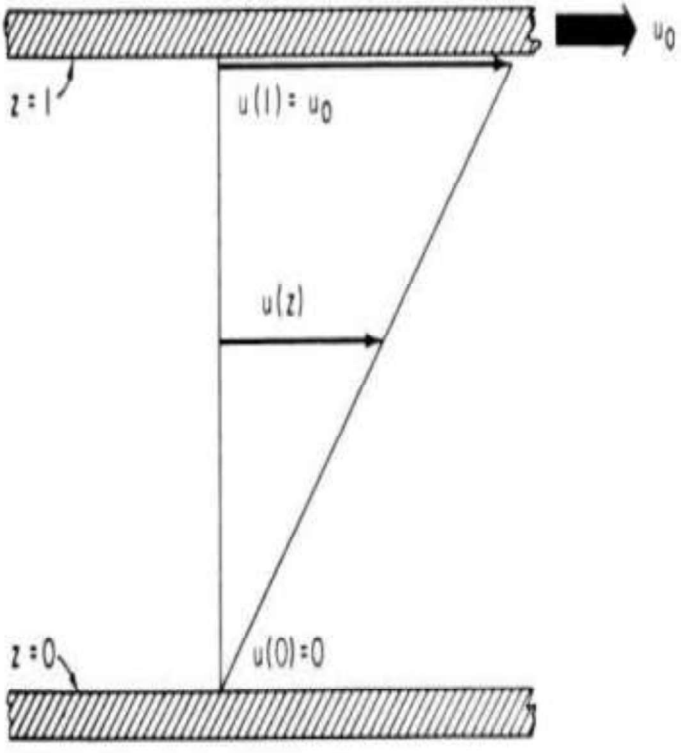

Figure 5.3: One dimensional steady-state viscous shear flow

Consider, for instance, the situation depicted in Figure 5.3 in which a plate, moving at speed u_0, is placed atop a column of fluid with depth l. The top layer of fluid moves at the velocity of the plate while the fluid at the bottom of the column has zero motion. Thus, a

shearing stress exists in the fluid and a force must be exerted on the plate in order that it be kept moving at speed u_0 along the top surface of the fluid. The requisite force is proportional to u_0 since a greater force will be required for a greater speed. Additionally, since molecules of fluid that reside at the bottom of the column, can influence the movement of the plate through momentum transport in the fluid column, the requisite force is also inversely proportional to the depth of the fluid. The force is also proportional to the area of the plate since a larger plate makes contact with more fluid than a smaller one. With these considerations, the force required to keep the plate moving by dimensional analysis is given by

$$F = \mu A \frac{du}{dz} \approx \mu A \frac{u_0}{l}$$

where μ is called the **dynamic viscosity coefficient**. The quantity du/dz is the change of velocity with height, also called the **vertical shear**. Physically, F represents the force required to overcome the viscous effect of the vertical shear. From the molecular viewpoint, a molecule moving to smaller z (i.e. toward the bottom of the fluid column) transports high momentum that it acquired from the motion of the plate to the surrounding fluid. Thus, there is a net downward transport of momentum and this momentum transport (per unit time) is the viscous force.

The above example can be applied to the atmosphere-Earth system where the bottom plate represents the surface of the Earth and the top plate represents the atmosphere. Based on the above analysis of our previous example, the effects of friction dominate near the surface where the momentum of air parcels is lost due to frictional dissipation with the surface. The region of the atmosphere where viscous forces become important is called the **boundary layer**. Observations of the mid-latitude synoptic environment suggest that top of the boundary layer is around 850 mb. As we will see later, surface friction will play a large role in the examination of the wind field.

**5.4.1: Derivation of the Viscous Force

In the above expression, F represents the x-direction force required to overcome the viscous effect of the vertical shear of the x-direction velocity component. Hence, as $\delta z \rightarrow 0$, the shearing stress, or viscous force per unit area, is given by

$$\tau_{zx} = \mu \frac{\partial u}{\partial z},$$

where the subscript 'zx' indicates that this is the component of the shearing stress (in the x direction) that arises from the vertical shear (z) of the x-direction (x) velocity component. The prior example considered the steady movement of a plate across the top of a fluid column. In nature, viscous forces result from *non-steady* shear flows.

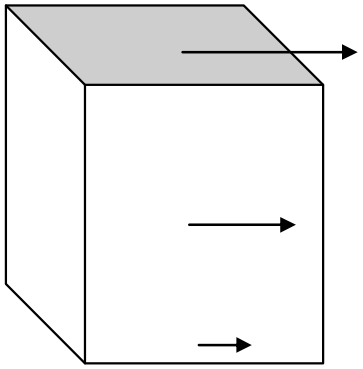

Figure 5.4 One dimensional shear-stress acting on a fluid element

In recognition of this fact, let's consider the volume element depicted in Figure 5.4, which represents the case of non-steady flow in a fluid of constant density. Analogous to our treatment of the pressure gradient force, we expand the shearing stress in a Taylor series in order to determine its value at the top and bottom (z-direction) facing sides of the volume element. The stress acting across the upper boundary on the fluid *below* it can be approximated as

$$\tau_{zx} + \frac{\partial \tau_{zx}}{\partial z}\frac{\delta z}{2}$$

while the stress acting across the bottom boundary on the fluid *below* it can be approximated as

$$\tau_{zx} - \frac{\partial \tau_{zx}}{\partial z}\frac{\delta z}{2}$$

According to Newton's 3rd law, this stress must be equal and opposite to the stress acting across the bottom boundary on the fluid *above* it. Since we are interested in the net stress acting on the volume element in Figure 5.4, we want to sum the forces that act on fluid *within* the volume element. Thus, we find that the net viscous force on the volume element acting in the x-direction is given by

$$\left(\tau_{zx} + \frac{\partial \tau_{zx}}{\partial z}\frac{\delta z}{2}\right)\delta x \delta y - \left(\tau_{zx} - \frac{\partial \tau_{zx}}{\partial z}\frac{\delta z}{2}\right)\delta x \delta y = \frac{\partial \tau_{zx}}{\partial z}\delta x \delta y \delta z$$

Dividing this expression by the mass of volume element, $\rho \delta x \delta y \delta z$, we have the viscous force per unit mass arising from the vertical shear of the x-direction motion:

$$\frac{1}{\rho}\frac{\partial \tau_{zx}}{\partial z} = \frac{1}{\rho}\frac{\partial}{\partial z}\left(\mu \frac{\partial u}{\partial z}\right)$$

If μ is constant, then the above expression can be reduced to

$$\frac{1}{\rho}\frac{\partial}{\partial z}\left(\mu\frac{\partial u}{\partial z}\right) = \nu\frac{\partial^2 u}{\partial z^2}$$

where $\nu = \mu/\rho$ is known as the **kinematic viscosity coefficient.** Analogous derivations can be performed to determine the viscous stresses acting in the other directions. The resulting frictional force per unit mass in the *x*, *y*, and *z* directions is

$$\vec{F}_{fr} = \nu\,\nabla^2\vec{v}$$

5.5: Introduction to the Apparent Forces

In expressing his first law, Sir Isaac Newton states: "Every body persists in its state of rest or of uniform motion in a straight line unless it is compelled to change that state by forces impressed on it." In other words, a mass in uniform motion relative to a coordinate system fixed in space will remain in uniform motion in the absence of any forces. Any motion relative to a coordinate system fixed in space is known as **inertial motion** and the reference frame in which that motion is measured is known as an **inertial reference frame**. Most of us live at a single location long enough to become accustomed to thinking of north, south, east, and west as fixed directions. In reality, however, the direction I call "north" is not the same, as viewed from the perspective of a space traveler orbiting Earth. If one considers the intersection of latitude and longitude lines on a globe as the intersections of a Cartesian x and y grid describing the Earth, then it is clear that since the Earth rotates, this coordinate system is accelerating and thus provides us with a non-inertial reference frame. It might appear that given our non-inertial reference frame we are not able to apply Newton's laws of motion to motion relative to the Earth. Of course, this is not true, but we do have to make some correction for the non-inertial nature of the reference frame by which we measure all such motion. We will make the necessary corrections by introducing the **centrifugal** and **Coriolis forces**, the so-called **apparent forces**. But first, it is instructive to consider physically why the coordinate system matters at all. We can do this by considering application of Newton's laws to experiments conducted inside a closed elevator car.

In the first case, let us imagine that the car is stationary or moving with a constant velocity, $\vec{V}$. Under such conditions imagine that a weight is dropped within the moving car. Upon

making the appropriate measurements and calculations, you would determine that the weight had fallen toward the floor of the car with a measurable, constant acceleration of $9.80\ m/s^2$. This acceleration would be observed relative to the walls and floor of the elevator car in a Cartesian coordinate system defined by the dimensions of the elevator car. In such a case, an observer in the elevator car would note complete agreement between the results of the experiment and Newton's laws of motion since the constant velocity elevator car provides an inertial reference frame for this experiment.

In the second case, we remotely observe the elevator car falling freely through the elevator shaft. If a similar weight is dropped within the car the weight appears to remain suspended in mid-air, at a constant elevation above the floor of the car. Measured relative to the coordinate frame of the car, the weight has zero acceleration even though to us remote observers it is clearly accelerating toward the ground at a rate of $9.80\ m/s^2$. Viewed from inside the car, Newton's laws seem to fail here, but this is because the coordinate system itself is accelerating and is therefore non-inertial. The latitude/longitude coordinate system on a rotating Earth is also accelerating and so we have to take that acceleration into account in order to apply Newton's laws accurately to objects moving relative to that Earth-based coordinate system.

5.6: The Centrifugal Force

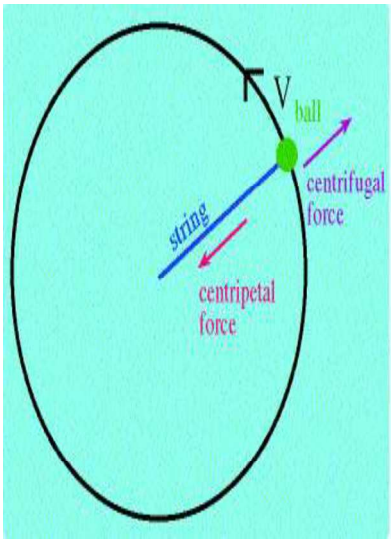

Figure 5.5 The rotating ball on a string experiences an inward-directed centripetal acceleration, indicated by the red arrow. To the observer on the ball, a compensating centrifugal force, indicated by the purple arrow, must be included to describe accurately motions on the ball itself.

Each of us is located a certain distance from the axis of rotation of the Earth. Depending upon the exact distance, we are rotating around that axis at a very high speed, but constant speed. Each of us is, therefore, not unlike the ball on the end of the string depicted in

Figure 5.5. The speed of the ball is $v = \omega r$, where ω is angular speed of the ball and r is the radius of rotation. However, the direction of the ball changes continuously and so, as viewed from the perspective of the ball, there is a uniform centripetal acceleration caused by the force of the string pulling on the ball directed toward the axis of rotation equal to

$$\frac{dv}{dt} = -\frac{v^2}{r} = -\omega^2 r$$

Suppose you are on the ball and rotating with it. From your perspective the ball is stationary but, in reality, a centripetal acceleration is still being exerted upon it. In order for a person on the ball to apply Newton's laws under this condition, an apparent force that exactly balances the true centripetal force must be included in the physics; this apparent force is known as the centrifugal force. In order to balance the centripetal acceleration, the centrifugal acceleration is directed outward along the radius of rotation and is given by $\omega^2 r$.

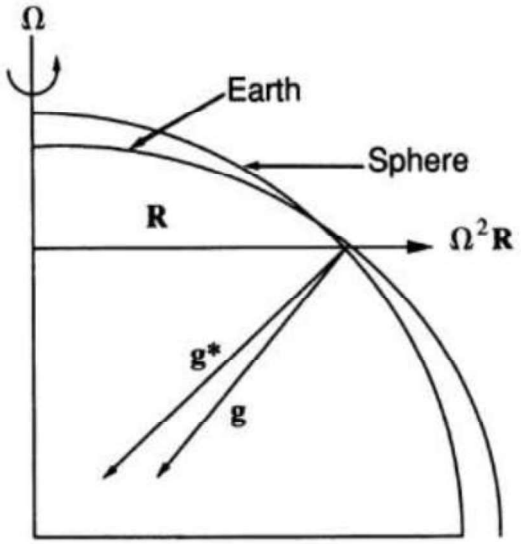

Figure 5.6 Relationship between the true gravitational vector g^* and gravity g on a rotating Earth.

As depicted in Figure 5.6, on a rotating Earth, the centrifugal force affects the vertical force balance. When the centrifugal force and gravitational force $\vec{g}^*$ are added, the result is called **effective gravity** ($\vec{g}$) and is given by $\vec{g} = \vec{g}^* + \Omega^2 \vec{R}$ where Ω is the rotation rate of the Earth, and $\vec{R}$ is the position vector from the axis of rotation to the object in question. Note that effective gravity, thus defined, is directed perpendicular to the local tangent of the surface of the Earth -- not necessarily toward the center of the Earth. In fact, since $\Omega^2 \vec{R}$ is directed away from the axis of rotation, $\vec{g}$ is *not* directed toward the center of the Earth except at the poles and the equator! Were the Earth a perfect sphere, this fact would result in the existence of a horizontal,

equatorward-directed component of gravity. The relatively malleable crust of the Earth has long since responded to this circumstance and adopted its oblate spheroidal shape with an equatorial radius some 21 km larger that its polar radius. Given such a slightly distorted shape, the local vertical direction everywhere on Earth is defined parallel to $\vec{g}$. The centrifugal force component of effective gravity is an example of the effect of rotation on objects at rest with respect to the Earth-based rotating frame of reference. In order to apply Newton's laws accurately to the motion of objects relative to that rotating frame an additional apparent force, the Coriolis force, must be considered.

5.7: The Coriolis Force

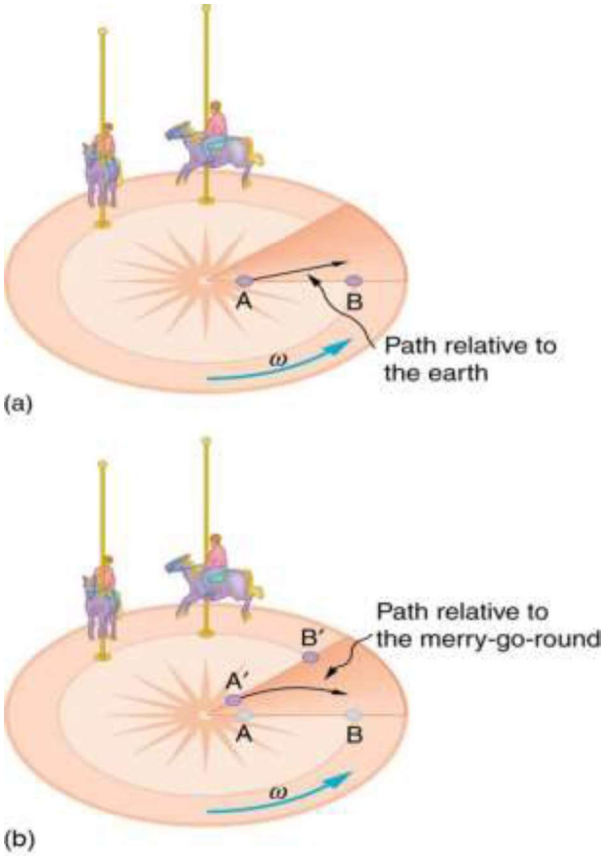

Figure 5.7 Schematic of merry-go-round illustrating the Coriolis force.

Consider a experiment in which one student takes a position on a merry-go-round and another student takes a position some distance above the ground in an adjacent tree. The merry-go-round is set spinning and a ball is pushed from the center of the merry-go-round toward the spinning student. From the vantage point of the tree, the motion of the ball appears as a straight

line, as it should since a uniform force was administered to it. But from the perspective of the rotating frame, the ball appears to accelerate in a curved path, away from the observer in a direction opposite to the direction of rotation. Upon consulting each other's notes, the students conclude that an apparent force, arising from the rotation of the merry-go-round, deflects the ball from its path. This apparent force is the **Coriolis force**.

A careful examination of our thought experiment above reveals more information and details about the Coriolis force.

- The magnitude of the Coriolis force depends on the rotation rate of the Earth. The deflection of the ball from its path would increase if the rotation rate of the merry-go-round increased.
- The magnitude of the Coriolis force depends on latitude. The deflection of the ball from its path is felt more at the rim of the merry-go-round than the center of the merry-go-round. On the Earth, the Coriolis force is zero at the equator and increases towards the poles.
- The magnitude of the Coriolis force is proportional to the velocity of the object. If the object's speed is zero, there is no relative motion and thus the Coriolis force is zero. Since an object's momentum increases with speed, a larger force is required to change its momentum. This suggests that the Coriolis force increases as the velocity of the object increases.
- The Coriolis force always acts to deflect an object to the right (left) of its direction of motion in the Northern (Southern) hemisphere (as shown in Figure 5.8). This also implies that the Coriolis force acts perpendicular to the direction of motion. Since the Coriolis force always acts perpendicular to the motion vector, it can do no work on the moving object. Thus, the Coriolis force can only change the direction of motion but cannot initiate motion in an object at rest.

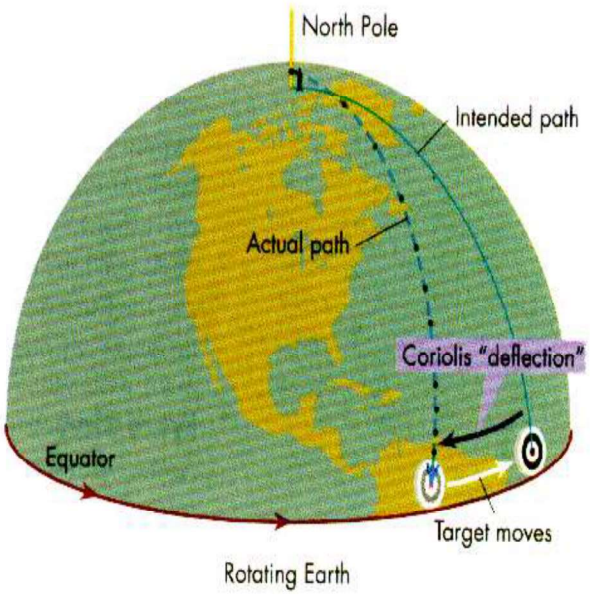

Figure 5.8: Schematic of Coriolis deflection in Northern Hemisphere

These considerations suggest that the magnitude of the Coriolis force depends upon wind speed, the rotation rate of the Earth, and the latitude. It can be shown that the magnitude of the Coriolis force is given by $F_{cor} = 2\Omega|\vec{V}|\sin\phi$ where Ω is the rotation rate of the Earth and ϕ is the latitude. Using a shorthand in which f, the so-called **Coriolis parameter**, is given by $f = 2\Omega\sin\phi$, we can rewrite the magnitude of the Coriolis force as $F_{cor} = f|\vec{V}|$. Because of the Coriolis force, an object moving eastward (westward) will deflect to the south (north) in the Northern Hemisphere. Similarly, an object moving northward (southward) will deflect to the east (west) in the Northern Hemisphere.

**5.7.1: Derivation of Apparent Forces

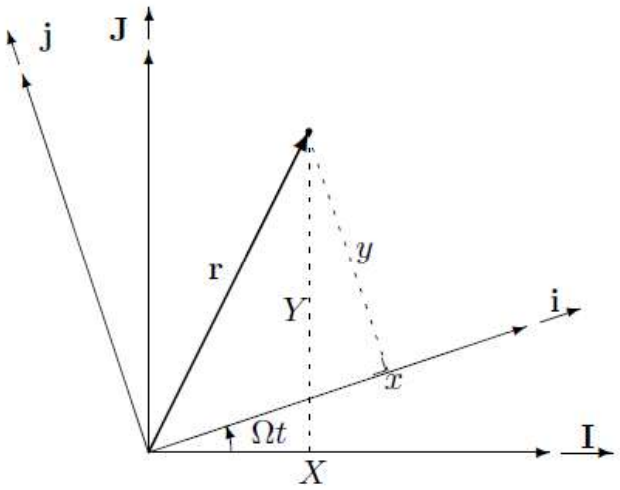

Figure 5.9 Fixed (X, Y) and rotating (x, y) reference frames.

To derive the apparent forces, let the X and Y axes form the inertial reference frame and the x and y axes be those of a rotating reference frame (with a rotation rate Ω) with the same origin as shown in Figure 5.9. The corresponding unit vectors are denoted $(\boldsymbol{I}, \boldsymbol{J})$ and $(\boldsymbol{i}, \boldsymbol{j})$. At any time t, the rotating x-axis makes an angle Ωt with the fixed X-axis. It follows that

$$\boldsymbol{i} = \boldsymbol{I}\cos\Omega t + \boldsymbol{J}\sin\Omega t\,, \quad \boldsymbol{I} = \mathbf{i}\cos\Omega t - \boldsymbol{j}\sin\Omega t$$
$$\boldsymbol{j} = -\boldsymbol{I}\sin\Omega t + \boldsymbol{J}\cos\Omega t\,, \quad \boldsymbol{J} = \mathbf{i}\sin\Omega t - \boldsymbol{j}\cos\Omega t$$

and that the coordinates of the position vector $\vec{r} = X\boldsymbol{I} + Y\boldsymbol{J} = x\boldsymbol{i} + y\boldsymbol{j}$ of any point in the plane are related by

$$x = X\cos\Omega t + Y\sin\Omega t\,, \quad y = -X\sin\Omega t + Y\cos\Omega t$$

The first time derivative of the above expression gives

$$\frac{dx}{dt} = \frac{dX}{dt}\cos\Omega t + \frac{dY}{dt}\sin\Omega t - \Omega X\sin\Omega t + \Omega Y\cos\Omega t = \frac{dX}{dt}\cos\Omega t + \frac{dY}{dt}\sin\Omega t + \Omega y$$

$$\frac{dy}{dt} = -\frac{dX}{dt}\sin\Omega t + \frac{dY}{dt}\cos\Omega t - \Omega X\cos\Omega t - \Omega Y\sin\Omega t = -\frac{dX}{dt}\sin\Omega t + \frac{dY}{dt}\cos\Omega t - \Omega x$$

A second derivative with respect to time provides in a similar manner

$$\frac{d^2x}{dt^2} = \left(\frac{d^2X}{dt^2}\cos\Omega t + \frac{d^2Y}{dt^2}\sin\Omega t\right) + 2\Omega\left(-\frac{dX}{dt}\sin\Omega t + \frac{dY}{dt}\cos\Omega t\right)$$
$$-\Omega^2(X\cos\Omega t + Y\sin\Omega t) = \left(\frac{d^2X}{dt^2}\cos\Omega t + \frac{d^2Y}{dt^2}\sin\Omega t\right) + 2\Omega V - \Omega^2 x$$

$$\frac{d^2y}{dt^2} = \left(-\frac{d^2X}{dt^2}\sin\Omega t + \frac{d^2Y}{dt^2}\cos\Omega t\right) + 2\Omega\left(\frac{dX}{dt}\cos\Omega t + \frac{dY}{dt}\sin\Omega t\right)$$
$$-\Omega^2(-X\sin\Omega t + Y\cos\Omega t) = \left(-\frac{d^2X}{dt^2}\sin\Omega t + \frac{d^2Y}{dt^2}\cos\Omega t\right) - 2\Omega U - \Omega^2 y$$

The relative acceleration (in the rotating frame) is given by

$$\vec{a} = \frac{d^2x}{dt^2}\boldsymbol{i} + \frac{d^2y}{dt^2}\boldsymbol{j}$$

The absolute acceleration (in the inertial frame) is given by

$$\vec{A} = \frac{d^2X}{dt^2}\boldsymbol{I} + \frac{d^2Y}{dt^2}\boldsymbol{J} = \left(\frac{d^2X}{dt^2}\cos\Omega t + \frac{d^2Y}{dt^2}\sin\Omega t\right)\boldsymbol{i} + \left(-\frac{d^2X}{dt^2}\sin\Omega t + \frac{d^2Y}{dt^2}\cos\Omega t\right)\boldsymbol{j}$$

Comparing these expressions gives

$$A_x = a_x - 2\Omega v - \Omega^2 x, \quad A_y = a_y + 2\Omega u - \Omega^2 y$$

We now see that the difference between absolute and relative acceleration consists of two contributions. The first contribution, proportional to Ω, is called the **Coriolis acceleration** and the second contribution, proportional to Ω^2, is called the **centrifugal acceleration**. The preceding results can also be written in vector form. Defining $\vec{\Omega} = \Omega\boldsymbol{k}$ where $\boldsymbol{k}$ is the unit vector in the third dimension, we have $\vec{A} = \vec{a} + 2\vec{\Omega}\times\vec{u} + \vec{\Omega}\times\left(\vec{\Omega}\times\vec{r}\right)$. We now see that

$$\vec{F}_{cor} = 2\vec{\Omega}\times\vec{u}, \quad \vec{F}_{cen} = \vec{\Omega}\times\left(\vec{\Omega}\times\vec{r}\right)$$

We have now considered all the forces necessary to accurately describe the dynamics of an air parcel in the atmosphere. We are now in the position to derive the fundamental equations of motion

**5.8: The Fundamental Equations of Motion

Recall that Newton's 2nd law is a statement of the conservation of momentum:

$$\frac{d}{dt}\left(m\vec{V}\right) = \vec{F}_{net}$$

However, it is strictly true, as we have already considered, only in an inertial frame of reference. As discussed previously, the five major forces that impact atmospheric motion are the pressure gradient force, the gravitational force, the frictional force, the centrifugal force, and the Coriolis force. This implies the acceleration of an air parcel following the relative motion in a rotating reference frame is equal to the sum of the atmospheric forces.

From section 5.7.1, we derived a relationship between the absolute acceleration of an air parcel $\left(\vec{A}\right)$ and the acceleration of the same air parcel relative to Earth $(\vec{a})$. Defining $\vec{A} = d_a\vec{V}_a/dt$ and $\vec{a} = d\vec{V}/dt$, we have

$$\frac{d_a\vec{V}_a}{dt} = \frac{d\vec{V}}{dt} + 2\vec{\Omega}\times\vec{V} + \vec{\Omega}\times\left(\vec{\Omega}\times\vec{r}\right)$$

In words, the above expression states that the Lagrangian acceleration in an inertial system is equal to the sum of (1) the Lagrangian change of relative velocity, plus (2) the Coriolis acceleration from relative motion in the relative frame, plus (3) the centripetal acceleration resulting from the rotation of the coordinate system. Recalling Newton's second law and the fact that we will consider the pressure gradient force, the frictional force, and gravitational force as the only real forces acting on the atmospheric fluid, we find that

$$\frac{d_a\vec{V}_a}{dt} = \frac{d\vec{V}}{dt} + 2\vec{\Omega}\times\vec{V} + \vec{\Omega}\times\left(\vec{\Omega}\times\vec{r}\right) = -\frac{1}{\rho}\nabla p + \vec{g}^{*} + \nu\,\nabla^2\vec{V}$$

Rearranging in terms of the relative acceleration gives

$$\frac{d\vec{V}}{dt} = -\frac{1}{\rho}\nabla p - 2\vec{\Omega}\times\vec{V} - \vec{\Omega}\times\left(\vec{\Omega}\times\vec{r}\right) + \vec{g}^{*} + \nu\,\nabla^2\vec{V} = -\frac{1}{\rho}\nabla p + \vec{g} + \nu\,\nabla^2\vec{V}$$

where the centripetal force has been combined with the gravitation force $\vec{g}^{*}$ in the gravity term $(\vec{g})$. This expression states that the acceleration following the relative motion in a rotating reference frame is equal to the sum of (1) the Coriolis force, (2) the pressure gradient force, (3) effective gravity, and (4) the friction force. This is a major result, but it remains in vectorial form

only – a form not particularly amenable to analysis. Since synoptic-scale weather systems of interest are sufficiently small relative to the size of the earth, it is acceptable to write the vector momentum equation in terms of Cartesian coordinates.

First, the component form of the pressure gradient force is given by

$$-\frac{1}{\rho}\nabla p = -\frac{1}{\rho}\frac{\partial p}{\partial x}\hat{\imath} - \frac{1}{\rho}\frac{\partial p}{\partial y}\hat{\jmath} - \frac{1}{\rho}\frac{\partial p}{\partial z}\hat{k}$$

The effective gravity, which acts downward in the local vertical direction, is represented by

$$\vec{g} = -g\hat{k}$$

while friction can be represented as

$$\nu\nabla^2\vec{V} = \nu\nabla^2 u\,\hat{\imath} + \nu\nabla^2 v\,\hat{\jmath} + \nu\nabla^2 w\,\hat{k}$$

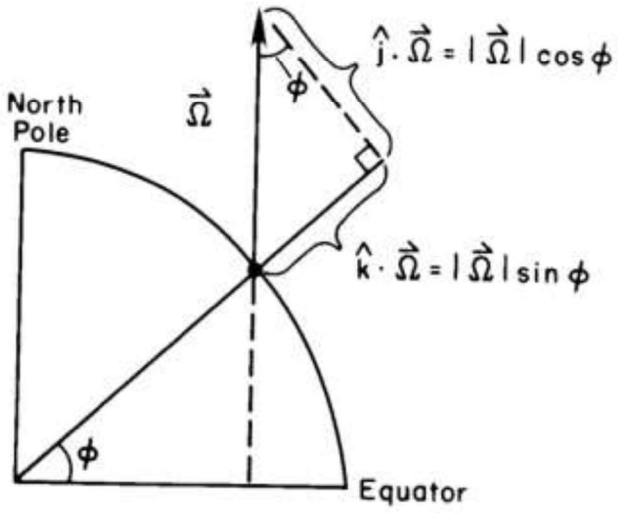

Figure 5.10 Partition of the rotation vector $\vec{\Omega}$ into its vertical and meridional components

Figure 5.10 demonstrates that the rotation vector $\vec{\Omega}$ is perpendicular to the x direction and so has components only in the positive $\hat{\jmath}$ and positive $\hat{k}$ directions. Considering the trigonometry in Figure 5.10, the $\hat{k}$ component of $\vec{\Omega}$ has magnitude $\Omega\sin\phi$ while the $\hat{\jmath}$ component has magnitude $\Omega\cos\phi$. Thus, the components of the Coriolis force term is given by

$$-2\vec{\Omega}\times\vec{V} = \begin{vmatrix} \hat{\imath} & \hat{\jmath} & \hat{k} \\ 0 & -2\Omega\cos\phi & -2\Omega\sin\phi \\ u & v & w \end{vmatrix}$$
$$= -(2\Omega\cos\phi\, w - 2\Omega\sin\phi\, v)\hat{\imath} - 2\Omega\sin\phi\, u\hat{\jmath} + 2\Omega\cos\phi\, u\hat{k}$$

Therefore, the three component equations of motion for flow on the rotating Earth is given by

$$\frac{du}{dt} = -\frac{1}{\rho}\frac{\partial p}{\partial x} + 2\Omega \sin\phi v - 2\Omega \cos\phi\, w + \nu\nabla^2 u$$

$$\frac{dv}{dt} = -\frac{1}{\rho}\frac{\partial p}{\partial y} - 2\Omega \sin\phi\, u + \nu\nabla^2 v$$

$$\frac{dw}{dt} = -\frac{1}{\rho}\frac{\partial p}{\partial z} + 2\Omega \cos\phi\, u + \nu\nabla^2 u$$

In the next chapter, we will use these equations to develop an understanding of synoptic-scale motions.

Chapter 6: The Governing Equations

In the previous chapter, we considered all the forces necessary to accurately describe the dynamics of an air parcel in the atmosphere. This led us to the fundamental equations of motion for the atmosphere. In this chapter, we will use these equations of motion to develop a practical, dynamical understanding of the atmosphere at the middle latitudes.

**6.1: Introducing Scale Analysis

The complete set of governing equations for the atmosphere is difficult to utilize and conceptually comprehend. For specific applications, the equations can be simplified through the elimination of terms that are unimportant to the situation in question. A procedure known as ***scale analysis*** is a systematic strategy to determine which terms in the equations, often associated with specific physical processes, are most important and which are negligible in a given meteorological setting. By characterizing the temporal and spatial scales associated with specific weather systems, we can systematically neglect "small" terms in the governing equations in the study of those systems. While these assumptions reduce accuracy, their use is justified by the physical insight obtained from the simplified equations.

Why is it important to derive customized equation sets and techniques for different classes of weather system, and why must students work through these derivations? In addition to the dynamical insight afforded by isolating the essential physics of a given weather system, one must know when to apply and when not to apply a given technique. Suppose that a particular weather forecasting technique is developed from simplified equations that are valid for synoptic-scale flows, and that this technique gains widespread acceptance in the forecasting community. If a forecaster were to apply this technique to a *mesoscale* weather system, the technique may fail, perhaps resulting in a poor weather forecast. This is one example of why students are required to derive equations, because it is important to know what assumptions were made in the development of a given technique, and this information is needed to deduce which tools are appropriate for which situations.

In addition, the ability to apply a systematic approach to the governing equations allows atmospheric scientists to develop new equations and techniques to study unique problems. In applying scale analysis to various weather systems, we must identify the characteristic horizontal length and time scales, and these are often related to one another. The length scale can be related to the size of a weather system, or how far an air parcel would travel within the system during a

given time interval. The time scale can be related to how long it would take an air parcel to circulate within the system, or to traverse the characteristic length scale (implying a characteristic velocity scale).

**6.1.1: Simplifying the Equations of Motion

The observationally based characteristic values for the set of variables in the equations of motion are given by

$U \approx 10\ m/s$	Characteristic horizontal velocity
$W \approx 1\ cm/s$	Characteristic vertical velocity
$L \approx 1000\ km = 10^6\ m$	Characteristic length scale of synoptic-scale features
$H \approx 10\ km = 10^4\ m$	Characteristic depth scale
$\delta p \approx 10\ mb = 1000\ Pa$	Characteristic horizontal pressure fluctuation
$P_0 \approx 1000\ mb = 10^5\ Pa$	Characteristic pressure
$t \approx L/U = 10^5\ s$	Characteristic time scale

We can now estimate the magnitude of each term in the equations of motion for a given latitude. For the midlatitudes, it is convenient to consider a disturbance centered at latitude $\phi_0 = 45°$ and introduce the notation

$$f_0 = 2\Omega \sin \phi_0 = 2\Omega \cos \phi_0 \approx 10^{-4}\ s^{-1}$$

Figure 6.1 shows the characteristic magnitude of each term in the horizontal equations of motion based on the scaling considerations given above. The molecular friction term is so small that it may be neglected for all motions except the smallest scale turbulent motions near the ground. It is apparent from Figure 6.1 that for midlatitude synoptic scale disturbances the Coriolis force (term B) and the pressure gradient force (term F) are in approximate balance. Retaining only these two terms gives as a useful simplification of the horizontal equations of motion

$$-fv \approx -\frac{1}{\rho}\frac{\partial p}{\partial x}; \quad fu \approx -\frac{1}{\rho}\frac{\partial p}{\partial y}$$

where $f \equiv 2\Omega \sin\phi$ is called the *Coriolis parameter.* This balance is known as **geostrophic balance**.

Scale Analysis of the Horizontal Momentum Equations

	A	B	C	D	E	F	G
x – Eq.	$\frac{Du}{Dt}$	$-2\Omega v \sin\phi$	$+2\Omega w \cos\phi$	$+\frac{uw}{a}$	$-\frac{uv\tan\phi}{a}$	$=-\frac{1}{\rho}\frac{\partial p}{\partial x}$	$+F_{rx}$
y – Eq.	$\frac{Dv}{Dt}$	$+2\Omega u \sin\phi$		$+\frac{vw}{a}$	$+\frac{u^2\tan\phi}{a}$	$=-\frac{1}{\rho}\frac{\partial p}{\partial y}$	$+F_{ry}$
Scales	U^2/L	$f_0 U$	$f_0 W$	$\frac{UW}{a}$	$\frac{U^2}{a}$	$\frac{\delta P}{\rho L}$	$\frac{\nu U}{H^2}$
($m\,s^{-2}$)	10^{-4}	10^{-3}	10^{-6}	10^{-8}	10^{-5}	10^{-3}	10^{-12}

Scale Analysis of the Vertical Momentum Equation

z - Eq.	Dw/Dt	$-2\Omega u\cos\phi$	$-(u^2+v^2)/a$	$=-\rho^{-1}\partial p/\partial z$	$-g$	$+F_{rz}$
Scales	UW/L	$f_0 U$	U^2/a	$P_0/(\rho H)$	g	$\nu W H^{-2}$
$m\,s^{-2}$	10^{-7}	10^{-3}	10^{-5}	10	10	10^{-15}

Figure 6.1: Scale analysis of the equations of motion

A similar scale analysis can be applied to the vertical component of the momentum equation. Because pressure decreases by about an order of magnitude from the ground to the tropopause, the vertical pressure gradient may be scaled by P_0/H, where P_0 is the surface pressure and H is the depth of the troposphere. The terms in the vertical momentum equation are also given in Figure 6.1. As with the horizontal momentum equations, we consider motions centered at 45° latitude and neglect friction. The scaling indicates that to a high degree of accuracy, the gravitational force and the pressure gradient force are in approximate balance. Retaining only these two terms gives as a useful simplification of the vertical momentum equation:

$$-g \approx -\frac{1}{\rho}\frac{\partial P}{\partial z}$$

This balance is known as **hydrostatic balance**.

Thus, an analysis of the momentum equations for mid-latitude synoptic-scale motions demonstrate that the vertical equation of motion is dominated by two terms, the vertical pressure gradient force and the gravitational force, and the horizontal equations of motion are dominated by two terms, the horizontal pressure gradient force and the Coriolis force. The first condition

leads to hydrostatic balance, whereas the second condition leads to a balanced condition called geostrophic balance. Thus, a scaling of the equations of motion for mid-latitude synoptic scale motions renders the following fundamental statement regarding the nature of the mid-latitude atmosphere on Earth:

To a first order, the mid-latitude atmosphere on Earth is in hydrostatic and geostrophic balance

6.2: The Hydrostatic Equation

Apart from performing a scaling analysis, another important way to describe the physical behavior of the atmosphere is to examine the fundamental conservative quantities that govern the atmosphere: mass, momentum, and energy. In the next sections, we will investigate the manner in which these quantities and their various interactions serve to describe the building blocks of a dynamical understanding of the atmosphere at the middle latitudes. The first quantity that we will study will be mass. For our purposes, we shall define mass as the measure of the substance of an object and make that measurement in kilograms (kg). We must first consider the distribution of mass in the atmosphere and the force balance that underlies this distribution. A number of insights concerning the vertical structure of the atmosphere proceed directly from this understanding.

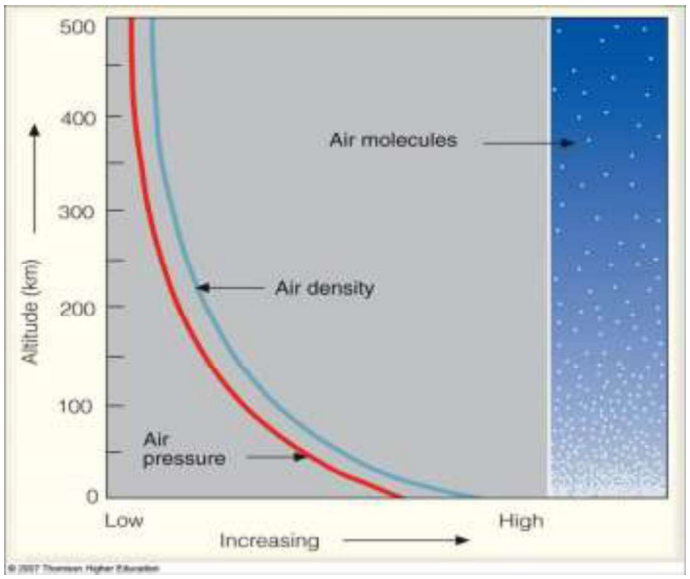

Figure 6.2 Schematic of the distribution of mass in the atmosphere

Observations show that the pressure decreases exponentially with height within the troposphere, which implies that most of the mass of the atmosphere resides near Earth's surface. As a consequence, there is a strong vertical pressure gradient force that exists throughout the atmosphere which compels air to move from higher pressure (near the surface) to lower pressure (above the surface) (i.e. the vertical pressure gradient force is an upward-directed force). The fact that the atmosphere does not race away into space under this forcing is a consequence of the fact that there is also the force of gravity acting on the atmosphere, pulling it downwards.

The atmosphere tends to exhibit a balance between this vertical pressure gradient force, which points upward, and the gravitational force, which points downward. We call this balance of forces **hydrostatic balance.** The condition for hydrostatic balance leads to the following expression:

$$\frac{dP}{dz} = -\rho g$$

This expression, known as the **hydrostatic equation**, represents a fundamental balance characteristic of the Earth's atmosphere. Though strictly true only for an atmosphere at rest (hence the static portion of the name), this hydrostatic balance is obeyed to great accuracy under nearly all conditions in the Earth's atmosphere.

6.3: The Thickness Equation

Consider the unit area column of atmosphere contained between 850 hPa and 500 hPa shown in Figure 6.3. Since pressure is defined as force per unit area, we have isolated in that column an atmospheric mass sufficient to exert 350 hPa of pressure. Such a slab of the atmosphere has a unique mass whether it extends from 850 to 500 hPa or from 717 to 367 hPa. In fact, the mass of this column can be precisely calculated as 3567.79 kg. Though the mass of a 350 hPa, unit area slab of the atmosphere is unique, its depth might be different from one day to the next. We will refer to this geometric depth as the **thickness** between two isobaric surfaces.

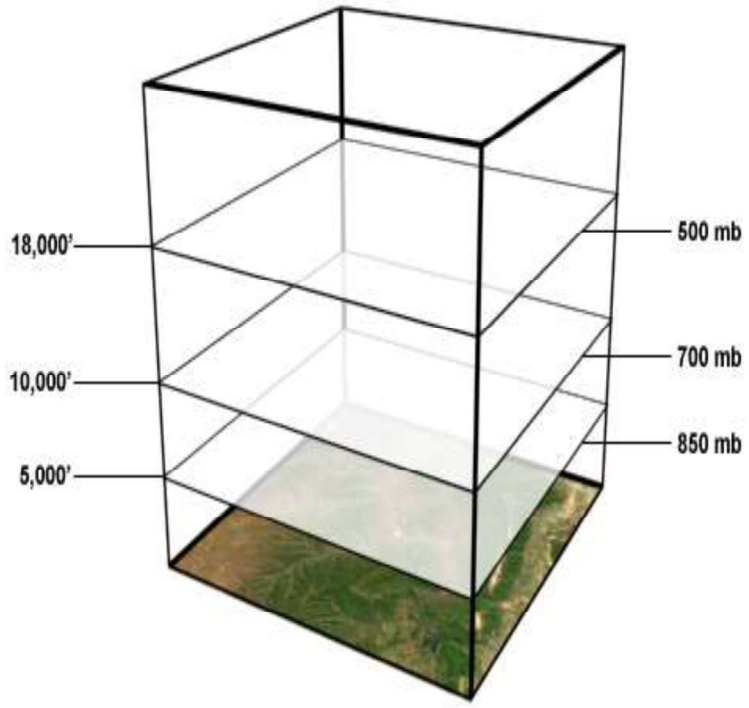

Figure 6.3 Schematic of pressure layers within the atmosphere

Clearly, if the thickness varies, then so does the volume of the unit area slab. The variation of the volume of the slab dictates that the density of the air contained within the slab varies as well: less (more) dense air will correspond to a greater (smaller) thickness. By the ideal gas law, less (more) dense air will correspond to a higher (lower) column average virtual temperature, T_v. Thus, column average virtual temperature should have a bearing on the thickness between two isobaric levels.

Combining the hydrostatic equation with the ideal gas law provides convincing evidence to support this hypothesis. Recall that the ideal gas law can be written as $P = \rho R_d T_v$ where P is the pressure, ρ is the density, R_d is the gas constant for dry air, and T_v is the virtual temperature. Using this expression, the hydrostatic equation can be rewritten as

$$\frac{dP}{dz} = -\frac{\rho g}{R_d T_v} \Rightarrow dz = -\frac{R_d T_v}{g}\frac{dP}{P}$$

If we integrate this expression between pressure levels P_1 and P_2 at which the heights are z_1 and z_2, we get

$$\frac{R_d \bar{T}_v}{g} \ln\left(\frac{P_1}{P_2}\right) = z_2 - z_1 = \Delta z$$

where $\bar{T}_v$ is the pressure-weighted, column average virtual temperature. This expression is known as the **thickness equation** and it quantifies our suspicion regarding the influence of column average temperature on the thickness of an isobaric column.

We can express the thickness equation (and, therefore, the hydrostatic equation) in terms of a quantity called **geopotential**, Φ. The geopotential is defined as the work required to raise a unit mass a distance dz above sea level. It quantifies the work (per unit mass) that is done against gravity in doing so. Mathematically, therefore, geopotential is given as $d\Phi = g\,dz$. Using this expression, we can rewrite the hydrostatic equation as

$$\frac{d\Phi}{dP} = -\frac{R_d \bar{T}_v}{P}$$

Correspondingly, the thickness equation can also be written as

$$R_d \bar{T}_v \ln\left(\frac{P_1}{P_2}\right) = g\Delta z = \Delta\Phi$$

Writing the geopotential in units of height gives us a new meteorology variable called **geopotential height**. The geopotential height is simply given by $Z = \Phi/g_0$ where g_0 is the global average gravity at sea level ($9.80\ m/s^2$). Thus, geometric height (z) and geopotential height Z are just about equal in the troposphere. Because geopotential height includes the variation of gravity with elevation, the geopotential height is sometimes referred to as a "gravity-adjusted height".

6.3.1: Reduction to Sea Level Pressure

There are several important applications of the hydrostatic and thickness equations that have a bearing on the analysis and understanding of mid-latitude weather systems. One of the most common analysis products used to characterize and understand the weather is a sea level pressure map (as shown in Figure 6.5). This is a map on which isobars of sea-level pressure are contoured in an attempt to identify and characterize the major circulation systems in a given location at a given time. In geographical regions characterized by high terrain, such as the Rocky Mountains of North America, the elevation is so far above sea level that use of the station pressure (i.e. the pressure actually measured with a barometer at the station) does not effectively

contribute to this goal. In such regions the thickness equation can be used to calculate a **reduced sea-level pressure** (i.e. an estimate of what the sea-level pressure would be were the surface elevation 0 m as shown in Figure 6.4). Consider the following example.

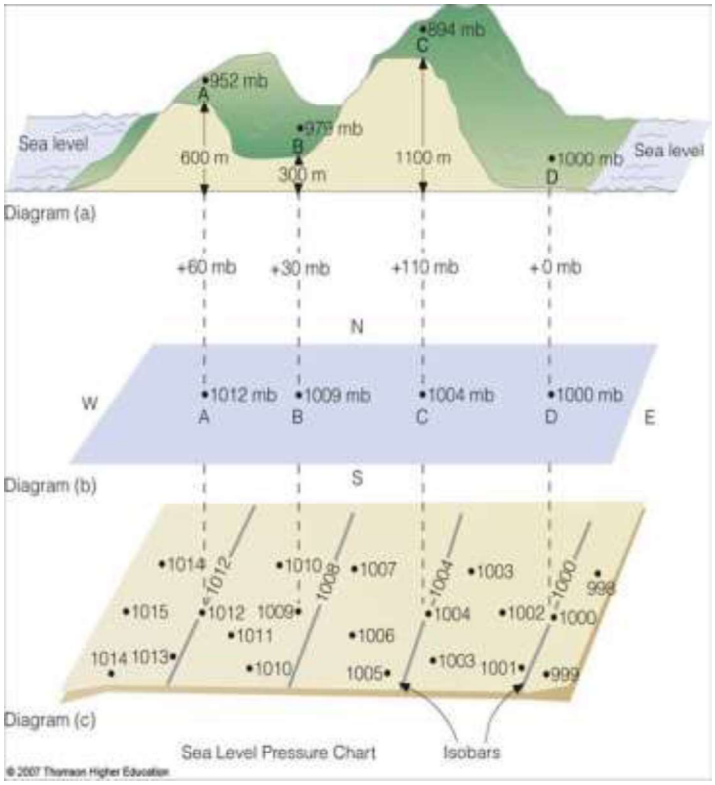

Figure 6.4 Schematic of sea-level pressure chart

In Figure 6.5, the station pressure at St Louis, Missouri (STL), a city close to sea level, on a certain day is measured to be 1010 hPa. Meanwhile, the station pressure at Denver, Colorado (DEN), whose elevation is 1609 m above sea level, is measured at 828 hPa. There is not a horizontal pressure difference of 180 hPa between STL and DEN. Most of the observed pressure difference is a consequence of the vertical variation of pressure. By reducing the station pressure to sea level at DEN, we attempt to discover how much of the observed pressure difference actually is a horizontal pressure difference.

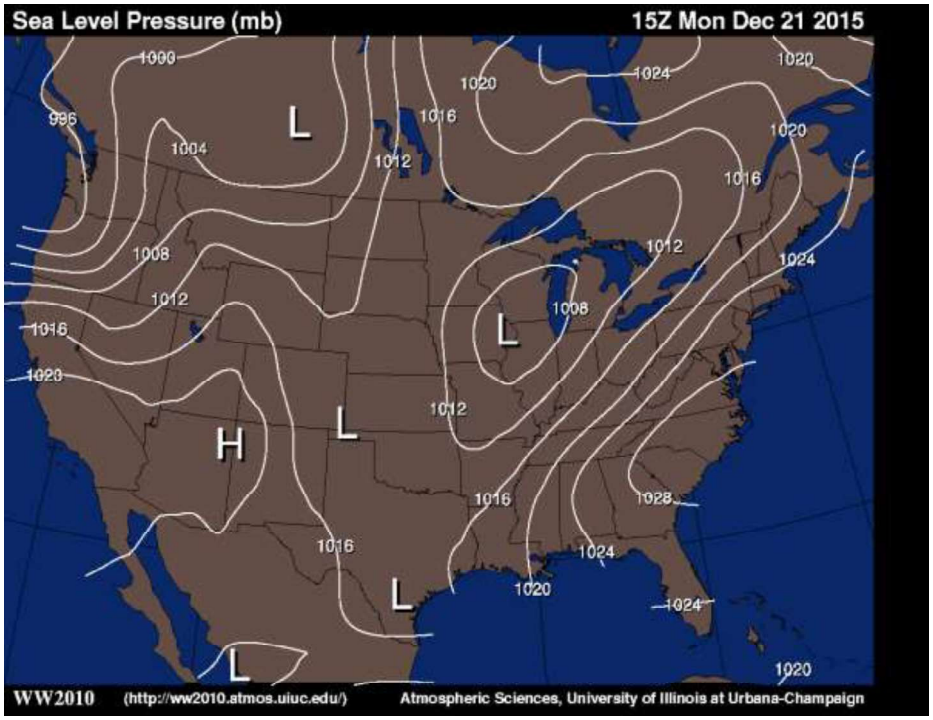

Figure 6.5 Sea-level pressure map of the continental U.S. for 21 December 2015 at 15 Z

We begin with the thickness equation $z_2 - z_1 = (R_d \bar{T}_v / g) \ln(P_1/P_2)$ with $z_2 = z_{DEN}$ and $z_1 = 0$ (the geometric height at sea level). Correspondingly, $P_2 = P_{STA}$ (observed station pressure) and $P_1 = P_{SLP}$ (the desired value we calculate as sea level pressure at DEN. Finally, $\bar{T}_v$ represents the average column temperature between sea level at DEN and the station elevation. Rearranging the thickness equation using the given variables, we have

$$\frac{g z_{DEN}}{R_d \bar{T}_v} = \ln\left(\frac{P_{SLP}}{P_{STA}}\right) \Rightarrow P_{SLP} = P_{STA} \exp\left[\frac{g z_{DEN}}{R_d \bar{T}_v}\right]$$

The above expression is known as the **altimeter equation** and is the standard expression for reducing station pressure to sea level. Supposing that the surface T_v at Denver is 20°C, we find that the reduced sea-level pressure at Denver would be 1012.5 hPa. This value can be usefully compared to the sea-level pressure at St. Louis on a synoptic weather chart.

6.3.2: Isobaric Charts

The definition of geopotential height and the thickness equation enables meteorologists to construct upper-air maps at constant pressure, also known as **isobaric charts** (as shown in Figure 5.5). By convention, radiosonde data records and reports upper air observations at 1000, 925, 850, 700, 500, 400, 300, 250, 200, 150, and 100 mb. Since pressure is fixed on isobaric charts, we can use the thickness equation to examine how geopotential height varies across that surface.

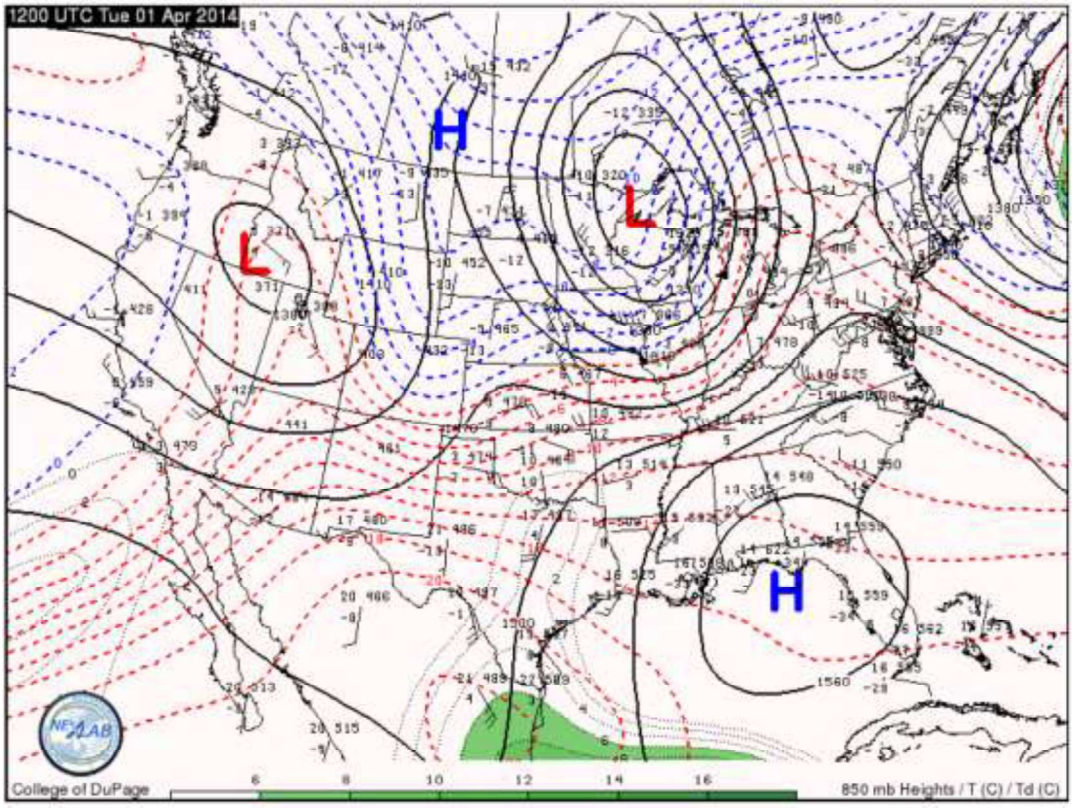

Figure 6.5 850-mb map analysis of the continental U.S. on 01 April 2014 at 1200 UTC. Black contours are geopotential height lines, red contours are isotherms greater than 0°C, and blue contours are isotherms less than 0°C

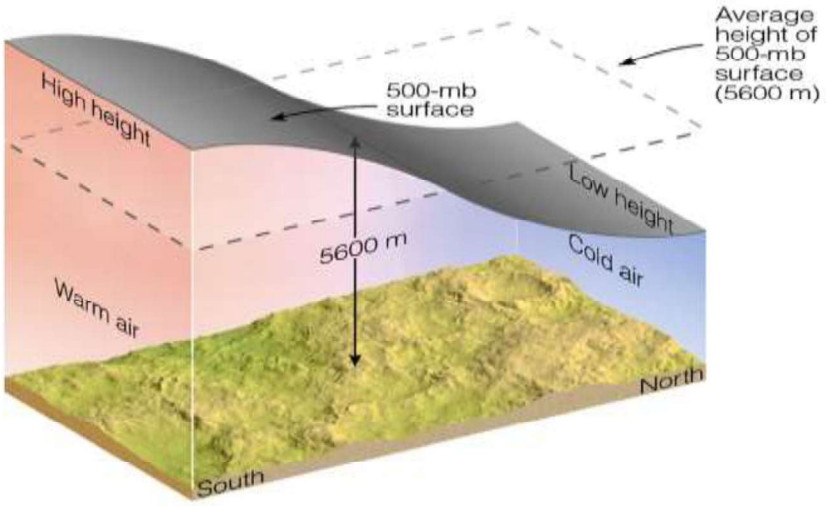

Figure 6.6 Schematic of geopotential height contours on a 500-mb isobaric chart

Since the atmospheric depth (i.e. thickness) is proportional to the mean atmospheric temperature, the isobaric surfaces will be located at higher level further south and at lower levels further north (as shown in Figure 6.6). Therefore, on an isobaric map, we plot lines of constant geopotential height (also called **isohypses**). Because of the relationship between pressure and height, the kinematics of pressure contours on a surface map is identical to the kinematics of geopotential height contours on upper-air isobaric charts. Thus, regions of low isohypse values are correlated with low pressure (trough) while isohypse values are correlated with high pressure (ridges).

6.3.3: Thickness and Temperature Advection

As mentioned previously, the thickness equation allows us to make a general relationship between temperature and geopotential heights on isobaric maps. As a rule, warmer temperatures in the lower troposphere imply higher geopotential heights at upper levels. Since warm air leads to a greater thickness than cold air, thickness is another easy way to diagnose where warm and cold air masses are present in the atmosphere. This also implies that thickness analyses can be used to locate synoptic fronts and to determine their intensity (since by definition a synoptic front must be associated with a horizontal thickness gradient). Consider the 500 mb map shown in Figure 6.7. Note that the regions of lowest thickness also correspond to the lowest geopotential heights. This means that a cold air mass is present in NE Canada and the wind field is advecting cold, polar air towards the northeast and Midwest US.

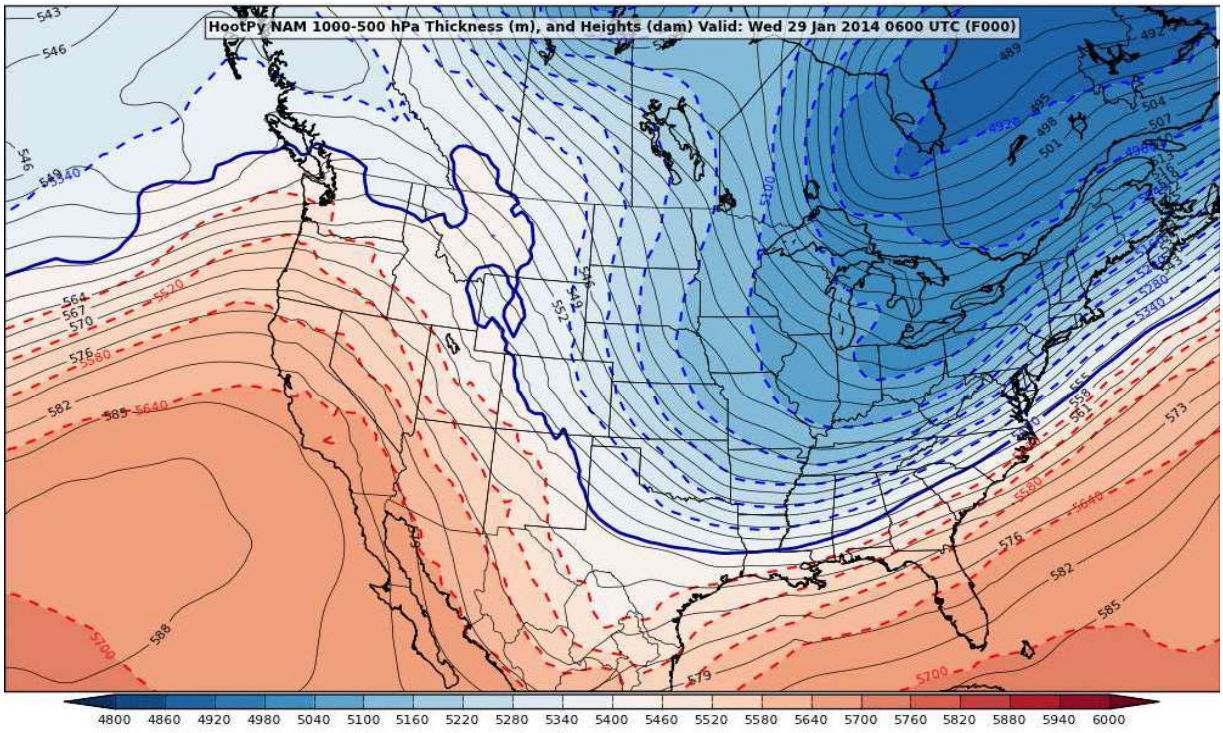

Figure 6.7 1000-500 hPa thickness and geopotential height map from 29 January 2014 at 06 Z

Thickness is often used to determine the 50% probability of snow, given that precipitation is occurring. This is referred to as the **rain-snow line**. Figure 5.8 shows thickness values for the 1000-500 mb layer associated with a 50% chance of snow given that precipitation is occurring. Comparing Figure 6.8 to Figure 6.7, it seems likely that if precipitation is occurring in the Midwest, then the 1000-500 mb layer indicate snow as the more probable form of precipitation. In the eastern US near sea level, $\Delta Z = 5400\ m$ for the 1000 to 500 mb layer (with mean virtual temperature of -7.1°C) closely corresponds to the 50% probability between rain and snow if precipitation is occurring. Consequently, the 5400 m line is used as an indicator of the rain-snow line. Note that the rain-snow line is substantially higher for sites at relatively high altitudes like Denver and Cheyenne since the warmest part of the layer is usually below the ground.

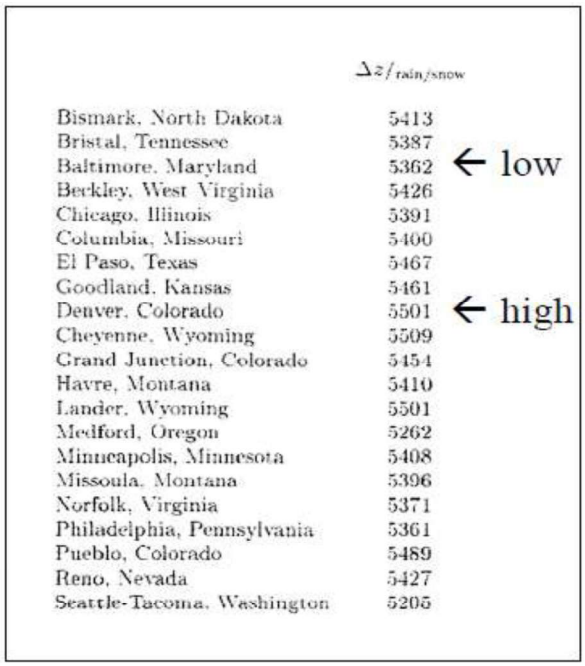

	$\Delta z/_{rain/snow}$	
Bismark, North Dakota	5413	
Bristal, Tennessee	5387	
Baltimore, Maryland	5362	← low
Berkley, West Virginia	5426	
Chicago, Illinois	5391	
Columbia, Missouri	5400	
El Paso, Texas	5467	
Goodland, Kansas	5461	
Denver, Colorado	5501	← high
Cheyenne, Wyoming	5509	
Grand Junction, Colorado	5454	
Havre, Montana	5410	
Lander, Wyoming	5501	
Medford, Oregon	5262	
Minneapolis, Minnesota	5408	
Missoula, Montana	5396	
Norfolk, Virginia	5371	
Philadelphia, Pennsylvania	5361	
Pueblo, Colorado	5489	
Reno, Nevada	5427	
Seattle-Tacoma, Washington	5205	

Figure 6.8 Thickness values for the 1000-500 mb layer associated with a 50% chance of snow given that precipitation is occurring

Now that we have acquired a perspective on the distribution of mass in the atmosphere, we turn to an investigation of how the conservation of mass relates divergence/convergence and vertical motion.

6.4: Mass Continuity Equation

Imagine trying to fill a small basin with water from a hose. If there's a leak in the basin, then one needs to know both the inflow rate from the hose as well as the outflow rate through the leak in order to accurately gauge the filling rate. If the inflow rate is suddenly increased while the outflow rate remains the same, it's simple to conclude that the mass of water in the basin will increase. If we designate the mass of water in the basin as M_w, then a simple expression of the mass continuity equation becomes

$$\frac{dM_w}{dt} = Inflow\ Rate - Outflow\ Rate$$

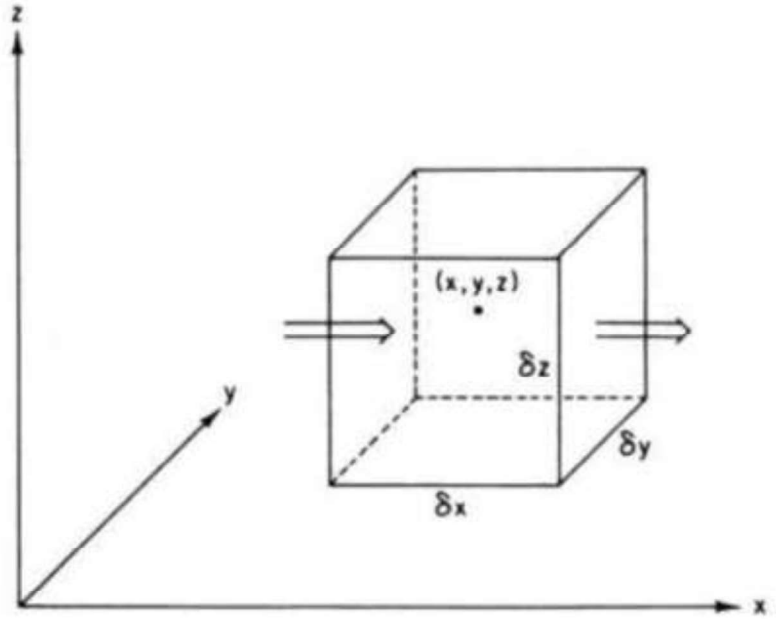

Figure 6.9 Schematic of cube, fixed in space, through which air flows

We can think of a slightly more abstract representation of this idea, illustrated in Figure 6.9, by considering an infinitesimal cube, fixed in space, through which air flows. The rate at which mass flows at the center of the cube (known as the **mass flux**) is given as the product of the velocity and the density of the air. If the inflow rate exceeds the outflow rate, we would say that mass is accumulating towards the center of the cube and thus there is net *convergence* into the infinitesimal cube. Conversely, if the outflow rate exceeds the inflow rate, we would say that mass is evacuating away from the center of the cube and thus there is net *divergence* out of the infinitesimal cube. In this way, we could define the divergence of the wind field as a measure of the rate at which mass is removed from a given volume of air and the convergence of the wind field as a measure of the rate at which mass is accumulates into a given volume of air. This physically suggests that the net rate of mass accumulation in the cube is represented by the divergence/convergence of the wind field. Writing this expression in terms of density gives

$$\frac{d\rho}{dt} \propto Net\ Divergence$$

In summary, the mass continuity equation states the regions of local convergence (divergence) leads to an increase (decrease) in mass. It is instructive at this point to consider the implications of the mass continuity equation for the atmosphere. A fluid in which individual parcels experience no change of density following the motion is known as an **incompressible fluid**. Even though the atmosphere is a compressible fluid, for many atmospheric phenomena the

compressibility is not a major physical consideration. In such cases, the mass continuity equation becomes a statement of zero velocity divergence throughout the depth of the entire atmosphere.

In synoptic meteorology, this statement can be explained in terms of **Dines compensation principle**. The Dines compensation principle states that there must be at least one level of nondivergence in the troposphere [typically called the **level of non-divergence** (LND)]. This level is usually around 550 mb, but can be highly variable depending on atmospheric stability. The compensation principle states that the convergence (divergence) that occurs above the LND tends to be offset by divergence (convergence) that occurs below the LND, as shown in Figure 6.10.

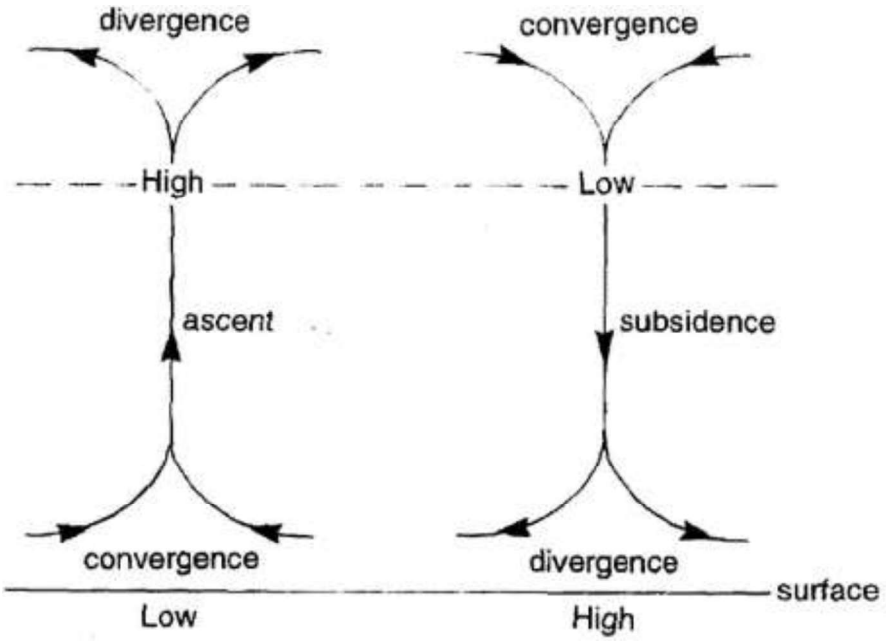

Figure 6.10 Dines compensation principle applied to large-scale circulations

Thus, if upper-level divergence occurs, the troposphere will attempt to compensate by initiating rising motion to "fill the void". Increased convergence in the lower troposphere will usually result. This process is sometimes referred to as the **chimney effect**. When air is forced to rise vertically from the surface, it rises into regions where pressure is lower. If the divergence aloft is stronger than the convergence in the lower levels, surface pressure falls will occur since mass is being removed from the column by divergence.

If upper-level convergence occurs, the troposphere will attempt to compensate by initiating sinking motion (also called **subsidence**). Increased divergence in the lower troposphere will usually result. This process is sometimes referred to as the "damper effect". If the convergence aloft is stronger than the divergence in the lower-levels, surface pressure rises will occur since mass is being added to the column by the convergence.

**6.4.1: Derivation of Mass Continuity Equation

As before, consider an infinitesimal cube, fixed in space, through which air flows, as shown in Figure 6.9. For such a fixed control volume, the net rate of mass inflow through the sides must equal the rate of accumulation of mass within the volume. The rate of inflow of mass through the left-hand face per unit area is

$$\left[\rho u - \frac{\partial}{\partial x}(\rho u)\frac{\delta x}{2}\right]$$

whereas the rate of outflow per unit area through the right-hand face is

$$\left[\rho u + \frac{\partial}{\partial x}(\rho u)\frac{\delta x}{2}\right]$$

Because the area of each of these faces is $\delta y \delta z$, the net flow rate into the volume due to the *x* velocity component is

$$\left[\rho u - \frac{\partial}{\partial x}(\rho u)\frac{\delta x}{2}\right] - \left[\rho u + \frac{\partial}{\partial x}(\rho u)\frac{\delta x}{2}\right] = -\frac{\partial}{\partial x}(\rho u)\delta x \delta y \delta z$$

Similar expressions hold for the *y* and *z* directions. Thus, the net rate of mass inflow is

$$-\left[\frac{\partial}{\partial x}(\rho u) + \frac{\partial}{\partial y}(\rho v) + \frac{\partial}{\partial z}(\rho w)\right]\delta x \delta y \delta z$$

and the mass inflow per unit volume is just $-\nabla \cdot \left(\rho \vec{V}\right)$, which must equal the rate of mass increase per unit volume. Now the increase of mass per unit volume is just the local density change $\partial \rho / \partial t$. Therefore, we have

$$\frac{\partial \rho}{\partial t} + \nabla \cdot \left(\rho \vec{V}\right) = 0$$

This is known as the **mass divergence form of the continuity equation.** An alternative form of the continuity equation is obtained by applying the vector identity

$$\nabla \cdot \left(\rho \vec{V}\right) = \rho \nabla \cdot \vec{V} + \vec{V} \cdot \nabla \rho$$

This gives

$$\frac{\partial \rho}{\partial t} + \rho \nabla \cdot \vec{V} + \vec{V} \cdot \nabla \rho = 0 \Rightarrow \frac{1}{\rho}\frac{D\rho}{Dt} = \nabla \cdot \vec{V}$$

This is known as the **velocity divergence form of the continuity equation.** This states that the fractional rate of increase of the density *following the motion* of an air parcel is equal to velocity convergence.

Following the scaling analysis of section 6.1 and assuming that $|\rho'/\rho_0| \ll 1$, we can approximate the velocity divergence form of the mass continuity equation as

$$\frac{1}{\rho_0}\left(\frac{\partial \rho'}{\partial t} + \vec{V}\cdot\nabla\rho'\right) + \frac{w}{\rho_0}\frac{d\rho_0}{dz} + \nabla\cdot\vec{V} \approx 0$$

where ρ' designates the local deviation of density from its horizontally averaged value, $\rho_0(z)$. For synoptic scale motions, $\rho'/\rho_0 \approx 10^{-2}$ so that using the characteristic scales in Section 5.1, we find that the first term has magnitude

$$\frac{1}{\rho_0}\left(\frac{\partial \rho'}{\partial t} + \vec{V}\cdot\nabla\rho'\right) \approx \frac{\rho'}{\rho_0}\frac{U}{L} \approx 10^{-7}s^{-1}$$

For motions in which the depth scale H is comparable to the density scale height, $d\ln\rho_0/dz \approx H^{-1}$, the second term scales as

$$\frac{w}{\rho_0}\left(\frac{d\rho_0}{dz}\right) \approx \frac{W}{H} \approx 10^{-6}s^{-1}$$

For synoptic scale motions, the third term scales as

$$\nabla\cdot\vec{V} \approx \frac{W}{H} + 10^{-1}\frac{U}{L} \approx 10^{-6}\,s^{-1}$$

Therefore, to a first approximation, the second and the third term balance in the continuity equation. To a good approximation then

$$\frac{\partial u}{\partial x} + \frac{\partial v}{\partial y} + \frac{\partial w}{\partial z} + w\frac{d}{dz}(\ln\rho_0) = 0 \Rightarrow \nabla\cdot\left(\rho_0\vec{V}\right) = 0$$

Thus, for synoptic scale motions, the mass flux computed using the basic state density ρ_0 is nondivergent. This approximation is similar to the idealization of incompressibility. However, an *incompressible* fluid has constant density following the motion and thus, the velocity divergence will vanish, i.e. $\nabla\cdot\vec{V} = 0$.

6.5: The Geostrophic Approximation

Recall that the horizontal equations of motion can be written as

$$\frac{d\vec{V}_H}{dt} = \vec{F}_{cor} + \vec{F}_{pressure} + \vec{F}_{friction}$$

If we perform a scaling analysis of this equation above the boundary layer (as shown in Section 6.1), we will see that the horizontal pressure gradient force is approximately balanced with the Coriolis force, leading to a condition known as **geostrophic balance.** Geostrophic balance can be expressed as

$$f\left|\vec{V}\right| = -\nabla\Phi$$

The wind field associated with geostrophic balance is called the **geostrophic wind**.

$$\left|\vec{V}_g\right| = \frac{\nabla\Phi}{f}$$

What kind of flow does geostrophic balance describe? We can get some insight into this question by considering the balance of forces involved. Consider the sea of sea-level isobars depicted in Figure 6.11. As mentioned earlier, the PGF vector is always directed from high to low pressure, perpendicular to the isobars as depicted in Figure 6.11. In order for there to be a force balance between the pressure gradient and Coriolis forces, the Coriolis force vector must be equal and opposite to the PGF vector as depicted. Since Figure 6.11 represents a hypothetical situation in the Northern Hemisphere, we know that the Coriolis force must be directed perpendicular to the motion of the air parcel and to the right. Consequently, as shown in Figure 6.11, the resulting geostrophic wind flows parallel to the isobars.

The same reasoning applies for upper-air charts where isohypses are plotted on isobaric maps. Here, the geostrophic wind is parallel to the geopotential height contours with a magnitude dependent on the magnitude of $\nabla\Phi$. For synoptic-scale motions, the actual wind is close to the geostrophic wind (within 10-15% of the observed wind).

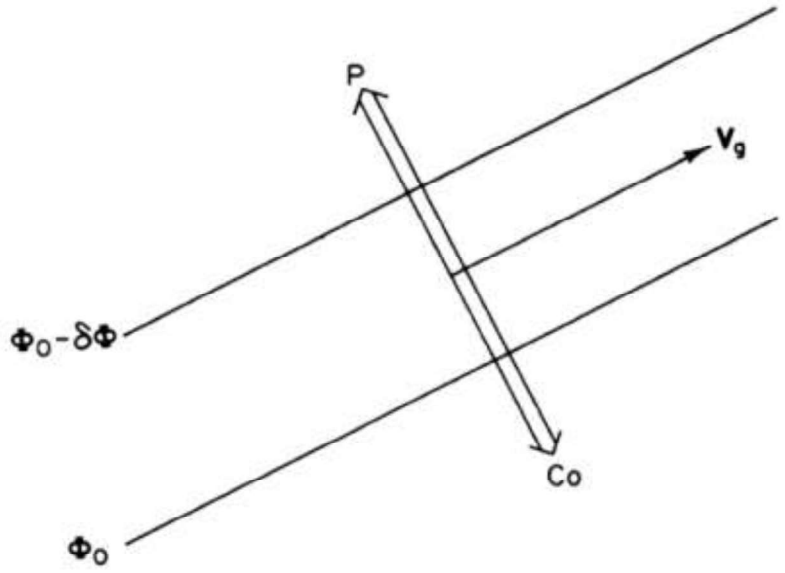

Figure 6.11 Illustration of the force balance resulting in the geostrophic wind $\vec{V}_g$. The arrow P represents the pressure gradient force and the arrow CO represents the Coriolis force. The thin dashed lines are isobars and *H* and *L* represent regions of high and low pressure, respectively.

Given that geostrophy is a balance between the PGF and Coriolis forces, we might inquire under which conditions is geostrophic balance met. Since there is no mention of $d\vec{V}/dt$ in the geostrophic approximation, the geostrophic wind is only strictly valid in regions of zero wind acceleration. Since the wind is a vector quantity, with magnitude and direction, if either of those properties is changed over time, the wind has been accelerated. Thus, two broad categories of flow in the atmosphere will violate the geostrophic balance: those characterized by (1) wind speed changes along the flow, and/or (2) wind direction changes along the flow. The along-flow speed changes are most prominent in the vicinity of the local wind speed maxima known as **jet streaks**. Along-flow direction changes are most obvious in the vicinity of troughs and ridges in the pressure field. We will discuss the dynamics of these types of flows in a future chapter.

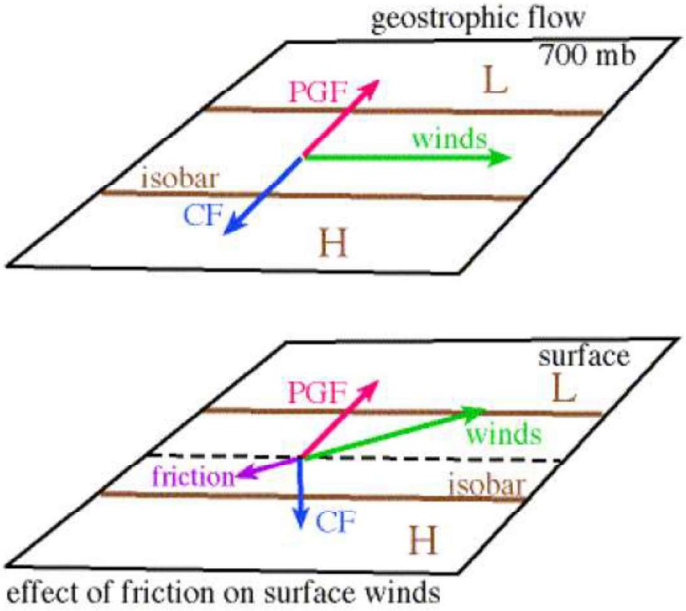

Figure 6.12 Schematic of the effect of friction on the wind field

Suppose we examine the wind field within the boundary layer. In this region, it is expected that friction will be significant. Within the boundary layer, friction will slow down the winds, which will reduce the magnitude of the Coriolis force. Assuming that the pressure gradient force remains the same within the boundary layer, this implies that the magnitude of the pressure gradient force will exceed the magnitude of the Coriolis force. Therefore, the winds will no longer flow parallel to isobars. The winds will cross the isobars directed towards the lower pressure, as shown in Figure 6.12.

Due to the frictional turning of the wind such that it crosses the isobars, there will be rising motion near the surface low and sinking motion near the surface high. Thus frictional convergence produces rising motion. An example is winds blowing across Lake Michigan and into Michigan itself; friction is less over the lake than on land, so the air slows over Michigan and convergence between the lake and the land wind results. Likewise, frictional divergence produces subsidence. An example of frictional divergence is wind coming out of a mountainous area and onto flat terrain. Friction decreases over the flat area and the wind speeds up. The area between the slow mountain and the fast plains wind is an area of divergence.

6.6: Thermal Wind Balance

An analysis of the momentum equations for mid-latitude synoptic-scale motions demonstrate that the vertical equation of motion is dominated by two terms, the vertical pressure gradient force and the gravitational force, and the horizontal equations of motion are dominated by two terms, the horizontal pressure gradient force and the Coriolis force. The first condition leads to hydrostatic balance, whereas the second condition leads to a balanced condition called geostrophic balanced as discussed previously. Therefore, **to a first order approximation, the mid-latitude atmosphere on Earth is in hydrostatic and geostrophic balance.** Combining the horizontal balance condition of geostrophic balance and the vertical balance condition of hydrostatic balance leads to a single balance condition called **thermal wind balance**. Thermal wind balance indicates that there is a relationship between the vertical shear of the geostrophic wind and the horizontal temperature gradient. Thermal wind balance provides us with a powerful diagnostic tool for understanding the structure, dynamics, and evolution of mid-latitude weather systems. We will illustrate this important balance condition below.

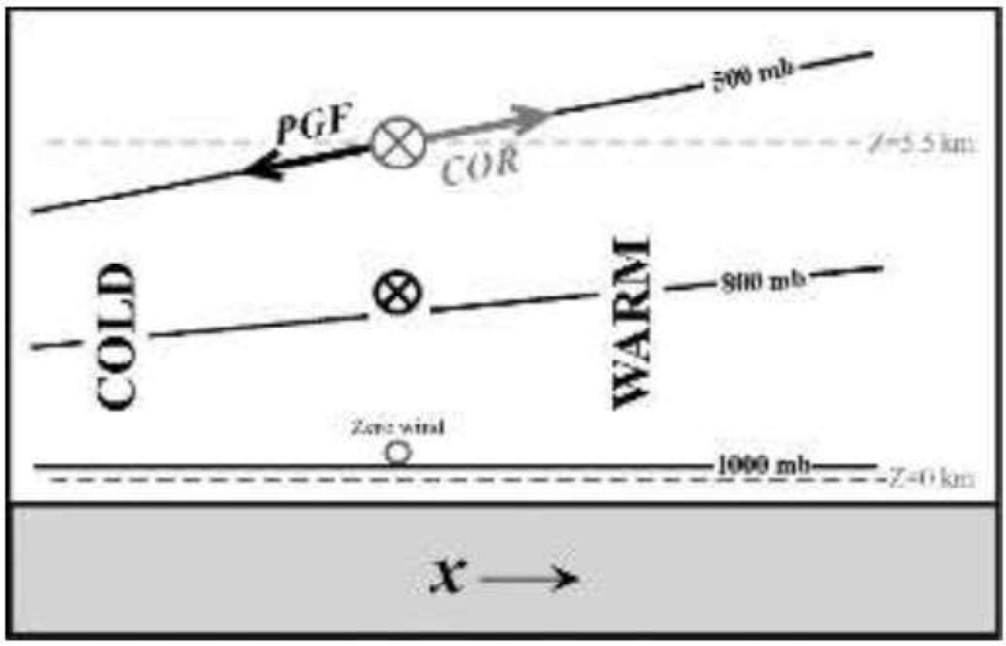

Figure 6.13 Schematic introducing thermal wind balance

Recall that the thickness equation suggested that the thickness between two isobaric surfaces is smaller in a cold column of air than in a warm column. Consider a hypothetical example in which a cold column and a warm column are horizontally juxtaposed, as in Figure 6.13. The distance between the 1000 and 800 hPa surfaces must be larger in the warm air than

the cold so that the 800 hPa surface slopes downward toward the cold air as illustrated. Similarly, the distance between the 800 and 500 hPa surfaces must be larger in the warm air than the cold and so the 500 hPa surfaces slopes even more dramatically downward toward the cold air. Thus, we find the slope of the isobaric surfaces increases with increasing height in the presence of a horizontal contrast in column average temperature. Of course, the slope of an isobaric surface is equivalent to the existence of a geopotential gradient along that surface since the geopotential is simply $g\Delta z$.

We now know that the pressure gradient force on an isobaric surface is related to the geopotential gradient on that surface. Thus, the increased slope to the isobaric surfaces in Figure 6.13 also means that the magnitude of the horizontal pressure gradient force increases with increasing height. Consequently, the geostrophic wind must be increasing with increasing height as well. Therefore, **there is a physical relationship between the vertical shear of the geostrophic wind (i.e. the manner in which the geostrophic wind changes with height) and the horizontal temperature gradient**. When the geopotential height gradient at one level of the atmosphere differs (in magnitude and/or direction) from that at another level, the geostrophic wind with at those levels will also be different. The **thermal wind** is defined as the vertical shear of the geostrophic wind (i.e. the change in the geostrophic wind with height).

We now explore the mathematical description of this relationship. From the discussion of geostrophic wind, we saw that the magnitude of the geostrophic wind speed was

$$\left|\vec{V}_g\right| = \frac{|\nabla\Phi|}{f} \approx \frac{1}{L}\frac{|\delta\Phi|}{f}$$

If we have geostrophic wind at two different isobaric levels, we can determine the magnitude of the thermal wind as $\left|\vec{V}_T\right| = \left|\vec{V}_{g,2} - \vec{V}_{g,1}\right|$ where

$$\left|\vec{V}_{g,1}\right| = \frac{1}{f}\frac{\delta\Phi_1}{L}, \qquad \left|\vec{V}_{g,2}\right| = \frac{1}{f}\frac{\delta\Phi_2}{L}$$

(assuming that $\Phi_2 > \Phi_1$). Using the expression for the geostrophic wind, the magnitude of the thermal wind becomes

$$\left|\vec{V}_T\right| = \frac{1}{f}\,\frac{\delta\Phi_2 - \delta\Phi_1}{L}$$

where $\delta\Phi_2 - \delta\Phi_1$ is the difference in the geopotential gradient at two different isobaric levels, say 1000 and 500 mb. The change in geopotential height is the same as the change in thickness for the layer. Thus, as the thickness gradient increases, the thermal wind increases, which means

that the shear in the geostrophic wind increases. Using the expression for the thickness equation, we have

$$\left|\vec{V}_T\right| = \frac{R_d}{f}\ln\left(\frac{P_1}{P_2}\right)\frac{\delta\overline{T}_{v,2} - \delta\overline{T}_{v,1}}{L}$$

where $\overline{T}_v$ is the column average virtual temperature. Therefore, the thermal wind is proportional to the temperature gradient in the layer. To summarize, just as the geostrophic wind is proportional to the geopotential height gradient on an isobaric surface, the thermal wind is proportional to the thickness gradient between two isobaric surfaces, which is determined by the temperature gradient. The thermal wind relationship suggests that wind, geopotential height, and temperature are all locked together such that a change in one results in a change in the others.

Just as the geostrophic wind flows parallel to geopotential height contours, the thermal wind "flows" parallel to thickness contours, with colder layers (with lower thickness) to the left, and warmer layers (with greater thickness) to the right in the Northern Hemisphere. Similar to the Coriolis force and the geostrophic wind, the thermal wind is also reversed in the Southern Hemisphere. In the Northern Hemisphere, you can remember the simple rule that "with the thermal wind at your back, cold air is to your left!"

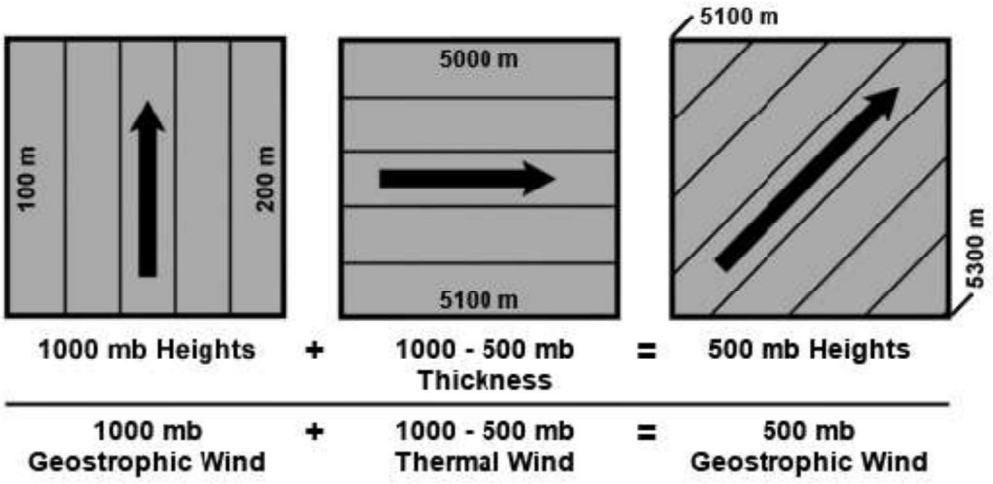

Figure 6.14 Schematic maps of heights and thickness (contour interval = 20 m) and geostrophic and the thermal winds.

In graphical form, the thermal wind vector is simply the vector difference between the geostrophic wind at some upper level in the atmosphere and the geostrophic wind at some lower level as shown in Figure 6.14. Mathematically, this is shown as $\left|\vec{V}_T\right| = \left|\vec{V}_{g,2} - \vec{V}_{g,1}\right|$, where $\left|\vec{V}_{g,2}\right|$

is at a higher level than $\left|\vec{V}_{g,1}\right|$. Using vector addition and subtraction, we see that when thickness contours are parallel to geopotential height contours, the geostrophic winds at different levels will be parallel. This implies that the thermal wind is parallel to the geostrophic wind.

However, when thickness contours are not parallel to geopotential height contours, the wind changes direction with height, as shown in Figure 6.14. In Figure 6.14, we have a Northern Hemisphere case with 1000 mb geopotential heights oriented perpendicular to thickness contours for the mean 1000-500 mb layer. This has several consequences:

- When cold air is to the north, the top of the 1000-500 mb thickness layer tilts down to the north. This makes the 1000-500 mb contours perpendicular to those at 1000 mb.
- Adding the 1000-500 mb thickness (that slopes down to the north) to the 1000 mb heights (that slope down to the west) results in 500 mb heights that slope down to the northwest and a little more steeply than 1000 mb heights. This requires that the wind is somewhat stronger at 500 mb.
- The thermal wind is oriented parallel to the thickness contours of the 1000-500 mb layer, which are parallel to the isotherms for the average temperature in the layer.
- This case clearly demonstrates the simple rule that (in the Northern Hemisphere) ``with the thermal wind at your back, cold air is to your left!"

Once again, we see that the wind, geopotential height, and temperature fields are all dynamically linked. A change in one results in a change in the others. For this reason, the thermal wind equation is an extremely useful diagnostic tool, which is often used to check analyses of the observed wind and temperature fields for consistency.

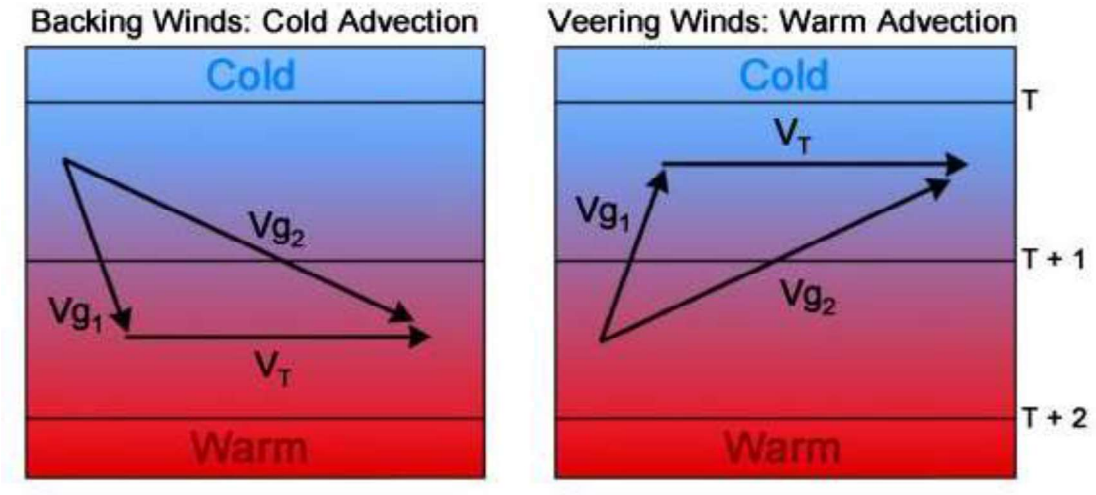

Figure 6.15 Relationship between turning of geostrophic wind and temperature advection: (a) backing of the wind with height and (b) veering of the wind with height

Another important characteristic of the thermal wind is that it can tell us whether the average temperature in a layer is warming or cooling. Since the thermal wind always has cold air to its left in the Northern Hemisphere, and it is simply the difference between the geostrophic winds at two levels, we can look only at the winds at those levels and determine if the temperature advection into the region is warm or cold.

Because the thermal wind blows parallel to thickness contours with the warm air to the right facing downstream in the Northern Hemisphere, a geostrophic wind that turns counterclockwise with height (called **backing**) is associated with cold advection. In Figure 6.15, wind backed from north-northwest wind at $\left|\vec{V}_{g,1}\right|$ to a northwesterly wind at $\left|\vec{V}_{g,2}\right|$ where $\left|\vec{V}_{g,1}\right|$ is at a lower elevation than $\left|\vec{V}_{g,2}\right|$. In this scenario, the geostrophic wind at both levels flows from colder to warmer air, indicated cold advection. Conversely, a geostrophic wind that turns clockwise with height (called **veering**) is associated with warm advection.

It is therefore possible to obtain a reasonable estimate of the horizontal temperature advection and its vertical dependence at a given location solely from data on the vertical profile of the wind given by a single sounding. Alternatively, the geostrophic wind at any level can be estimated from the mean temperature field, provided that the geostrophic velocity is known at a single level. Thus, for example, if the geostrophic wind at 850 hPa is known and the mean horizontal temperature gradient in the layer 850-500 hPa is also known, the thermal wind equation can be applied to obtain the geostrophic wind at 500 hPa.

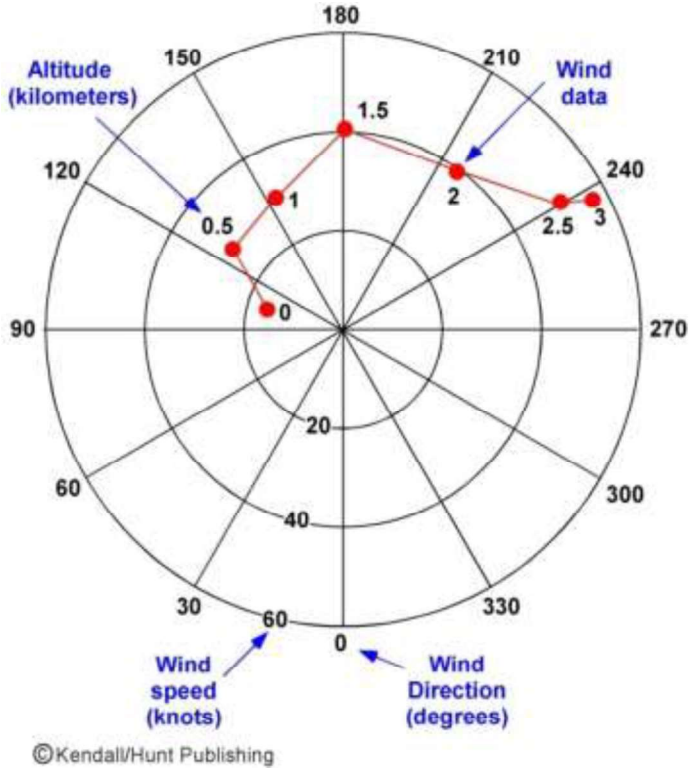

Figure 6.16: An example of a hodograph. The points shown are heads of the wind vectors (the tails are at the origin) at the indicated heights (km) above mean sea level.

Because of the thermal wind relationship, meteorologists are often interested in how the wind direction changes with respect to time, or across a given space. The vertical variation of the wind field at a fixed location is sometimes plotted as a **hodograph**, as shown in Figure 6.16. A **hodograph** is the locus of points formed by the heads of all the wind vectors at a given location at adjacent heights. The difference between the wind vector aloft and the wind vector below, the vertical-shear vector, is tangent to the hodograph at any height. Thus, hodographs are useful not only because they depict the wind as a function of height, but they also because they show the vertical wind shear as a function of height. If the meteorological wind direction increases with time or height, then the wind field is veering with time or height. If the wind direction decreases with time or height, then the wind field is backing with time or height. For example, a southerly wind that later becomes easterly is thus said to have **backed**, and a vertical profile in which the surface wind is southeasterly and the wind aloft is westerly is thus said to **veer** with height. Thus, hodographs can be used to anticipate warm air advection and cold air advection into a region.

As we've shown above, the thermal wind relationship forms the cornerstone of modern dynamical meteorology as well as the first-order balance for the flow in the middle latitudes on Earth. This latter point is a direct consequence of the fact that the mid-latitude atmosphere is, to first order, geostrophically and hydrostatically balanced.

**6.6.1: Full Derivation of Thermal Wind Balance

To derive the expression for thermal wind balance, it is convenient to change our vertical coordinates to height coordinates to isobaric coordinates. Writing the hydrostatic equation in isobaric coordinates gives

$$\frac{\partial \Phi}{\partial P} = -\frac{R_d T_v}{P}$$

The geostrophic wind can be determined from the expression of geostrophic balance in isobaric coordinates

$$\vec{V}_g = \frac{\hat{k}}{f} \times \nabla_p \Phi$$

The vertical derivative of the geostrophic wind relationship is

$$\frac{\partial \vec{V}_g}{\partial P} = \frac{\hat{k}}{f} \times \nabla \frac{\partial \Phi}{\partial P}$$

Using the isobaric form of the hydrostatic equation yields

$$\frac{\partial \vec{V}_g}{\partial P} = -\frac{R_d \hat{k}}{fP} \times \nabla T_v$$

Thus, we have the vertical shear of the geostrophic wind vector (i.e. the thermal wind). The component form of the thermal wind equation yields

$$\frac{\partial u_g}{\partial P} = \frac{R_d}{fP}\frac{\partial T_v}{\partial y}$$
$$\frac{\partial v_g}{\partial P} = -\frac{R_d}{fP}\frac{\partial T_v}{\partial x}$$

In Figure 6.13, we see that $\partial T_v/\partial x > 0$ and $\partial v_g/\partial P < 0$, which says that an increasing horizontal temperature gradient leads to stronger geostrophic wind aloft.

We can also express the thermal wind in terms of the geopotential difference using the thickness equation

$$\frac{\partial u_g}{\partial P} = \frac{R}{fP}\frac{\partial T_v}{\partial y} \qquad \frac{\partial v_g}{\partial p} = -\frac{R}{fP}\frac{\partial T_v}{\partial x}$$

Integrating these expressions gives

$$u_T = -\frac{R_d}{fP}\frac{\partial \overline{T}_v}{\partial y}\ln\left(\frac{P_0}{P_1}\right) = \frac{1}{f}\frac{\partial}{\partial y}(\Phi_1 - \Phi_0)$$
$$v_T = \frac{R_d}{fP}\frac{\partial \overline{T}_v}{\partial x}\ln\left(\frac{p_0}{p_1}\right) = \frac{1}{f}\frac{\partial}{\partial x}(\Phi_1 - \Phi_0)$$

Thus, the vector form of the thermal wind relation is

$$\vec{V}_T = \frac{R_d}{f}\ln\left(\frac{P_0}{P_1}\right)\hat{k} \times \nabla\bar{T}_v = \frac{\hat{k}}{f} \times \nabla(\Phi_1 - \Phi_0)$$

Thus, the thermal wind is proportional to the thickness gradient between two isobaric surfaces, which is determined by the temperature gradient, as suggested previously.

Chapter 7: Introduction to Quasigeostrophic Theory

The governing equations that describe the behavior of the atmosphere as described in Chapter 5 and 6 are quite complex. Even when written in Cartesian form and with simplifying assumptions such as the hydrostatic approximation, it remains difficult to conceptualize the dynamical essence of synoptic-scale weather systems using the full set of equations. However, early pioneers in meteorology, including Reginald Sutcliffe, Carl-Gustaf Rossby, Jule Charney, and Arnt Eliassen, recognized that the equations could be greatly simplified by utilizing the observation that the flow in synoptic-scale weather systems is *approximately* geostrophic. Jule Charney presented on the earliest quasigeostrophic (QG) derivations; the motive of this work was, in part, to provide a useful set of equations for early numerical weather prediction efforts.

By using a carefully designed set of assumptions, the governing equations can be simplified and combined in ways that retain the fundamental dynamics of weather systems and yet are simple enough to comprehend. The simplified QG framework provides many tools for dynamic analysis of the atmosphere while suggesting specific applications for weather forecasting. This system allows us to understand and diagnose the processes leading to vertical air motion and weather system development or decay, along with explaining why weather takes place.

Our aim is to understand the underlying assumptions of the QG equations and to understand the physical implications of QG theory. As we will see, the implications of QG theory form the conceptual framework of synoptic-scale forecasting and provide us physical insight into the nature of mid-latitude weather systems and the mid-latitude synoptic-scale flow. The QG framework allows us to simplify the equations of motion and reduce the system to two dependent variables that are useful in weather analysis and forecasting: the vertical velocity, which is closely related to the formation of clouds and precipitation, and the geopotential tendency, which is related to the development and movement of weather systems. We begin this chapter by examining departures from geostrophic balance in the atmosphere.